Dissertation

submitted to the

Combined Faculties for the Natural Sciences and for Mathematics

of the Ruperto-Carola University of Heidelberg, Germany

for the degree of

Doctor of Natural Sciences

presented by

Diplom-Biol. Steve Wagner

born in: Bad Salzungen

Oral-examination: 17.09.2013

Identification of Tumor Initiating Cells in a Patient-Matched Model of Serous Ovarian Carcinoma

Referees: Prof. Dr. Andreas Trumpp

Prof. Dr. Petra Boukamp

The work presented in this thesis was started in February 2011 and completed June 2013 under the supervision of Prof. Andreas Trumpp in the research group “Stem Cells and Cancer” at the German Cancer Research Center (DKFZ), Heidelberg as well as at the Heidelberg Institute for Stem Cells and Experimental Medicine (HI-STEM), Heidelberg.

Conference presentations:

Wagner *et al.*

"Comparison of Conventional Cell Lines and Improved Models for Ovarian Carcinoma: Drug Targets and Cancer-Stem Cell Markers"

(EACR22 2012, Barcelona, Spain)

Wagner *et al.*

"Novel Primary Models for Human Ovarian Carcinoma to Identify Cancer-Stem Cell Markers and Putative Drug Targets"

(ISREC Symposium 2011 – Lausanne, Switzerland)

1 Summary

Serous ovarian adenocarcinoma (SOC) is one of the most devastating diseases among women worldwide. Despite improvements in early diagnosis and therapy in the last decades, the five-year survival rate remains at 30%. Poor prognostic outcome can be mainly explained by the fast relapse rate observed in most patients after cytoreductive surgery and chemotherapeutic treatment. Of note here is that intrinsically resistant cell populations, the so-called cancer stem cells, have been recently associated with tumor recurrence, treatment failure and subsequent disease relapse. However, the lack of models that faithfully recapitulate the heterogeneity of serous ovarian cancer hindered so far the study of these phenotypically and functionally heterogeneous cancer cells.
Hence, the aim of this thesis was to establish and to evaluate a personalized model system that fully mimics SOC. Furthermore, this novel model system serves as a platform to study the cellular and molecular processes involved in metastasis development and drug resistance, as well as to identify tumor initiating cell populations.

Our advanced model system combines serum-free culture of primary cancer cells with xenotransplantation assays. Xenograft tumors established upon transplantation of primary SOC cells show histopathological features of SOC and express the two clinically used SOC specific markers CA125 and WT1. We were able to demonstrate that this model system displays major hallmarks of SOC such as the development of ascites and metastatic colonization of the diaphragm. Additionally, the molecular characteristics of the respective tumor are preserved throughout our models and the recently identified four transcriptional subtypes of SOC are conserved within our *in vitro* cultured primary cell lines as well as the corresponding xenograft tumors.

Using this model system, we were able to identify the heterogeneously expressed surface marker CD151, which defines a functionally different subpopulation within the tumor. Xenotransplantation assays demonstrated that exclusively $CD151^+$ cells possess tumor initiation capacity whereas $CD151^-$ cells do not. Gene expression profiling predicted a selective subpopulation-specific activation of various proliferation-associated pathways in $CD151^+$ cells. Determination of the phosphorylation status of key

pathway members of the JNK/MAPK- and EGFR signaling as well as members of the Src kinases (SFKs) verified these findings. Ablation of CD151 almost completely abrogated the activating phosphorylation suggesting CD151 to play a central in regulation of described pathways.
Analysis of a patient cohort, comprising 489 SOC patients, resulted in a significant correlation of CD151 expression with an advanced disease stage and a shorter overall survival in low-grade tumor patients.

Taken together, our data indicate that CD151 defines a tumor initiating subpopulation of cells in SOC and also plays a functional role in mediating the activation of various proliferative pathways. Thus, CD151 should be evaluated as a prognostic marker as well as a target of therapeutic treatment in SOC.

2 Zusammenfassung

Das seröse Ovarialkarzinom ist eines der verheerendsten Erkrankungen bei Frauen weltweit. Trotz Verbesserungen in der Früherkennung und der Therapie in den letzten Dekaden, beträgt die 5-Jahres Überlebenswahrscheinlichkeit gerade einmal 30 Prozent. Diese schlechte Prognose ist größtenteils auf den relativ schnell verlaufenden Rezidiv der Patientinnen nach zytoreduktiver Operation und Chemotherapie zurück zu führen.
Mehrere Beweise machen eine kleine resistente Population von Zellen, die sogenannten Krebsstammzellen, für diesen Rezidiv verantwortlich. Eine der größten Schwierigkeiten bei der Untersuchung phänotypischer und funktioneller Heterogenität von Krebszellen des serösen Ovarialkarzinoms war bisher der Mangel an Modellen, welche die Erkrankung wirklichkeitsgetreu abbilden.

Das Ziel dieser Arbeit war die Entwicklung und Beurteilung eines fortgeschrittenen und personalisierten Modells für das seröse Ovarialkarzinom, welches die Erkrankung möglichst wirklichkeitsgetreu widerspiegelt. Des Weiteren, sollte dieses Modell als Basis für die Aufklärung von Metastasierungsprozessen, Therapieresistenz und der Identifikation von Tumor induzierenden Zellen verwendet werden.
Das von uns entwickelte fortgeschrittene Modellsystem kombiniert die Serum-freie Kultivierung primärer Krebszellen mit deren Transplantation in immundefiziente Mäuse. Xenografttumore, welche durch die Transplantation primärer Zellen des serösen Ovarialkarzinoms erzeugt wurden, zeigen histopathologische Eigenschaften des serösen Ovarialkarzinoms und exprimieren die beiden klinischen Marker für das seröse Ovarialkarzinom; CA125 und WT1.
Wir konnten zeigen, dass dieses Modell wichtige Charakteristika des serösen Ovarialkarzinoms widerspiegelt, wie die Entwicklung von Aszites und die Metastasierung der Krebszellen in das Diaphragma. Darüber hinaus, werden die molekularen Eigenschaften der jeweiligen Tumore in unseren Modellen erhalten und die vier kürzlich beschriebenen Subtypen des serösen Ovarialkarzinoms widergespiegelt.

Mit Hilfe dieses Modellsystems waren wir in der Lage den heterogen exprimierten Marker CD151 zu identifizieren, welcher eine funktionell verschiedene Population von

Zellen definiert. Xenotransplantationsversuche demonstrierten, dass $CD151^+$ Zellen die Fähigkeit besitzen neue Tumore zu erzeugen wohingegen $CD151^-$ diese Fähigkeit nicht besitzen. Genexpressionsanalysen sagten die Subtyp-spezifische Aktivierung verschiedener proliferativer Signalwege in den $CD151^+$ Zellen voraus. Die Bestimmung des Phosphorylierungsstatus von Schlüsselkomponenten des JNK/MAPK- und EGFR-Signalweges, als auch der Src Kinasen (SFKs) bestätigte diese Resultate. Die Herunterregulation von CD151 hob diese aktivierenden Phoshorylierungen nahezu vollständig auf.

Die Analyse einer Patientenkohorte, bestehend aus 489 Patientinnnen des serösen Ovarialkarzinoms, ergab eine signifikante Korrelation der Genexpression von CD151 mit einem fortgeschrittenen Krankheitsstadium und einer verkürzten Überlebenszeit in Patientinnen mit einem gering-gradigen Tumor.

Zusammenfassend, deuten unsere Daten darauf hin, dass CD151 eine Tumor induzierende Subpopulation von Zellen beim serösen Ovarialkarzinom definiert, die auch funktionell eine Rolle spielt. Daher sollte CD151 als prognostischer Marker sowie auch als Ziel therapeutischer Behandlung evaluiert werden.

3 Introduction

Ovarian cancer

Ovarian cancer represents the fifth leading cause of cancer related death among women in the United States, accounting for 6% of all female cancer deaths. In 2013, an estimated 22.240 new ovarian carcinomas will be diagnosed, and approximately 14.030 ovarian carcinoma-related deaths are expected **(Figure 1)** [1]. Despite improvements in therapy, ovarian cancer remains the most deadly type of gynaecological cancers. Sixty-nine percent of all ovarian cancer patients will succumb to their disease, as compared with 19% of those suffering from breast cancer. This can be mainly explained due to late diagnosis as a result of the absence of an effective screening strategy [2]. Still, only 20% of the ovarian cancer patients are diagnosed while the tumour is still localized to the ovaries. At this stage, more than 80% of the patients can be cured by conventional surgery and chemotherapy [3]. Once the tumour has spread to the pelvic organs, the abdomen or beyond the peritoneal cavity, the five-year survival rate decreases below 40% [4].

Described risk factors for the development of ovarian carcinoma include age, obesity, family history of ovarian and other associated malignancies, like breast, uterine and colorectal carcinomas as well as inherited mutations in carcinoma predispositing genes [5-7]. Various studies also revealed that the risk of ovarian carcinoma might be increased by hormonal and reproductive factors like prolonged consumption of unopposed estrogen replacement therapy, infertility or long-term use of fertility drugs and low parity or nulliparity.

Approximately 10-15% of invasive ovarian carcinomas are the result of hereditary susceptibility [8,9]. The most common germline mutations are in the *BRCA1* and *BRCA2* genes, followed by the *MLH1* and *MSH2* genes, which are also implicated in hereditary nonpolyposis colorectal cancer [7]. The risk of suffering from ovarian cancer, carrying a *BRCA1* mutation lies between 30% and 60%; when carrying a *BRCA2* mutation the risk lies between 10% and 27% to develop ovarian cancer [8,9].

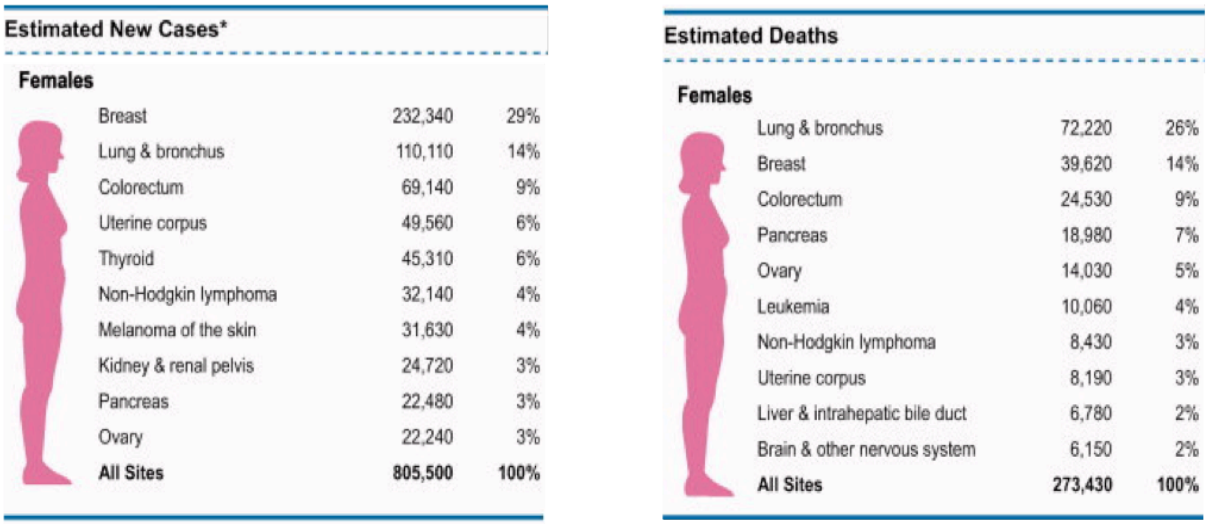

Estimated New Cases*

Females

Breast	232,340	29%
Lung & bronchus	110,110	14%
Colorectum	69,140	9%
Uterine corpus	49,560	6%
Thyroid	45,310	6%
Non-Hodgkin lymphoma	32,140	4%
Melanoma of the skin	31,630	4%
Kidney & renal pelvis	24,720	3%
Pancreas	22,480	3%
Ovary	22,240	3%
All Sites	**805,500**	**100%**

Estimated Deaths

Females

Lung & bronchus	72,220	26%
Breast	39,620	14%
Colorectum	24,530	9%
Pancreas	18,980	7%
Ovary	14,030	5%
Leukemia	10,060	4%
Non-Hodgkin lymphoma	8,430	3%
Uterine corpus	8,190	3%
Liver & intrahepatic bile duct	6,780	2%
Brain & other nervous system	6,150	2%
All Sites	**273,430**	**100%**

Figure 1- Cancer statistics published by Siegel et al. [1] depicting estimated new cases (left table) and estimated cancer deaths (right table) in the United States, 2013.

Pathophysiology

Ovarian cancers are remarkably heterogeneous at the cellular and the molecular level. More than 90% show an epithelial histology. Epithelial ovarian cancer is thought to arise from cells that cover the ovarian surface or that line subsurface inclusion cysts [10]. These cells are derived from the coelomic epithelium in fetal development, which is also involved in formation of the Müllerian ducts. The Fallopian tubes, uterus, cervix and the upper vagina evolve from these ducts.

Clinically, epithelial ovarian tumors often present as a complex cystic mass with solid components in the pelvis. Ovarian cancer cells most frequently spread initially within the peritoneal cavity where they implant on the peritoneal surface, the diaphragm, the bladder and the liver. This is associated with the development of ascites – a typical symptom of all types of ovarian cancer. Outside the peritoneal cavity, metastasis can occur in the parenchyma of the lung or the lymph nodes [11]. Unlike other cancers, no anatomical barrier exists for the invasion of ovarian cancer cells throughout the peritoneal cavity.

Five distinct main histologic subtypes have been described for epithelial ovarian cancer: low-grade and high-grade serous ovarian carcinoma, which both resemble cells that line the fallopian tube, the endometrioid- (endometrium), the mucinous- (endocervix), and the clear cell ovarian carcinoma (mesonephros) histotype **(Figure 2)**. The classification of ovarian tumors into these subtypes is of great importance as mucinous tumors have a

significantly worse prognosis than serous and endometrial cancers and respond less favourably to platinum- and taxane based chemotherapies [12].

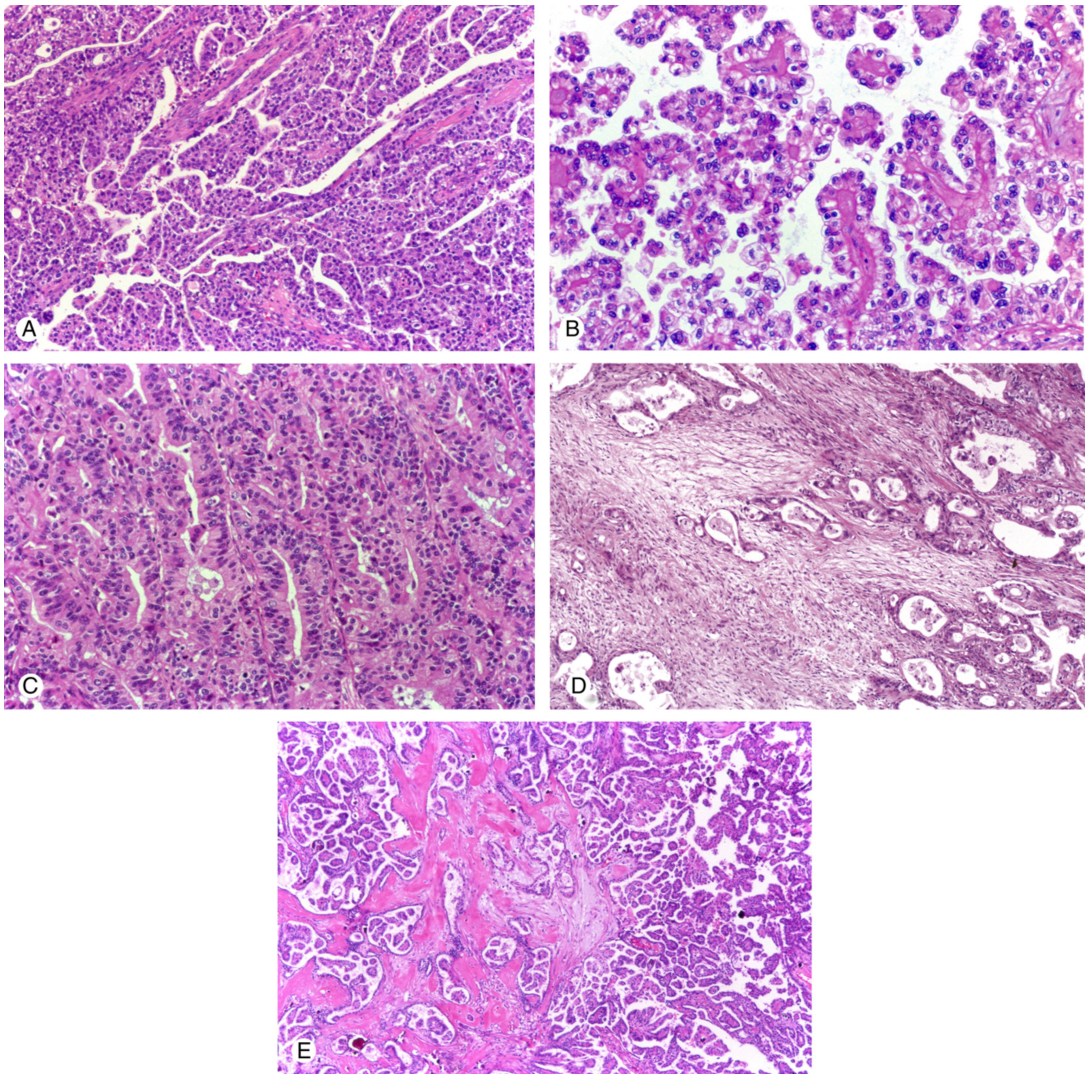

Figure 2 - Histopathological staining of the five different main subtypes of epithelial ovarian cancer. These histotypes bear strong resemblance to the normal cells lining different organs in the female genital tract. (A) High-grade serous ovarian carcinoma, (B) clear cell ovarian carcinoma, (C) endometrioid ovarian carcinoma, (D) mucinous ovarian carcinoma, (E) low-grade serous ovarian carcinoma (Figure adapted from Gilks *et al*. [13])

Diagnosis and staging

80% of patients with ovarian cancer have symptoms when the tumour is still localized, only 20% of these patients are diagnosed at this stage. The main reason for this is the rather unspecific nature of these symptoms. Typical presented symptoms range from diffuse abdominal complaints, changes in bowel habits, and unexplained weight loss to

massive abdominal swelling [14]. Unfortunately, these symptoms are rather unspecific and shared with many more common gastrointestinal, genitourinary and gynaecological conditions, which makes early diagnosis difficult. The cancer antigen 125 (CA125) is, among the serum markers, the most frequently used biomarker for the detection of ovarian cancer at early stages. In combination with transvaginal sonography (TVS) or by monitoring CA125 levels over time a high specificity can be achieved, but it is not sensitive and specific enough to be used alone when measured on a single occasion [15]. The development of novel biomarkers for early stage ovarian cancer is still in progress. Furthermore, multiplex technologies, which simultaneously measure several serum markers instead of one single marker, are very promising [2,16].

The most valuable diagnostic imaging procedure for the detection of ovarian cancer is transvaginal ultrasound. Computed tomography or magnetic resonance imaging is less sensitive and does not always reflect the whole extent of peritoneal and mesenteric carcinomatosis, which is common in ovarian cancer at an advanced stage. At the moment, surgical staging is still the most reliable procedure for the assessment of surgery feasibility for ovarian cancer [17].

Staging of ovarian cancer is determined according to the staging system developed by the International Federation of Gynaecology and Obstetrics (FIGO) **(Table 1)**. The 5-year survival rate of ovarian cancer is closely related to the stage at diagnosis. In the majority of cases ovarian cancer is not diagnosed until the cancer has reached an advanced stage, FIGO IIB – IV [4]. In these stages the tumor has already disseminated within the pelvis or elsewhere in the abdomen. A preferably complete removal of all macroscopically identifiable tumor manifestations is a crucial factor for patient survival. Post-operative residual tumor is the strongest independent parameter in prognosis after disease stage. Patients with a complete tumor resection survive in the median five years longer than those with post-operative residual tumor [12].

Table 1 – Staging of ovarian cancer according to TNM and International Federation of Gynaecology and Obstetrics (FIGO) [18]

Stage	Tumor grade	Nodal Status	Distant metastasis	FIGO	5-year survival	Characteristics
IA	*T1a*	*N0*	*M0*	*IA*	87%	Tumor limited to 1 ovary, capsule intact, no ascites present
IB	*T1b*	*N0*	*M0*	*IB*	71%	Tumor limited to both ovaries, capsules intact, no ascites present
IC	*T1c*	*N0*	*M0*	*IC*	79%	Tumor stage IA or IB, tumor on surface of 1 or both ovaries with capsule ruptured, ascites present
IIA	*T2a*	*N0*	*M0*	*IIA*	67%	Extension and/or metastases to the uterus and/or tubes
IIB	*T2b*	*N0*	*M0*	*IIB*	55%	Extension to other pelvic tissues
IIC	*T2c*	*N0*	*M0*	*IIC*	57%	Tumor stage IIA or IIB, tumor on surface of 1 or both ovaries, with capsule(s) ruptured, ascites present
IIIA	*T3a*	*N0*	*M0*	*IIIA*	41%	Tumor grossly limited to the true pelvis, negative nodes, but with histologically confirmed microscopic seeding of peritoneal surfaces or small bowel mesentery
IIIB	*T3c*	*N0*	*M0*	*IIIB*	25%	Tumor of 1 or both ovaries, peritoneal metastasis ≤ 2 cm in diameter, negative nodes
IIIC	*T3c, Any T*	*N0 N1*	*M0*	*IIIC*	23%	Peritoneal metastasis beyond the pelvis > 2 cm in diameter and/or positive retroperitoneal or inguinal nodes
IV	*Any T*	*Any N*	*M1*	*IV*	11%	Tumor involving 1 or both ovaries with distant metastases, parenchymal liver metastasis qualifies as stage IV disease

Molecular genetics

Several genetic and epigenetic changes have been found in ovarian cancers from different patients. As in other solid tumors, ovarian cancer develops from a progeny of single cells that have accumulated a series of five or more genetic alterations. Around 30 of these genetic abnormalities in oncogenes or tumor suppressor genes have been described for ovarian oncogenesis [19].

The most frequent genetic abnormality, shared by 60% to 80% of patients, is the mutation or loss of the tumor suppressor *TP53* [20]. The encoded protein p53 acts as a crucial regulator of G1/S transition in cell cycle and induces apoptosis upon DNA damage. Loss or mutation of *TP53* enables neoplastic cells to avoid apoptosis and hence cell division will occur despite DNA damage resulting in the accumulation of further genomic rearrangements [21].

As mentioned above, hereditary defects in DNA repair genes themselves account for 10-15% of ovarian cancer cases [22,23]. For carriers of these mutations the lifetime risk to develop ovarian cancer varies between 30-60% for *BRCA1*, 15-30% for *BRCA2* and 7% for *MLH1* and *MLH2.* BRCA1 and BRCA2 play a crucial role in the reliable repair of DNA double strand breaks by homologous recombination [8,9]. Like in familial breast cancers, all ovarian cancer cells inherit an inactivated allele. Loss of *BRCA1* or *BRCA2* function occurs through loss of the normal allele (loss of heterozygosity or LOH).

Around 15 different oncogenes have been found in ovarian cancers, and 11 of them showing genomic amplification [19,24]. One of the most common amplified genes in ovarian cancers is the small G-protein Rab25. Rab25 is involved in the regulation of motility, aggressiveness, apoptosis and autophagy [25]. It also has been shown to mediate survival in response to stress, as induced by chemotherapy, ultraviolet radiation, serum depletion or glucose starvation [26].

Other common amplified oncogenes in ovarian cancer are Aurora kinases, which are essential for cell proliferation. They are required for the completion of cytokinesis and their dysregulation leads to aneuploidy, which is a trait of many cancers [27].

Studies relating genetic alterations to clinical presentation and tumor morphological features indicate that low-grade and high-grade serous ovarian carcinomas may arise via different genetic pathways [28-30]. Low-grade tumors (neoplasms), develop in a known stepwise fashion from adenoma to low malignant state and ultimately to a low-grade serous carcinoma. This tumors are characterized by mutations in *KRAS*, *BRAF* and *PIK3CA* and LOH on Xq, suggesting that these tumors develop by a dysregulated RAF/MAPK pathway [31,32] **(Figure 3A)**. The mutated *KRAS* encodes for an abnormal protein, which is constitutively active and thereby aberrantly activating downstream effector pathways, namely PI3K, RAF/MAPK, and RAL-GEFs.

In contrast, high-grade tumors develop *de novo* from the surface epithelium. They grow rapidly and show no morphologically recognizable precursor lesions. High-grade serous

tumors have a high frequency of mutations in *TP53* and potential aberrations in *BRCA1* and *BRCA2* as well as LOH on 7q and 9p [33,34]. Thus, these tumors most probably arise via *TP53* mutations and BRCA1 or BRCA2 dysfunction [35-37] **(Figure 3B)**.

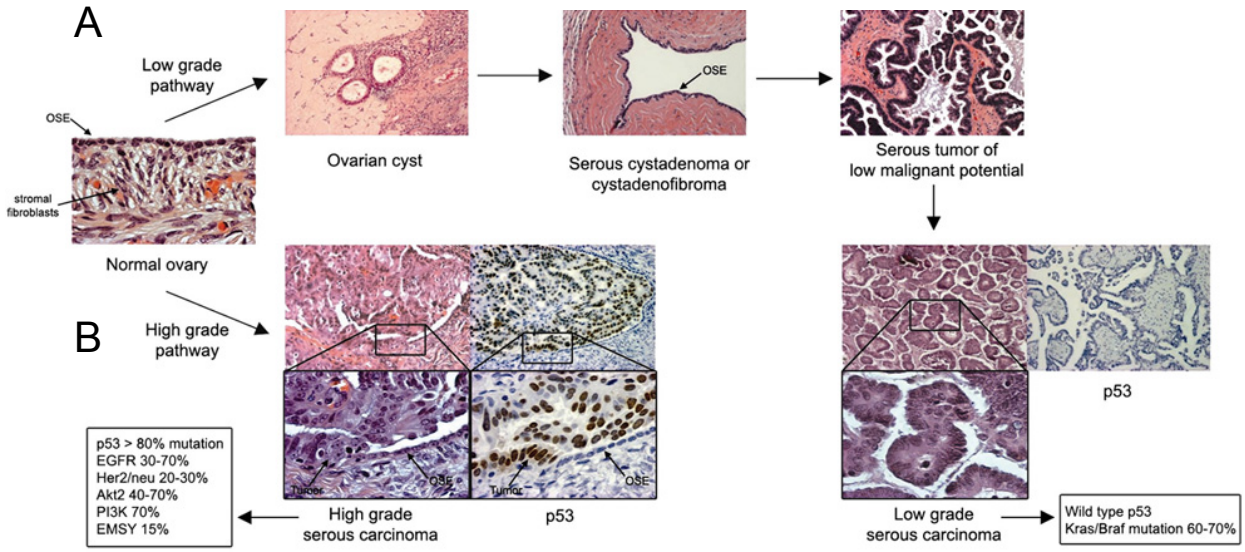

Figure 3 – Dualistic models for the development of Serous ovarian adenocarcinoma (SOC). (A) Development of low-grade serous carcinoma is characterized by morphologically recognizable precursors, from inclusion cystadenoma or cystadenofibroma to serous tumor of low malignant potential and low-grade serous carcinoma. They show a high frequency of *KRAS* and *BRAF* mutations. (B) High-grade serous tumors are characterized by a high frequency of *TP53* mutations and the absence of *KRAS* and *BRAF* mutations. They develop *de novo* without a recognizable intermediate. (Figure adapted from Rosen *et al.* [38])

Signaling pathways

More than 50% of ovarian cancers show an activation of at least one out of seven certain signaling pathways [26]. The most frequent triggered pathway, shared by approximately 70% of ovarian cancers, is the Phosphatidylinositide 3-kinase (PI3K) pathway.
Activation of the PI3K pathway can be driven by direct mutation or amplification of genes encoding key members of the pathway like *PIK3CA* and *AKT2*, or by inactivating mutations of *PTEN* [39-41]. In many cancers autocrine or paracrine signaling by receptor tyrosine kinases also trigger this pathway [42,43].
Signaling via the PI3K-Akt promotes survival and cell growth by several mechanisms **(Figure 4)**. Akt inhibits the pro-apoptotic Bcl-2 family members Bad and Bax [44,45]. It also impedes negative regulation of the transcription factor NF-κB, which leads to an increased transcription of anti-apoptotic and pro-survival genes. By phosphorylation of Mdm2 Akt antagonizes p53-mediated apoptosis. Akt also reduces the production of cell

death promoting proteins by down regulation of forkhead transcription factors [46]. In addition, cell proliferation can be stimulated by Akt mediated activation of mTor [47]. mTor is crucial for the regulation of translation in response to nutrients and growth factors by phosphorylating members of the protein synthesis machinery. This includes the ribosomal protein S6 kinases (p70S6K) and the 4E-binding protein (4E-BP). The latter is responsible for the release of translation initiation factor eIF4E, which is known to have transforming and anti-apoptotic activities *in vitro* [47-50].

Inhibitors against PI3K and Akt have been shown to inhibit the growth of ovarian cancer xenografts and could potentiate the cytotoxic effects of chemotherapeutics used against ovarian cancer [51].

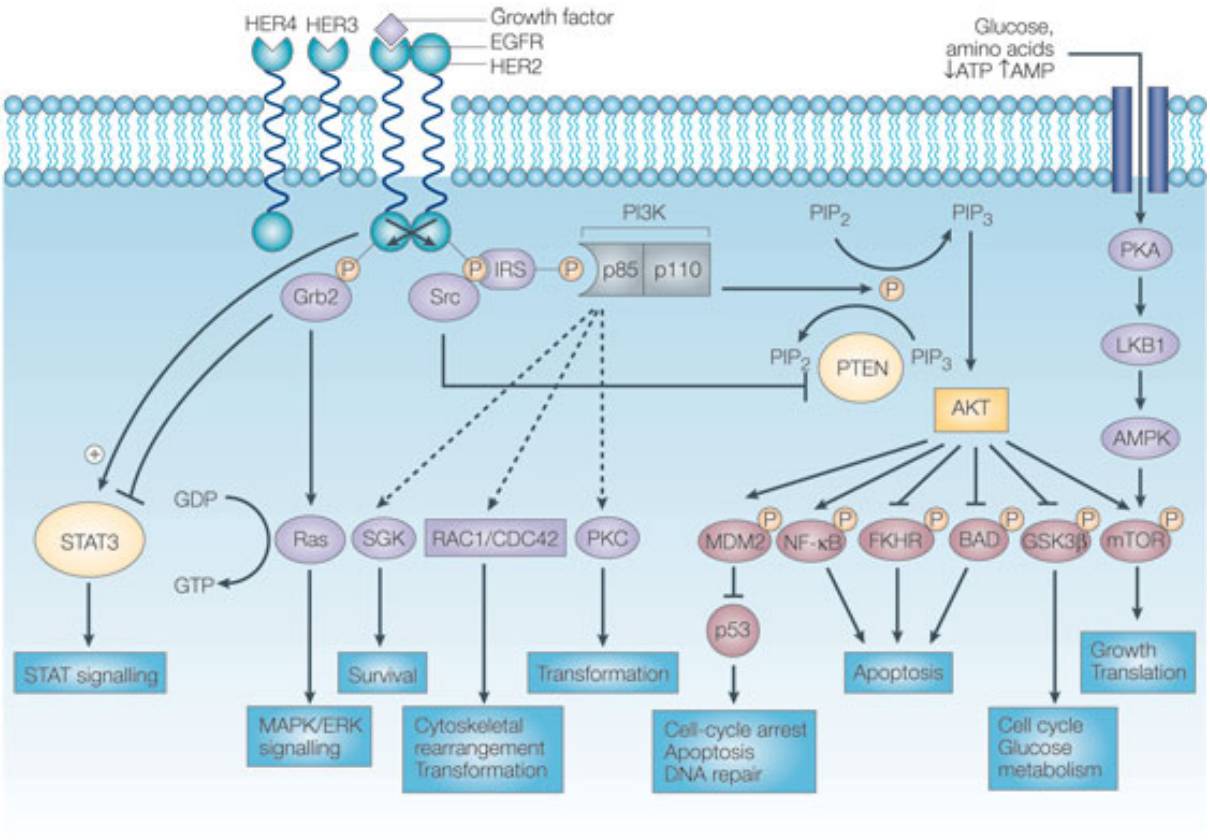

Figure 4 – The Phosphatidylinositide 3-kinase (PI3K) signalling cascade. PI3K signaling impacts on cell growth, survival and metabolism. (Figure modified from Hennessy *et al.* [52])

The pro-inflammatory cytokine IL-6 is overexpressed in most ovarian cancers. This leads to an autocrine stimulation of the IL-6 receptor, which triggers the activation of Janus kinas 2 (JAK2). JAK2 activation facilitates the phosphorylation and nuclear translocation of Signal Transducer and Activator of Transcription 3 (STAT3), resulting in

the upregulation of genes that stimulate proliferation, inhibit survival and induce angiogenesis [53]. More than 70% of ovarian cancers exhibit nuclear localization of phosphorylated STAT3, an observation associated with decreased overall survival [54].

The transcription factor NF-κB is constitutively activated in more than half of ovarian cancers [55] and has been implicated as a major regulator that controls cancer cell survival, proliferation and metastasis [56,57]. NF-κB is composed primarily of heterodimeric complexes of Rel family proteins p65 and p50. Several cytokines such as IL-1 and TNFα and growth factors like EGF bind to their receptors and trigger a cascade of signaling events that ultimately leads to the release of NF-κB from its inhibitor IκB [58]. Mitogen-activated protein kinase kinase kinase 3 (MEKK 3), which is one of several kinases that can induce the release of NF-κB [59,60], is overexpressed in more than 50% of ovarian cancers. As a result, NF-κB translocates to the nucleus where it binds to regulatory DNA elements. The expression of many genes essential for growth regulation and differentiation, such as cytokines, growth factors or angiogenic factors [60] and their receptors, are regulated by NF-κB [56,61-63]. It also induces the upregulation of genes, which are important for the control of cell survival such as Bcl-2, Bcl-xl, Survivin and the Iap family [61,63]. Consistent with these data, NF-κB has been correlated with resistance of cancer cells to radiation- and chemotherapeutic agent-induced apoptosis. Hence, NF-κB has also been associated to the development of resistance of tumor cells to apoptosis.

Molecular classification of tumors

Cancer subtypes

In the past, cancer was considered as one disease with varying histopathological features and response to systemic treatment. However, DNA sequencing and gene expression analysis have changed this view. Today, several cancer entities are not longer regarded as single diseases, but rather as a collection of different diseases, which need distinct therapeutic approaches.

The first clinically relevant tumor subtyping started in the 1970s with the division of breast cancer on the basis of estrogen receptor (ER) expression. To date, patients are classified into five main subtypes according to the expression of estrogen receptor (ER), progesterone receptor (PR), epidermal growth factor recptor 2 (HER2) as well as the proliferative index assessed by Ki67 [64]. Treatment decisions are made based on this

classification in combination with clinicopathological variables such as tumor size, lymph node involvement, and histological grade. Although, this strategy has been very successful as seen in a steady reduction in breast cancer mortality in the last decades, it is still not sufficient for the implementation of personalized therapy into clinical practise.

The rapid technical development in DNA sequencing- and genome expression profiling techniques allowed the identification of mutations that are common and shared by tumors of different entities.

The aim of these studiesis to exploit the existence of these molecular changes for targeted therapy. The paradigms are patients with EGFR mutations in lung cancer, patients with a non-mutated KRAS in colon and pancreas or a subset of patients with a BRAF mutation in melanoma [65]. Additionally, gene expression analyses could enable the identification of patients with a significantly worse prognosis by the use of transcriptional signatures predicting progression or overall survival. These patients might then be treated with a more aggressive therapy [65]. In summary, in the last years has been demonstrated that intrinsic molecular characteristics of the tumors are often better prognostic factors of treatment response than anatomical variables such as tumor size or nodal status [64].

In the next five years more than 25000 cancer genomes are expected to be sequenced by the Cancer Genome Atlas Research Network (TCGA) and the International Cancer Genome Consortium (ICGC) in cooperation with many individual partners from academia [64]. First studies describing novel subtypes based on gene expression patterns in several tumor entities have been already published in the last years [66,67]. The results obtained from these studies will lead to a new stratification of patients according to subtypes, pathway dependency or important mutations.

Ovarian cancer subtypes

Ovarian cancer is clinically classified according to the histology of the tumor into five main histotypes. These histotypes reflect the epithelial lining they arise from: low-grade and high-grade serous ovarian carcinoma (from the fallopian tube), endometrioid (endometrium), mucinous (endocervix), and clear cell (mesonephros) **(Figure 2)**. Additionally, the histotypes show differences in gene expression, tumor markers and therapy response [12]. Approaches to further classify these histotypes were based on

genetic alterations. According to the mutational spectra together with the clinical presentation and morphological features it could be shown that low-grade and high-grade serous ovarian carcinomas arise via different genetic pathways [28-30].

As mentioned above, low-grade tumors are characterized by mutations in *KRAS*, *BRAF* and *PIK3CA* and LOH on Xq [31,32], high-grade serous tumors show a high frequency of mutations in *TP53* and potential aberrations in *BRCA1* and *BRCA2* as well as LOH on 7q and 9p **(Figure 3B)** [33,34]. These data highlight the importance of large scale sequencing and expression profiling for the classification of individual tumors and suggest different treatment strategies for the individual patient.

The researchers of The Cancer Genome Atlas Research Network (TCGA) did these in lines for serous ovarian cancer in a study in 2012 [66]. They generated gene expression profiles of 489 high-grade serous ovarian tumors and performed non-negative matrix factorization consensus clustering in order to identify transcriptional subtypes. This analysis yielded in four clusters. The same analysis was applied to a previously published dataset and also resulted in four clusters. Additionally, the comparison of these two sets of four clusters showed a clear correlation. According to these results, the authors of the study concluded that at least four robust expression subtypes exist in high-grade serous ovarian carcinoma. The subtypes were termed 'differentiated', 'immunoreactive', 'mesenchymal' and 'proliferative' on the basis of gene content in the clusters [66]. However, this study did not include any subtype specific pathway analysis or researches on drug sensitivities of the different subtypes in e.g. available human ovarian cancer cell lines.

Taken together, several studies already described subtypes based on differential gene expression for serous ovarian cancer [68,69]. However, until now none of them have been evaluated in clinical trials or have led to an improvement of treatment strategies. As shown for breast cancer, the inclusion of gene-expression-based-assays and the subgrouping of patients can have a strong clinical impact and is a first step towards an individualized therapy [70].

Treatment of ovarian cancer

Surgery

For ovarian cancer, post-operative residual tumor is the most crucial independent parameter in prognosis after disease stage [12]. Therefore, it is one of the few malignancies in which cytoreductive surgery is carried out to eliminate the bulk of the tumor, even when complete resection is impossible [26]. Recent data from the analysis of three different large studies showed that patients with a complete tumor resection survived a median of five years longer than patients with post-operative residual tumor [12]. Even for patients with advanced ovarian cancer, a residual tumor of less than 1 cm can be achieved, if specialists in gynaecological oncology perform the surgery [71]. The appropriate surgery mostly depends if the tumor is still limited to the ovaries (FIGO stages I to IIA) or already metastasized within the pelvis or elsewhere in the abdomen (FIGO stages IIB to IV). To date, longitudinal laparotomy is the state of the art technique for examination of the abdominal cavity, as laprascopy does not provide the same value and oncological safety [72]. This approach involves a vertical midline incision to allow sufficient exposure of the upper abdomen and pelvis. Typically, a total abdominal hysterectomy and bilateral salpingo-oophorectomy are carried out. This goes along with careful examination of all peritoneal surfaces, omentectomy, biopsy of paraaortic lymph nodes and peritoneal washings. The dissection of the paraaortic lymph nodes is especially important in patients with low stage disease, since such patients may have more advanced disease [73].

The 5-year overall survival rate for ovarian cancer patients, which underwent surgery, ranges from 40% to 46%. Independent poor prognostic factors are advanced tumor stage, age, general health, post-operative residual tumor, high-grade or clear-cell histology and pre-operative ascites [71,74-77]. Approximately 69% of patients operated will develop recurrent disease [2].

Early ovarian cancer (FIGO stages I to IIA)

For patients with early stage ovarian cancer an adequately surgically staging is essential because of the significant incidence of microscopic metastases. Therefore, a systemic examination of the whole abdomen with multiple peritoneal biopsies as well as the

removal of macroscopic tumor manifestations is carried out. This procedure also includes, pelvic and paraaortic lymph node dissection because of the affection of the retroperitoneal lymph nodes in 20-25% of patients in stage T1 [72]. The aspiration of ascetic fluid and peritoneal washings for cytology studies is also performed and integrated in the assessment of stage.

Following surgery, patients with early stage ovarian cancer (except patients with stage IA, grade 1) receive three to six cycles of platinum-based chemotherapy. This adjuvant treatment leads to an increase in the 5-year overall survival from 74% to 82% and disease-free survival from 65% to 76% [78]. For the reasons mentioned below, postoperative chemotherapy with a combination of carboplatin and paclitaxel is commonly used for early stage ovarian cancer patients. The optimum number of cycles that should be applied is discussed controversy. A randomized trial by the Gynecologic Oncology Group (GOG) showed no significant difference in overall survival between groups treated with three cycles versus six cycles of Carboplatin and Paclitaxel chemotherapy in early stage disease [79]. However, for patients receiving a three-cycle regimen, a higher rate of relapse has been reported [80].

Even if adjuvant radiotherapy of the whole abdomen is used in some selected high-risk patients with early stage ovarian cancer, platinum-based chemotherapy is the state-of-the-art therapy and most widely applied [81].

Advanced ovarian cancer (FIGO stages IIB to IV)

Only 20% of patients with ovarian cancer are diagnosed while cancer is limited to the ovaries [2]. The remaining part already shows metastatic spread to the pelvic organs, the abdomen or beyond the peritoneal cavity. For these patients a complete tumor resection or at least a reduction of post-operative residual tumor to less than 1 cm is the strongest factor in prognosis [12]. In approximately 30-50% of cases an intestinal surgery is necessary to reduce the tumor burden to less than 1 cm. This could include partial resection of the liver or pancreas, splenectomy, cholecystectomy or diaphragm stripping [72]. This applies even for stage IV patients, which benefit more from complete tumor reduction or tumor reduction to less than 1 cm than patients with larger residual tumor [82-85].

To date, only one prospective study could show a therapeutic benefit of systematic pelvic and paraaortic lymph node removal in advanced ovarian cancer. The systematic

lymph node removal significantly prolonged progression-free survival but had no influence overall survival, when compared to patients who underwent removal of enlarged lymph nodes only [86].

The current standard of post-operative care for patients with advanced ovarian cancer is six cycles of platinum- and taxane-based chemotherapy. Carbo- and cisplatin have been shown to be the most active drugs against ovarian cancer. They mediate their effects by the formation of DNA intrastrand crosslinks. Taxanes such as paclitaxel and docetaxel act by a different mechanism. They exert their cytotoxic effects by binding and stabilization of tubulin polymers, thereby inhibiting the process of cell division [87]. Meta-analysis of studies performed so far showed that the combination of platinum and taxane is superior to platinum monotherapy [88]. In total, the risk of death decreases about 30% when paclitaxel is included in first-line therapy [89,90]. The combination of paclitaxel and carboplatin is as effective as Paclitaxel and Cisplatin in first-line therapy, but was reported to have less side effects like emesis, leukopenia and nephropathy [91,92]. Even for patients with advanced ovarian cancer who had undergone optimal surgery, this treatment regimen resulted in a median overall survival of nearly five years [91]. Despite improved treatment strategies, the majority of patients with advanced disease still undergo relapse and only 10-30% of such patients have long-term survival. Factors that predict poor survival include an advanced tumor stage, an age of more than 65 years, post-operative residual tumor, high grade or clear-cell histology, pre-operative ascites, a increased CA-125 level even after three cycles of chemotherapy, and a CA-125 level of more than 20 U/ml at end of first line therapy [12,71,74-77].

Treatment of advanced disease

Recurrent disease after platinum-based first-line chemotherapy is a major problem for patients with advanced ovarian cancer. In these cases a hormonal therapy with Tamoxifen or an aromatase inhibitor is often considered [93,94]. Even if less than 20% of patients respond to hormonal therapy, some patients have a prolonged period of stable disease and less side effects as for cytotoxic treatment.

Generally, the choice of second-line chemotherapy depends on the duration of the prior remission. A relapse after more than six months after completion of first-line therapy points to a platinum-sensitive disease [95,96]. For these patients single agent chemotherapy with carboplatin is often considered. A platinum-based combination therapy may be

reasonable for selected patients with more severe symptoms and a rapidly progressive disease [97].

Patients, who have a relatively short remission, lasting less than six months after first-line therapy, usually have a platinum-resistant disease [98]. They are normally treated with a regimen that does not contain platinum. Possible agents for treatment include liposomal Doxorubicin, Topotecan, Gemcitabine, Paclitaxel, oral Etoposide and Vinorelbine [95,99-102]. The overall response rate for each of these drugs ranges between 10 to 20 % in patients with platinum-resistant ovarian cancer. The decision, which drug should be administered, is often made according to the side effect profile and the convenience of administration.

Targeted therapy

The significance of targeted therapies is increasing in several tumor types. Based on specific molecular and biochemical pathways that cause the malignant phenotype, a number of compounds are under clinical investigation. These drugs target proliferation, angiogenesis, invasion, metastasis and decreased apoptosis and rely on the differential expression of specific targets in ovarian cancer compared to normal epithelial cells. They are under evaluation as single agents and in combination with chemotherapy [103]. However, until now no targeted therapy has been approved for the treatment of ovarian cancer.

The expression of epidermal growth factor receptor (EGFR) in ovarian cancer has been shown to be associated with poor prognosis. EGFR is known to activate cellular processes that drivee a malignant phenotype are initiated by EGFR activation [104]. Signal transduction by EGFR can be disturbed by monoclonal antibodies such as Cetuximab that block ligand binding or by inhibition of the enzymatic activity of EGFR tyrosine kinase by small molecule inhibitors as Gefintinib, Lapatinib or Erlotinib [105,106]. A recent phase II study of Erlotinib treatment in combination with Carboplatin treatment resulted in a response rate of 57% in platinum sensitive recurrent ovarian cancer and 7% in platinum-resistant patients [107]. In contrast, a phase II study with Erlotinib, Carboplatin and Paclitaxel as first-line therapy showed no significant better response rates compared to historical controls [108]. The monoclonal antibody Cetuximab failed to demonstrate a benefit in progression-free survival in a phase II study, when combined with Carboplatin and Paclitaxel [105].

Also inhibitors that affect other members of the epidermal growth factor receptor family such as HER2 have entered clinical evaluation. Clinical trials with the two monoclonal antibodies Trastuzumab and Pertuzumab showed modest activity in ovarian cancer [109,110]. Nevertheless, HER2 expression in ovarian cancer has not been studied, as extensively as in breast cancer and data on the impact of HER2 on survival of ovarian cancer patients are still inconsistent.

Angiogenesis plays a crucial role in ovarian cancer metastasis and ascites development [111]. In this context, vascular endothelial growth factor (VEGF) has been shown to be important regulator of angiogenesis and is involved in various aspects of ovarian carcinogenesis [112]. Bevacizumab, a monoclonal antibody targeting VEGF-A, showed in two phase II clinical trials a response of 16 to 21% when used as single agent [113,114]. Phase III studies of Bevacizumab in combination with chemotherapy resulted in a modest improvement of progression-free survival, but showed a greater survival benefit for patients with a high risk for progression [115].

Further compounds which are currently under clinical evaluation in phase I/II target different specific pathways, which have been implicated in ovarian cancer tumorigenesis, metastasis development and relapse [103,116]. These studies include PARP inhibitors such as ABT 888 and Olaparib, mTOR pathway inhibitors such as Temsirolimus and Everolimus, or MAPK pathway inhibitors such as Cabozantinib.

Even though many of such compounds are currently investigated in clinical trials, targeted therapy in ovarian cancer is for almost all cases still experimental and no targeted drug has been approved as clinical standard so far. Further studies are needed to identify subgroups of patients that would benefit of a specific targeted therapy.

Therapy resistance

Resistance of tumors against certain drugs causes treatment failure and death in more than 90% of patients with advanced disease. Already small-fold changes in the sensitivity of the tumor cells can lead to clinical resistance. A main reason for this phenomenon is the low therapeutic index of most chemotherapeutic agents. Drug resistance result mainly from three different factors: pharmacokinetics, properties of the tumor microenvironment and specific molecular alterations inherent to the cancer cells **(Figure 5)** [117].

According to experimental data, some cases of drug resistance might be explained by interpatient differences in pharmacokinetic variables. As a consequence of these differences between patients only an insufficient intratumor drug concentration is reached, which leads to the development of drug resistance. Pharmacokinetic parameters that influence drug concentration in the tumor include first-pass metabolism, conversion of prodrugs into active metabolites, renal clearance, hepatic drug metabolism and tumor vascularity [118].

As stated above, also the tumor environment modulates the response to certain drugs. For the resistance against radiotherapy it has been known for a long time that hypoxia plays an important role. This could now also been translated to chemotherapy [119]. Consequences of a hypoxic environment that influence resistance might be related to lower amount of proliferating cells and therefore a decreased generation of free radicals, an increased drug degradation, increased genomic instability as well as a HIF1-mediated transcriptional activation of survival genes and inhibition of apoptosis [120]. Additionally, it has been shown that stromal cells can also activate anti-apoptotic signalling pathways [121].

The genetic background of cancer cells present in a tumor can be very different in distinct patients. It is a well-accepted model that tumors consist of quite heterogeneous populations of cells. Even if they are clonally derived, several clones can co-exist within one tumor. The acquisition of somatic mutations or epigenetic changes induces the expression of a huge variety of drug tolerance genes, which are the basis of resistance development [122]. During treatment the high genetic instability of cancer cells promotes the selection of drug resistant clones, which results in the outgrowth of these clones.

It is important to keep in mind that cytotoxic agents target primarily proliferating cells, however, tumors consist also of a significant proportion of quiescent cells. These cells therefore show a higher degree of drug resistance compared to proliferating cells. This subpopulation of cells within the tumor bulk often exhibits a higher expression of multidrug efflux transporters or pro survival pathways being able to regrow the tumor after the treatment. These cells are called cancer stem cells. In haematological malignancies such as CML this model has already been substantiated [123].

In summary, resistance to a certain therapy is influenced by multiple mechanisms and probably different between patients. Large scale sequencing as well as expression profiling of individual tumors might improve the identification of molecular targets and lead to a more individualized treatment of each patient in the future.

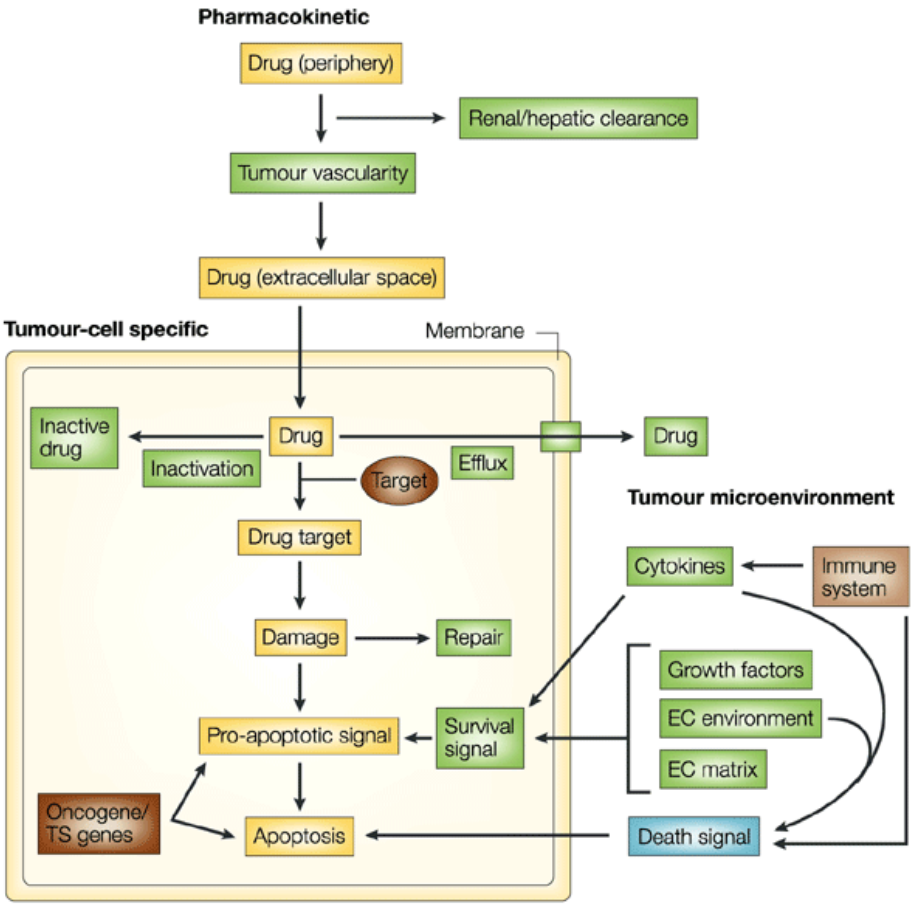

Figure 5 – Overview of the three categories of drug resistance: pharmacokinetics, the tumor micro-environment or cancer-cell-specific properties. Yellow – pathway of drug action; blue – pathways promoting cell death; green – pathways mediating drug resistance; brown – pathways with potentially pro- and anti-cytotoxic effects; TS – tumor suppressor; EC – extracellular (Figure adapted from Agarwal et al. [117])

Cancer Stem Cells

Heterogeneity within cancer

Nowadays, it is well accepted that many tumors consist of cancer cells, which are phenotypically and functionally heterogeneous. This so called intratumoral heterogeneity can arise in multiple ways. The best-established model uses stochastic genetic or epigenetic changes (clonal evolution) to explain intrinsic differences among cancer cells **(Figure 6A)** [124]. Alternatively, extrinsic factors such as interactions between tumor cells and different microenvironments might also play a substantial role in the determination of tumor heterogeneity. For example, cancer cells adjacent to blood vessels have a different supply with nutrients compared to cancer cells in distance from

blood vessels. **(Figure 6B)** [125,126]. The third possible explanation for heterogeneity within a tumor is that some cancers follow the so-called stem cell model. According to this model tumorigenic cancer stem cells "differentiate" into nontumorigenic cancer cells in a hierarchical organization **(Figure 6C)** [127,128]. This model would allow the explanation of phenotypic and functional differences that cannot be attributed to clonal evolution or environmental differences. In addition, the different models are not mutually exclusive and may influence the tumor each at different extents depending on the tumor **(Figure 6D)**. However, the perception that heterogeneity can arise through multiple mechanisms alone does not automatically prove the existence of a cancer stem cell hierarchy.

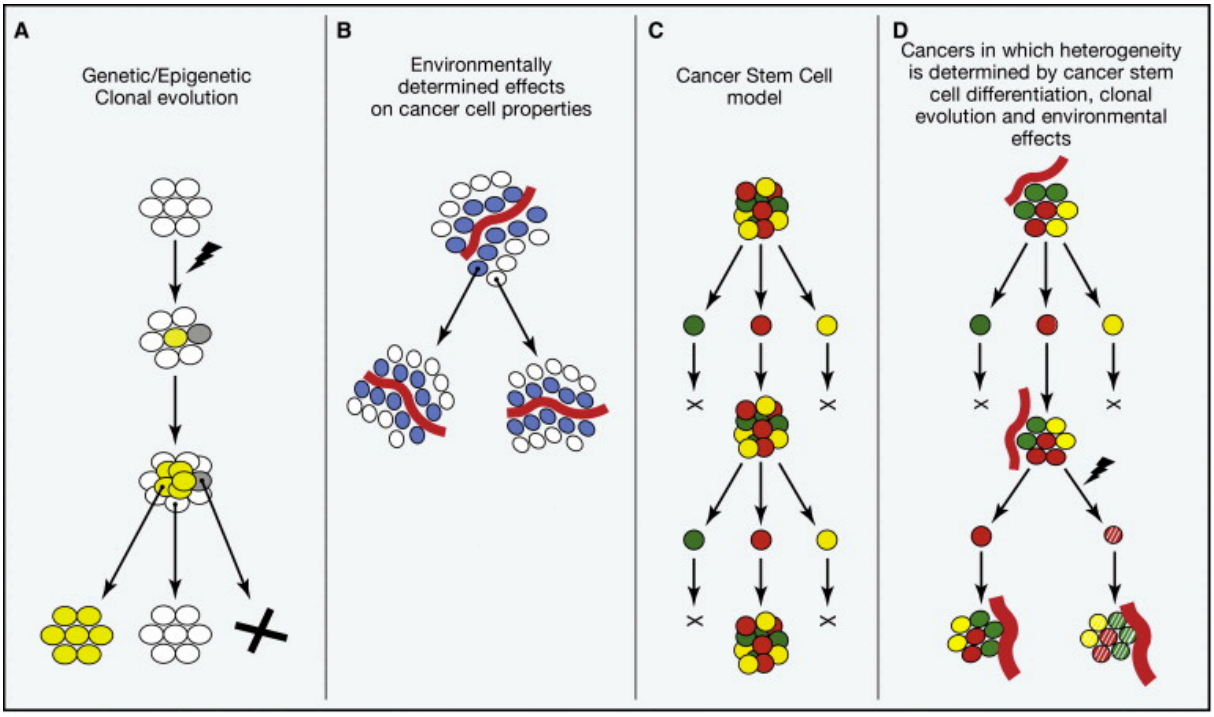

Figure 6 – Overview of different possible sources of heterogeneity within cancer. (A) Heterogeneity in tumors can arise via stochastic genetic changes (clonal evolution). (B) Extrinsic environmental differences can be a source of heterogeneity within tumors. (C) According to the stem cell model, cancers contain intrinsically different subpopulations of tumorigenic and nontumorigenic cells organized in hierarchical fashion. (D) The different sources of heterogeneity are not mutually exclusive and may influence the tumor each at variable extents depending on the cancer. (Figure modified from Magee *et al.* [124])

The Cancer Stem Cell Model

For several cancers it has been shown decades ago that they can differentiate into progeny, which have limited proliferative potential compared to their malignant

progenitors [129,130]. For some germ lineage cancers it could be shown that the presence of only differentiated cells after chemotherapy is a favourable prognostic factor, whereas the presence of undifferentiated cells predicts disease recurrence [131]. According to this data undifferentiated cells would be mainly responsible for tumor growth and disease progression.

Similar results were obtained for neuroblastomas, which also exhibit variable degrees of differentiation [124]. Patients with broad differentiated neuroblastomas in general have a better prognosis than patients with low degree of differentiation [132]. Additionally, patients with neuroblastomas showed an improved survival when treated with therapies that promote differentiation [133].

Taken together these clinical observations support the cancer stem model showing that undifferentiated tumor cells are the ones most likely driving cancer progression.

However, the cancer stem cell model became ever more important when first evidence emerged suggesting that this model could be also relevant for more common adult cancer types. By the comparison of the tumorigenic potential of phenotypically distinct subpopulations separated according to specific markers by flow cytometry, Dick and colleagues could show that some acute myeloid leukemias follow the cancer stem cell model [134]. Later on, the presence of a subpopulation with the exclusive ability to initiate new tumors was also verified for breast cancers [135] opening the possibility that the cancer stem cell model might be applicable to a broader spectrum of cancers.

Indeed, further studies using similar approaches have been now used to study the cancer stem cell model in colon cancer [136,137], pancreatic cancer [138], brain tumors [139] and ovarian cancer [140-143]. In every case, the ability to form tumors was restricted to a small subpopulation of cells, what indicates that tumorigenic cells are rare. These studies suggest that therapies that only shrink the tumor mass might not be curative if they fail to eliminate the cancer stem cells.

Cancer stem cells in ovarian cancer

As stated above, several studies focused on the identification of tumor initiating subpopulations in ovarian cancer. Anyhow, the distinct phenotype of the ovarian cancer stem cell population has not been defined sufficiently. Ovarian cancer initiating cells have been described to be enriched in $CD24^+$ [144], $CD44^+$ [140], $CD44^+CD117^+$ [143], $CD133^+$ [141] subpopulations. However, the study describing CD24 as a putative stem cell marker was

based only on one patient tumor and hence has been considered carefully. The tumor initiating properties of the $CD44^+CD117^+$ subpopulation could not been confirmed when evaluated in large cohort of ovarian cancers. Most of the ovarian cancers showed no expression of the $CD44^+CD117^+$ subpopulation. For the tumors expressing both markers, an increased tumorigenic potential in the described subpopulation could not be observed [142]. Another marker defining a putative cancer stem cell population in ovarian cancer is CD133. Curley *et al.* reported tumorigenic ovarian cancer cells to be enriched in the $CD133^+$ subpopulation. Also these data could not been confirmed in larger cohort of ovarian cancers. In some cases CD133 enriched for tumorigenic ovarian cancer cells and in others not. Furthermore the expression levels of CD133 changed on some tumorigenic cells during passaging [142]. A possible explanation could be that CD133 marks ovarian cancer initiating cells only under distinct conditions in some patients.

It appears to be difficult to confirm cancer stem cell markers in a number of solid cancers. As stated above, not every patient even expressed certain markers, raising the possibility that there is a particular diversity among patients in terms of the expression of these markers [124].

Experimental models for ovarian cancer

Genetically Engineered mouse models targeting the ovarian surface epithelium

Genetically engineered mouse models are indispensable for the understanding of the etiology and early stages of epithelial ovarian cancer, as well as the development and assessment of novel therapeutics. Advancement in knowledge about initiation and progression of ovarian cancer was hampered mainly due to the lack of appropriate experimental models, which adequately recapitulate the human disease. Until now, the lack of specific promoters that could drive transgene expression exclusively in the ovarian surface epithelium made the development of traditional transgenic mouse models for ovarian cancer very difficult. For the generation of epithelial ovarian cancer models only two candidate promotors have been reported: the Ovarian Specific Promotor 1 (OSP-1) [145] and the Mullerian Inhibiting Substance Type II Receptor promotor (MISIIR) [146] **(Table 2)**. However, expression of the early region of simian virus

40 T antigen (SV40 TAg) under the control of the OSP-1 promotor in transgenic mice revealed a leaky expression leading to the appearance of tumors in multiple tissues. In addition, ovarian tumors that developed, originated from the granulosa cell compartment and not from ovarian surface epithelium [147].

Connolly *et al.* reported the first successful transgenic mouse model for ovarian cancer [146]. Therefore they generated transgenic mice expressing the early region of SV40 under the control of the MISIIR promotor, which has been shown to be specific for female reproductive organs, including the fallopian tubes, uterus, and upper vagina. The transgenic mice developed bilateral ovarian tumors in about 50% of cases within 1.5-3 months of age. The appearance of tumors was associated with peritoneal dissemination as well as the development of ascites. However, SV40 Tag has not been shown to be a genetic contributor of ovarian carcinogenesis [148-150] and this model did not accurately represent human epithelial ovarian cancer.

Table 2 – Summary of promoters and targeted genes for ovarian epithelial tumorigenesis.

Presentation	Promotor	Targeted gene	Age of detection (months)	Frequency (%)	References
Poorly differentiated carcinoma with serous elements	MISIIR	SV40 TAg	1.5-3	50	Connolly *et al.* (2003)
Poorly or undifferentiated, carcinoma, some serous tumors	AdCre	*p53*$^{-/-}$ & *Rb*$^{-/-}$	3.5-10.5	97	Flesken-Nikitin *et al.* (2003)
Endometroid ovarian cancer	AdCre	*Kras* ^{G12D} & *Pten* $^{-/-}$	2-6.5	100	Dinulescu *et al.* (2005)
Endometroid ovarian cancer	AdCre	*Apc*$^{-/-}$ & *Pten* $^{-/-}$	1.5-5	100	Wu *et al.* (2007)
Adenoma	FSHR	*Cre, Brca1 -/-*	-	-	Chondankar *et al.* (2005)
Hyperplasia	AdCre	*Brca1* $^{\Delta 5-13}$	2-8.5	-	Clark-Knowles *et al.* (2007)
No tumorigenesis	MISIIR	*Pttg*	-	-	El-Naggar *et al.* (2007)
Hyperplasia	MISIIR	*PI3KCA*	-	-	Liang *et al.* (2009)

Improved mouse models for the development of epithelial ovarian cancer are based on the Cre-loxP recombination system **(Figure 7)**. A significant advantage of this system is the independence from an ovarian surface epithelium specific promotor. The Cre-recombinase is used for the excision of parts of the DNA flanked by loxP sites. This can lead to activation of "lox-stop" oncogenes or the inactivation of floxed tumor suppressors. For the induction of ovarian cancer in transgenic mice an adenoviral vector expressing Cre-recombinase (AdCre) has been injected under the ovarian bursal membrane. In the first study applying this system for the generation of ovarian cancer, mice with LoxP sites containing TP53 and Rb alleles were used to assess gene inactivation of two major tumor sppressors genes [151,152]. Upon intrabursal delivery of AdCre, mice in which both the *p53* and *Rb* genes had been inactivated developed epithelial ovarian tumors at a mean time of 7.5 months after virus application. Tumours were histopathological classified as either well-differentiated serous neoplasms or poorly differentiated epithelial tumors. This model faithfully recapitulates the development of epithelial ovarian cancer in terms of the pathology of the tumor as well as the appearance of ascites and metastatic disease in liver and lungs of mice.

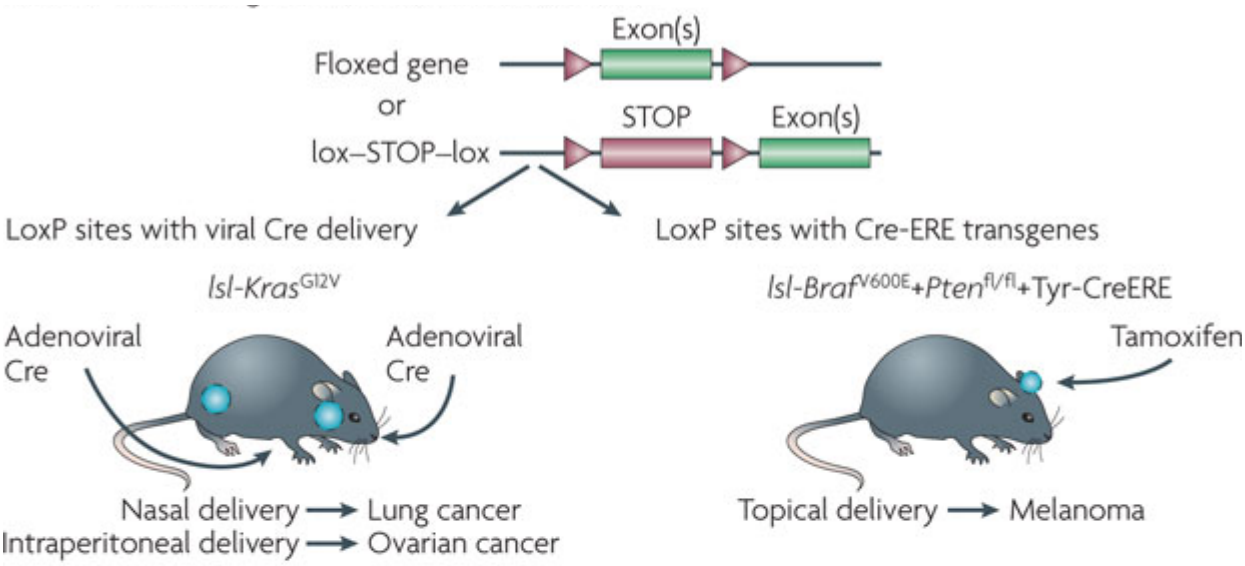

Figure 7 – Conditional genetically engineered mouse models. Activation of Cre in a tissue-specific manner is achieved by either adenoviral delivery (AdCre) or Cre-estrogen response element (ERE)-mediated tamoxifen administration. Examples are shown for lung cancer [153] and ovarian cancer [154], and melanoma [155] (Figure adapted from Heyer *et al.* [156]).

Primary xenograft models

The transplantation of primary patient tumor specimen at heterotopic or orthotopic sites of immunodeficient mice represents another strategy for the generation of suitable tumor models. In this context, great efforts have been made to establish proper mouse models for xenotransplantation, especially for human cells. First studies were based on nude mice, which are defective in the thymus and thus have a T-cell deficiency [157]. Since this time many attempts have been made to develop modified severe combined immunodeficiency (SCID) mice by genetic crossings with inbred or other mutant strains of mice to obtain an even more efficient model [158-161]. Finally, the establishment of nonobese diabetic mice with severe combined immunodeficiency (NOD/SCID) by Greiner *et al.* could improve the model and show that these mice are superior recipients for human cells [162]. These mice are characterized by an immunological multidysfunction, including reductions in macrophage function, complement-dependent hemolytic activity, and NK cell activity [163]. The NOD/SCID mouse model also has been considered as an appropriate model of human stem cell development and function [164]. However, residual NK cell activity in these mice still might interfere with engraftment efficiency [165,166]. A genetic variant of NOD/SCID mice, lacking functional NK cells (NOD/SCID Il 2rg$^{-/-}$), allowed a further increase of the transplantation efficiency up to the successful engraftment of single tumor cells [164].

Advantages of human primary xenograft models are the preservation of heterogeneity of the original tumor in the xenograft, recapitulation of interactions between tumor and microenvironment and most important the faithful recapitulation of disease progression [141]. Primary xenografts mimic the patient situation better than conventional cell line derived tumors, as they still contain stromal compartments and genetically represent the original patient carcinoma.

However, large scale drug-screening experiments are not feasible and would be far to expensive by using only xenograft models. Furthermore the site of tumor cell implantation is crucial as it also influences the growth of the tumor. Tumors transplanted at subcutaneous sites in general are barely vascularized and contain larger necrotic areas as orthotopic transplanted tumors. The preparation of the patient sample also plays an important role and has a huge influence on engraftment of the primary patient tumor.

Primary tumors are heterogeneous, have a distinct morphology and express a certain

panel of histopathological markers. Therefore studies using xeongraft models have to ensure that each established tumor still faithfully recapitulates the original patient tumor. In summary primary xenograft models accurately mimic the human disease, however the site of implantation as well as the site origin from the patient influence features of the xenograft. In addition, as highly immunodeficient mice are used for xenograft studies, the influence of the immune system on tumor progression is not considered in primary xenograft models.

In vitro cultivation of ovarian cancer cells

Conventional cancer cell lines cultured in fetal calf serum (FCS) have been the standard both for studies on human tumor biology and as a preclinical platform for screening of potential therapeutic agents for decades [167]. The advantages of these cell lines are their easy maintenance in culture by simple media formulations, the possibility to manipulate them and their good engraftment efficiency in initial as well as serial transplantation experiments. However, it has become increasingly clear that many of these repeatedly *in vitro* passaged cancer cell lines not accurately mirror the human disease. Long-term FCS-based *in vitro* cultivation leads to a multitude of genetic aberrations and changes in phenotypic characteristics, which often bear little resemblance to those of the corresponding primary human tumor **(Figure 8)** [167,168]. Selective pressure within these cultures may also lead to selection and outgrowth of sub-clones, decreasing the significance of results obtained from such cell lines. Moreover, morphological features and the expression of histopathological markers often change or get lost in xenografts generated from these cell lines compared to the original patient tumor. The result is a rather undifferentiated mass of tumor cells.

Taken together, studies based on conventional FCS-cultured cell lines contributed several major points to our knowledge about the biology of cancer such as pathways involved in tumor maintenance, tumor progression and metastasis development. However, data generated by use of these models has been interpret carefully and the predictive value of clinical performance for novel therapeutic agents determined in such a preclinical setting is limited [169].

These facts gave rise to the development of more biologically relevant cell culture systems for the exploration of tumor biology and for the screening of new therapeutic agents. Initial primary cell cultures omitting FCS in the media were established in the

field of neuronal stem cells research. There it was clearly shown that serum-based cultivation of neuronal stem cells leads to an irreversible differentiation and an accumulation of *de novo* alterations **(Figure 8)**. A major step was thus the development of *in vitro* cultivation models based on FCS-free media formulations, which allowed the growth of an undifferentiated multipotent population of NSCs [170,171]. This cultivation method was then applied to several experimental systems such as stem cell enrichment assays [172], comparative gene expression profiling [173], and *in vitro* models for the development of the nervous system. Also normal stem cells from different organs such as mammary progenitor/stem [174] cells as well as malignant stem like cells from glioblastoma [175] and colon [137] could be cultured using this methodology. However, these studies were based on growth of cells as spheroids, which has several limitations as also progenitor cells proliferate in suspension culture, true clonal analysis is impeded by sphere aggregation, and treatment for the identification of novel therapeutic agents is almost impossible. Very problematic in the sphere environment is the spontaneous differentiation and cell death of cultured cells [176]. An argument against the cultivation of cells as spheres is also the fact that epithelial cells *in vivo* need adhesion to avoid anoikis. More recent studies introduced an improved cultivation in a more physiological setting on adherent substrates [176,177] and showed an enrichment of tumor initiating cells *in vivo* [178]. Adherent cultures of primary cells maintain the stability of the genotype and features of the original tumor *in vivo* to the same extent like spheroid cultures [176]. In addition, adherent cultures provide a uniform access to growth factors for all cells, thereby limiting spontaneous differentiation and cell death and allow an easy manipulation or treatment of cells. In summary, the cultivation of primary cells in the absence of FCS represents advancement in the development of *in vitro* model systems and provides a closer match to the clinical situation. Therefore it is expected that findings made by the use of these improved systems can be more easily translated to the clinical situation.

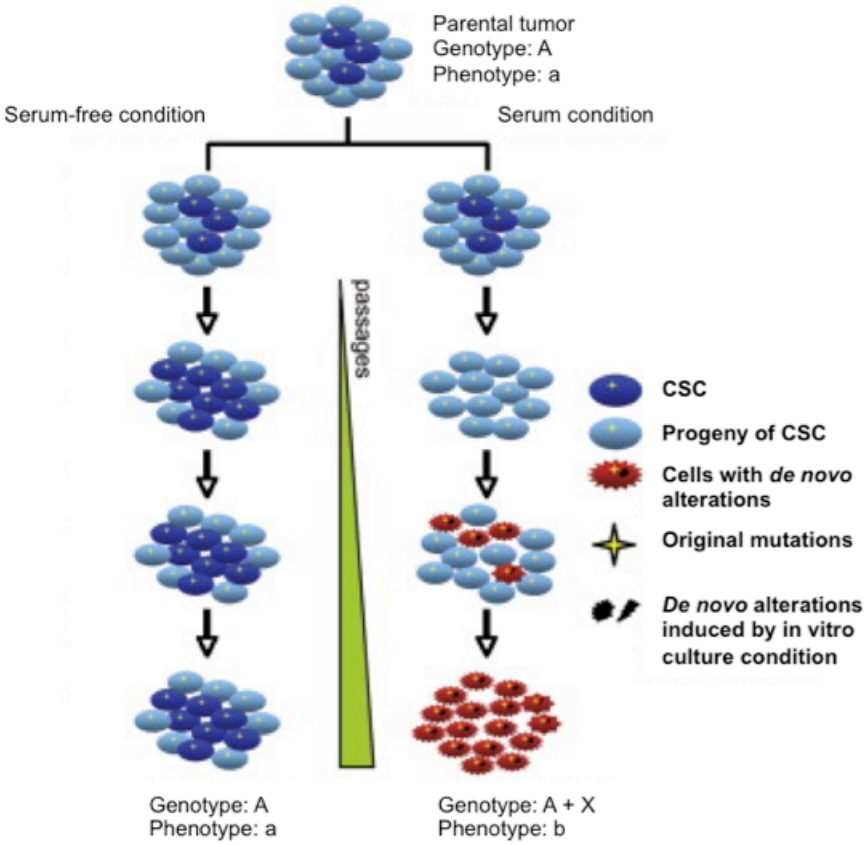

Figure 8 – A hypothetical model depicting the relationship between primary patient tumors, primary CSC culture and conventional FSC-based culture. The heterogeneous nature of the original primary tumor is quickly lost through differentiation in media with serum. Continuous culturing of cells in serum conditions result in outgrowth of subpopulations of cells exhibiting additional genetic and/or epigenetic changes (Figure modified from Lee *et al.* [167]).

Aim of the study

Ovarian cancer is one of the leading causes of cancer-related deaths among women worldwide with only minor improvements in cure in the last decades. This is mainly attributed to the lack model systems faithfully recapitulating this remarkably heterogeneous disease. Therefore, novel models are required in order to study tumor initiating cells, metastasis development and drug resistance in serous ovarian cancer.

The aim of this study was the establishment and evaluation of an advanced personalized model system for serous ovarian cancer that fully recapitulates the human disease. Based on this model, processes involved in metastasis development, drug resistance as well as the identification of tumor initiating cells should be dissected.
We conclusively prove that our model system displays all hallmarks of SOC and further preserves the heterogeneous nature of the original patient tumor. As a first application of our model we wanted to identify functionally different subpopulations within the tumor bulk showing properties of tumor initiating cells. This subpopulation should be further characterized in terms of molecular mechanisms promoting the TIC phenotype.

4 Materials and Methods

Materials

Mouse strains

NOD.Cg-*Prkdc*^{scid} *Il2rg*^{tm1Wjl} (NSG) mice were obtained from Jackson Laboratory (Bar Harbor, USA) and bred in the DKFZ animal facility. All mice were housed under specific pathogen-free conditions and used for experiments at 10-15 weeks of age. All animal care and procedures followed German legal regulations and were previously approved by the governmental review board of the state of Baden-Wuerttemberg, Germany.

Cell lines

Name	Origin	Media
SKOV-3	ATCC (HTB-77)	McCoy´s 5a + 10% FCS
OVCAR-3	ATCC (HTB-161)	RPMI-1640 + 20% FCS

Cell culture products

Product	Company	Catalog No.
15 ml canonical falcon tubes	TPP	Z707724
40 µM cell strainer	BD	352340
5 ml round-bottom polypropylene tubes	BD	352008
5 ml round-bottom polypropylene tubes	Sarstedt	55.526
50 ml canonical falcon tubes	Greiner	T2318
50ml reagent reservoir, sterile	Corning	4870
70 µM cell strainer	BD	352350
ART XLP 1000, 200, 10 µl Reach filter tips	VWR	732-2215, 732-

		2233, 732-2221
Cryotube, 1.8 ml sterile	Nunc	375418
Nalgene Freezing Container Mr.Frosty	Bunc	5100-0001
Primaria Cell Culture Flask, 25 cm^2	BD	353808
Primaria Cell Culture Flask, 75 cm^2	BD	353810
Primaria Cell Culture Plate, 24-well	BD	353847
Primaria Cell Culture Plate, 6-well	BD	353846
Primaria Cell Culture Plate, 96-well	BD	353872
Safe lock tubes: 0.5, 1.5, 2.0 ml	Eppendorf	13625, 12682, 12776
Serological Pipettes: 2, 5, 10, 25 and 50 ml sterile	BD	3565-07/-29/-30/-35/-50

Cell culture media

Product	Company	Catalog No.
Advanced DMEM medium	Life Technologies	12491015
Basic-FGF	Peprotech	100-18B
ß-Estradiol	Sigma	E2758
Bovine Serum Albumine	PAA	K35-011
Chorionic Gonadotropin	Sigma	C1063
CO2-independent medium	Life Technologies	18045088
Collagen	Life Technologies	A1048301
Cryostor CS10	Sigma	C2874
D-PBS	Sigma	P5368
EGF	Peprotech	100-15
FCS Gold	PAA	A11-151
Fetal Calf Serum, Origin: EU approved	Life Technologies	10270
Fungizone (Amphotericin B)	Life Technologies	15290-018
Gentamycine (50mg/ml)	Life Technologies	15750-060

Glucose 45% solution, sterile	Sigma	D8769
Growth factor reduced Matrigel	BD	354230
Heparine	Sigma	H-3149-10KU
HEPES	Life Technologies	15630106
Heregulin beta -1	Peprotech	100-03
IGF-R3	Sigma	I1271
IMDM	Life Technologies	12440061
L-Glutamine 200mM (100x)	Life Technologies	25030
L-Glutathione	Sigma	G6013
Lipid-Mixture	Sigma	L0288-100ML
Menopausal Gonadotropin	Sigma	G5270
N-2 supplement	Life Technologies	17502048
Penicillin/Streptomycin	Sigma	P4333
Trace Elements A, B, C	VWR	99-182-Cl, 99-175-Cl, 99-176-Cl
Water for Injection (WFI) for Cell Culture	Life Technologies	A12873-01
Y-27632	Selleck	S1049
β-Mercaptoethanol	Life Technologies	31350010

Kits

Product	Company	Catalog No.
BCA Protein Assay Kit	Pierce	23227
miRNeasy Mini kit	Qiagen	217004

Antibodies

FACS

Antigen	Clone	Company	Catalog No.
CD133 – PE	AC133	Miltenyi	130-080-801
CD44 – PB	IM7	Biolegend	103020
CD24 – APC	ML5	Biolegend	311118
CD151 - PE	14A2.H1	BD	556056
CD117-APC	YB5.B8	BD	550412
EpCAM – FITC	EBA-1	BD	347197
H2-kD – AlexaFluor647	SF1-1.1	Biolegend	116612

Isotype controls	Clone	Company	Catalog No.
AlexaFluor647 Mouse IgG2a	MOPC-173	Biolegend	400234
APC Mouse IgG1	MOPC-21	BD	550854
APC Mouse IgG2a	MOPC-173	Biolegend	400246
FITC Mouse IgG1	MOPC-21	Biolegend	400108
PB Mouse IgG2a	MOPC-173	Biolegend	400260
PE Mouse IgG1	MOPC-21	Biolegend	400114
PE Mouse IgG1	MOPC-21	BD	556650

Western Blot

Antigen	Company	Catalog No.
ATF-2 Thr71	Cell Signaling	9912
c-Jun Ser63		
c-Src	Millipore	14-117
Donkey Anti-Rabbit IgG-HRP	Southern Biotech	6445-02
ERK	Cell Signaling	4695

ERK1/2 Tyr202/204	Cell Signaling	4730
Goat Anti-Mouse IgG(H+L), Human ads-HRP	Southern Biotech	1031-05
SAPK/JNK Thr183/Tyr185	Cell Signaling	9912
SEK1/MKK4 Ser257	Cell Signaling	9912
Src Tyr419	Cell Signaling	2101
Vinculin	Cell Signaling	4650

Immunohistology

Antigen	Company	Catalog No.
CA125	Dako	M3520
WT1	Dako	M3561
Ki67	Dako	M7240
CD151	Sigma	HPA011960
Venus	Abcam	Ab290

Chemical and biological reagents

Product	Company	Catalog No.
Accutase	Life Technologies	A11105
ACK Lysis Buffer	Lonza	10-548E
CellTiterBlue	Promega	G8081
Ethylenediaminetetraacetic acid (EDTA)	Sigma	E9884
FiColl Paque Plus	GE	17-1440-02
Halt™ Protease/Phosphatase Inhibitor Cocktail	Pierce	78440
Isofluran B	Braun	6724123.00.00
Matrigel	BD	356234
NuPAGE® Antioxidant	Life Technologies	NP0005
NuPAGE® LDS Sample Buffer	Life Technologies	NP0007

NuPAGE® MOPS SDS Running Buffer	Life Technologies	NP0001
NuPAGE® Sample Reducing Agent	Life Technologies	NP0004
Phenylmethanesulfonyl fluoride (PMSF)	Sigma	P7626
Propidium Iodide	Biolegend	421301
Western Blot Stripping Buffer	Pierce	21059
DNase	Sigma	D4263
Collagenase IV	Sigma	C5138
RIPA Buffer (10x)	Cell Signaling	9806
MagicMark™ XP Western Protein Standard	Life Technologies	LC5602
Novex® Sharp Pre-stained Protein Standard	Life Technologies	LC5800
Tween 20	Sigma	P5927
Ponceau S solution	Sigma	P7170
Staurosporine	LC Labs	S-9300

Solutions and media formulation

Cancer Stem Cell Medium
500 ml Advanced DMEM/F12
5 ml N2 Supplement
2 mM Glutamine
1.7 ml Glucose (45%)
500 µg GSH (250 ul Stock)
500 µl each Trace Elements B, C
250 µl Trace Elements A
25 ml Sterile H_2O Cell Culture Grade
5mM HEPES for cell culture
2 µg/ml, Heparine
1ml Sigma Lipid Mixture-1
50 ng/ml hBasic-FGF
20 ng/ml hEGF
10 ng/ml IGFR3
100 µM β-Mercaptoethanol
5 µg/ml Insuline
36 ng/ml Hydrocortisone
0,5 ng/ml ß-Estradiol

PEB Buffer
1x PBS
1% BSA
2 mM EDTA

CBP Buffer
500 ml CO_2-independent medium
1% BSA
2 mM Glutamine

10x TBS Buffer (1L)
24.2 g Tris base
80 g NaCl
adjust pH to 7.6

20x Transfer Buffer (100ml)
10.2 g Bicine
13.1 g Bis-Tris

Laboratory equipment

Equipment	Name	Company
Analytical scale	AE163	Mettler Toledo
Caliper	Digital Caliper	Langirele
Centrifuge	5810R	Eppendorf
Flow Cytometer	BD FACS LSR Fortessa	BD
Flow hood	1300 Series A2 Class II	Thermo
Freezer -20°C	G1221	Liebherr
Freezer -80°C	Forma 904	Thermo
Fridge	Premium, Profi Line	Liebherr
Ice Machine	SCE170	Hoshizaki
Incubator	HERAcell 150i / 240i	Thermo
Microplate reader	SpectraMax	Molecular Devices
Microscope	OPMI PENTERO® 900	Zeiss
Multiwell pipet (8-well / 12-well)	Multipette Plus	Eppendorf
pH meter	S20 SevenEasy	Mettler Toledo
Pump	Vacusafe	Integra
Rotator	MACSmix™ Tube Rotator	Miltenyi
Thermomixer	Thermomixer comfort	Eppendorf
Tissue homogenizer	gentleMACS™ Dissociator	Miltenyi
Vortexer	Vortex Genie	VWR
Surgical clamps	Surgical clamp	Fine Science Tools
Suture	Safil	B.Braun

Bioinformatic tools

Tool	Version	URL
Gene Set Enrichment Analysis	3.7	www.broadinstitute.org/gsea
Gene Mania	3.1.2	http://www.genemania.org
Gene Pattern	2.0	http://www.broadinstitute.org/cancer/software/genepattern
GraphPad Prism	5	www.graphpad.com
R	2.15	www.**r**-project.org
TMeV Experiment Viewer	4.8	www.tm4.org/mev

Methods

Xenograft methods

Human Tissue Specimen

All human tissue samples were obtained from the Gynaecological Hospital, University Clinic Mannheim, with written informed consent under protocols approved by the review board of the Medical Faculty of the University of Heidelberg. Serous ovarian cancer tissue was collected from patients undergoing routine therapeutic surgery and was confirmed as serous ovarian carcinoma.

Xenografts of Primary Tumor Specimens and SOC Cell Lines

To establish primary xenografts, tumors enzymatically disaggregated to obtain a single cell suspension and depleted for contaminating $CD45^+$ using anti-CD45 paramagnetic microbeads. At least $1x10^5$ – $1x10^6$ ovarian tumor cells were injected intraperitoneal into NOD.Cg-*Prkdc*^{scid} *Il2rg*^{tm1Wjl} (NSG) mice, bred in the animal facility of the German Cancer Center. For the generation of xenografts from the SOC-cell lines, a suspension of 10^2-10^4 cultured cells diluted in media was prepared and injected intraperitoneal into NSG mice.

Successful engraftment of tumors and subsequent growth was monitored by regular palpation of the implantation site. All animal care and procedures followed German legal regulations and were previously approved by the governmental review board of the state of Baden-Wuerttemberg, Germany.

Dissociation of tumor material

Primary patient specimen and first passage xenografts were first finely cut using sterile scalpels into small pieces <0.1 mm^3 and dissociated into single cells by incubation with 1 µg/ml Collagenase IV for 2h at 37°C fixed on the MACSMix rotator with occasional periods of vortexing. The resulting suspension was filtered through a 40 µm mesh following which cell debris and dead cells were removed by density centrifugation. Remaining erythrocytes were removed using ACK Buffer. Contaminating $CD45^+$ leukocytes could be depleted using anti-CD45 paramagnetic microbeads.

Cryopreservation of single cells derived from xenograft tumors

Single cell suspensions derived from xenografted tumors were cryopreserved as described for the SOC cultures.

Serial transplantation assay

Xenografts derived from SOC cells were processed into single cell suspensions as described. For analysis of serial transplantation efficacy, $1x10^5$ xenograft-derived cells were injected intraperitoneal into secondary respectively tertiary recipient NSG mice.

Determination of *in vivo* repopulation frequency

SOC cells were processed into a single cell suspension and cell number was determined as described below. A group of three female NSG mice were injected intraperitoneal with 10^4, 10^3 or 10^2 SOC cells, respectively. After 100 days follow-up, mice were euthanized by cervical dislocation and evaluated for tumor growth at the injection site. Tumors were fixed in 10% PFA/PBS for subsequent histological analyses. Resulting repopulation frequencies were determined using the ELDA webtool (http://bioinf.wehi.edu.au/software/elda).

***In vivo* bioluminescence imaging using the Xenogen system (IVIS-200 Caliper)**

Mice were injected intraperitoneally with D-Luciferine Firefly Potassium salt (15 mg/ml in PBS) at a dose of 10 µl per gram body weight (Biosynth) 10 minutes before imaging. The animals were anesthetized using 4.5% isoflurane in oxygen (0.9 l/min), maintained at 1.5 % isoflurane in oxygen and analyzed in the heated camera chamber. The Living Image software was used according to the manufacturer's instructions (IVIS 200, Caliper).

Cell culture methods

Coating of tissue culture flasks

For coating of tissue culture flasks, Collagen at 50µg/ml, Matrigel at 50 µg/ml and FCS at 3% were added for to tissue-culture treated flasks for 4h at 37°C. After a wash with PBS, flasks were either directly used or store until further use at 4°C.

Generation of SOC cultures

For establishing SOC culture, single cells (0,5 - 1 x 10^5) derived from xenograft explants were seeded in T25 Primaria flasks in CSC medium supplemented with 50 µg/ml

Gentamycin, 0.5 µg/ml Fungizone and 10 µM Y-27632. Adherent monolayer cultures were maintained and incubated at 37°C and 5% CO_2. After outgrowth of tumor cells, contaminating fibroblasts were removed by trypsinization with Accutase and cells were subsequently propagated in antibiotic/ROCK-inhibitor-free CSC medium.

Splitting of SOC cultures

Medium was removed from culture flasks and 3 ml Accutase per T75 flask was added to remove the cells from the substrate. After 10-15 minutes, cells dislodged from the surface and the single cell suspension was transferred into a falcon tube as a 2:1 dilution in CBP medium. After centrifugation (1200 rpm, 5 min, 4°C), the supernatant was removed and the pellet re-suspended in 1-5 ml of CBP buffer depending on the application.

Freezing of SOC cultures

For cryopreservation of SOC cells, single cell suspensions were pelleted as described above and the resulting pellet was dissolved in Crystor CS10 and subsequently aliqouted into cryovials. The vials were placed on ice for 10 minutes after which they were transferred, placed in a pre-cooled Mr.Frosty, to the -80°C freezer. Approximately 5 hours later, the cells were placed in the liquid nitrogen tank for long-term storage.

Determination of cell number

An aliquot of cell suspension was diluted 1:10 – 1:50, depending on the expected number of cells, with trypan blue solution (0.05% w/v) to quantify the amount of viable cells. Cells were counted with a Neubauer chamber, whereas the number of viable cells was calculated according the formula:

Average cell number/chamber square x dilution factor x 10^4

Proliferation assay

SOC cells were seeded into 96-well plates at 1000 cells/well on Day 0. Cell number was determined as a measure of cell viability using the CellTiterBlue assay as described in the manual. In order to establish a baseline, the first row was evaluated 4h post cell plating, setting the derived emission values in relation to the plated cell number. Each day, subsequent rows were evaluated accordingly, thereby normalizing the derived emission values to the baseline derived from Day 0. Therefore, cell growth was expressed as a function with respect to the initial number of cells.

Determination of *in vitro* repopulation frequency

SOC cells were plated in 96-well plates in a limiting dilution assay, starting from 5000 cells per well in Row 1, diluted 2-fold in the subsequent rows. Plates were wrapped in saran wrap and incubated for 72h in a humidified environment. After this incubation period, each well was evaluated for clonal outgrowth. A well was scored positive if it contained a substantial cell clone, mostly comprised of more than 10 cells. If no or only small clusters of cells (<10 cells/clone) were present, the well was scored negative. Resulting repopulation frequencies were determined using the ELDA webtool (http://bioinf.wehi.edu.au/software/elda).

Flow cytometric analysis of SOC cells and xenograft-derived cells

For staining of cell surface antigens, $1x10^6$ single cells were placed in PEB Buffer. In case of primary tumor cells and xenograft-derived tumor cells, Fc receptors were blocked by incubation at 4°C for 15 min with 50 µg/ml Intratect human IgG fraction.

For surface staining, antibodies were added in appropriate dilutions and incubated in the fridge for at least 20 minutes. Following this incubation, cells were washed with PEB buffer and filtered through a mesh prior to FACS analysis. Staining of equal amounts of cells were prepared with corresponding isotypes for each antibody. Just prior to analysis, 1 µg/ml Propidium Iodide was added for death cell exclusion.

Samples were acquired on a FACS LSR Fortessa cytometer and data was analysed with FlowJo analysis software.

Transduction of primary serous ovarian cancer cell lines

SOC cells were dissociated using Accutase and single cell suspensions were seeded in T24 Primaria flasks. Polyprene (10µg/ml) was added to the medium prior to transduction. After successful transduction of the serous ovarian cancer cells, the cells were sorted for the respective reporter such as Venus or GFP.

Gene expression analyses

RNA isolation

Total RNA was isolated from different SOC lines (80% confluent) or tumor tissue (30 mg) using the miRNeasy kit according the provided manual. SOC cells were directly lysed in the supplemented QIAZol Buffer, tumor tissue was submerged in the same

buffer, using the GentleMACS Dissociator according the manufacturer's instruction. RNA quantity was determined using the NanoDrop, quality and integrity of the RNA samples were assessed on the Agilent Bioanalyzer, using a NanoChip. Only samples with a RNA Intergrity Number (RIN) greater than 8 were subjected to expression analysis.

Microarray analysis and data processing

Hybridization and data normalization was performed by the Genomics core facility of the German Cancer Research Center

Gene expression analysis was performed using the Illumina BeadChip Technology (HumanHT-12v4). cDNA and cRNA synthesis , hybridization and scanning was performed according to the manufacturer's instruction. Signal-to-noise ratio was very high across all chips analyzed with minimal background interference in all experiments. Raw data from the microarray analysis was background subtracted and median-normalized using the Illumina BeadStudio software workbench.

Data and gene-set-enrichment analysis

For analysis of differential gene expression and clustering we employed the TM4 Microarray Software Suite. Significant Analysis of Microarray (SAM) was used to identify differentially regulated genes between subtypes selected at a FDR < 0.05 and with a fold change of > 2. Correlation plots and respective Pearson coefficients (R^2) between samples were generated using 'R'. Gene set enrichment analysis on normalized data was conducted as described previously [179] using the complete MSig database on the Broad Institute server. Gene sets were considered significantly enriched with an FDR < 0.2.

Immunohistology methods

Immunohistology and initial evaluation of staining and tissue morphology were performed by the department of Pathology, University Clinic Heidelberg

Immunohistology

Tumor specimens were fixed in 10% PFA overnight and embedded in paraffin. For immunohistochemistry, slides were de-paraffinized and rehydrated. Antigens were retrieved by boiling in in a steam pot at pH 6 (Dako target retrieval solution, Dako, Glostrup) for 15 min, allowed to cool for 30 min and washed in distilled water. Nonspecific binding was blocked using the Linaris Avidin/Biotin blocking Kit (Vector Labs, Burlingame) according to the manufacturers instructions. Slides were incubated

with primary antibodies for 30 min, rinsed in PBS-T (PBS with 0.5% Tween-20), incubated for 20 min with the appropriate secondary antibody using the Dako REAL Detection System and rinsed in PBS-T. After blocking of endogenous peroxidase and incubation with Streptavidin HRP (20 min at RT), slides were developed with AEC and counterstained with Hematoxylin.

Primary antibodies were used at the following dilutions CA125 1:25, WT1 1:100, Ki67 1:200, CD151 1:50 and Venus 1:500. All antibodies were diluted in Dako antibody diluent and two pathologists scored all sections independently.

Western Blot methods

Cell lysis

SOC cells were seeded into T75 flasks and grown till 80-90% confluence. After three washing steps with ice-cold PBS, remaining PBS was drained and 400 µl of 1x RIPA Buffer supplemented with 1x HALT Proteinase/Phosphatase Cocktail, 1mM EDTA and 1mM PMSF was evenly dispersed onto the cells. Flasks were incubated for 5 minutes on ice with occasional rocking of the flask. After the incubation, the cells were scraped with sterile spatulas and the resulting homogenate was transferred into a pre-cooled Eppendorf tube. The lysate was vortexed at full speed for one minute and transferred into a pre-cooled centrifuge (15 min, 20.000 rpm). The resulting supernatant was transferred into a new Eppendorf tube and separated in 20 µl aliquots. Protein content was determined with a BCA Protein Assay as described in the manufacturer's protocol.

Immunoblotting

Samples were prepared for western blotting prior to loading the gel. 20 µg per sample were mixed with 1x SDS Buffer and 1x reducing agent and heated to 70°C for 10 minutes. After that, the sample was loaded onto a NuPage 4-12% Bis/Tris Gel. A mixture of 2 µl MagicMarkXP and 10 µl Per-Stained Marker was loaded in the first well of each gel and served as marker for determining molecular weight of the detected proteins. Gels were run in 1x MOPS Buffer as described by the manufacturer for 1 h at 120 V/250 mA. Blotting of proteins to nitrocellulose membranes was performed as depicted in the NuPage manual as a wet-blot setup for 2 h at 25V/300mA using transfer buffer as described above. A brief Ponceau S staining prior to blocking of the membrane verified successful transfer of proteins to the membrane.

Membranes were blocked by incubating for 2h at room temperature on an orbital shaker with TBS + 0.1% Tween (TBS/T) + 5% milk. After that the blot was washed 5-times 5 minutes with TBS/T. Primary antibodies were diluted as indicated in the datasheet in TBS/T + 5% milk, in case of phospho-antibodies, 5% BSA was used instead, and incubated at 4°C over night. After another wash (5-times 5 minutes with TBS/T), isotype-matched secondary antibodies were incubated at 1:10000 dilution in TBS/T + 5% milk for 1h at room temperature. After a final wash (5-times 5 minutes with TBS/T), blots were developed using ECL development reagent. An initial 10-second exposure was used to determine the proper exposure time.

Re-probing of blots

Blots were stripped using 10 ml of Stripping Buffer as indicated in the manual. After a brief wash with TBS/T, the membrane was blocked with TBS/T with 5 % milk and re-probed with the desired primary antibody as described above. Blots were generally re-probed only three times until they were discarded.

5 Results

An improved model system for human Serous ovarian carcinoma

Establishment of a primary xenograft model for Serous ovarian carcinoma

Long-term serum cultured cell lines often fail to recapitulate the heterogeneity and characteristics of the original patient disease [137,167,180]. Therefore, we wanted to establish an improved *in vitro* culture model, able to faithfully reflect the unique features of each patient´s tumor. For this purpose, we evaluated the direct culture of cells isolated from primary tumor tissue specimens as well as serous effusions from the peritoneal- or pleural cavity. However, only the cultivation of cells from serous effusions resulted in the efficient outgrowth of tumor cells in culture (data not shown). In order to expand the tumor material for further studies, we decided to establish a murine xenograft model in parallel **(Figure 9A)**. To achieve a preferably high engraftment rate, we chose the NOD.Cg-*Prkdc*^{scid} *Il2rg*^{tm1Wjl} (NSG) mouse model, which has been described to be more permissive to xenotransplants compared to NOD/SCID mice [181,182]. For every clinical specimen, we injected at least three of these immunodeficient mice with $1x10^5$ – $1x10^6$ ovarian tumor cells into the peritoneal cavity, respectively. Contaminating human $CD45^+$ cells could be depleted using anti-CD45 paramagnetic microbeads before injection.

In cooperation with Gynaecological Hospital, University Clinic Mannheim, we received from March 2011 to May 2013 in total 15 primary ovarian tumor samples and 9 serous effusions in total. Out of these 23 (96%) were histologically verified as serous ovarian adenocarcinoma, one was classified as a mucinous ovarian carcinoma **(Appendix, Table 1)**. From a total number of 23 transplanted primary tumors we were able to establish 15 (65%) xenograft models. The established primary serous ovarian carcinoma (SOC) xenografts recapitulated many characteristics of the human disease such as the development of ascites and tumor growth at the ovaries and the abdomen **(Figure 9B)**. All xenografted tumors were stained for the expression of serous ovarian

adenocarcinoma specific markers and histologically classified as serous ovarian adenocarcinoma **(Appendix, Table 1)**.

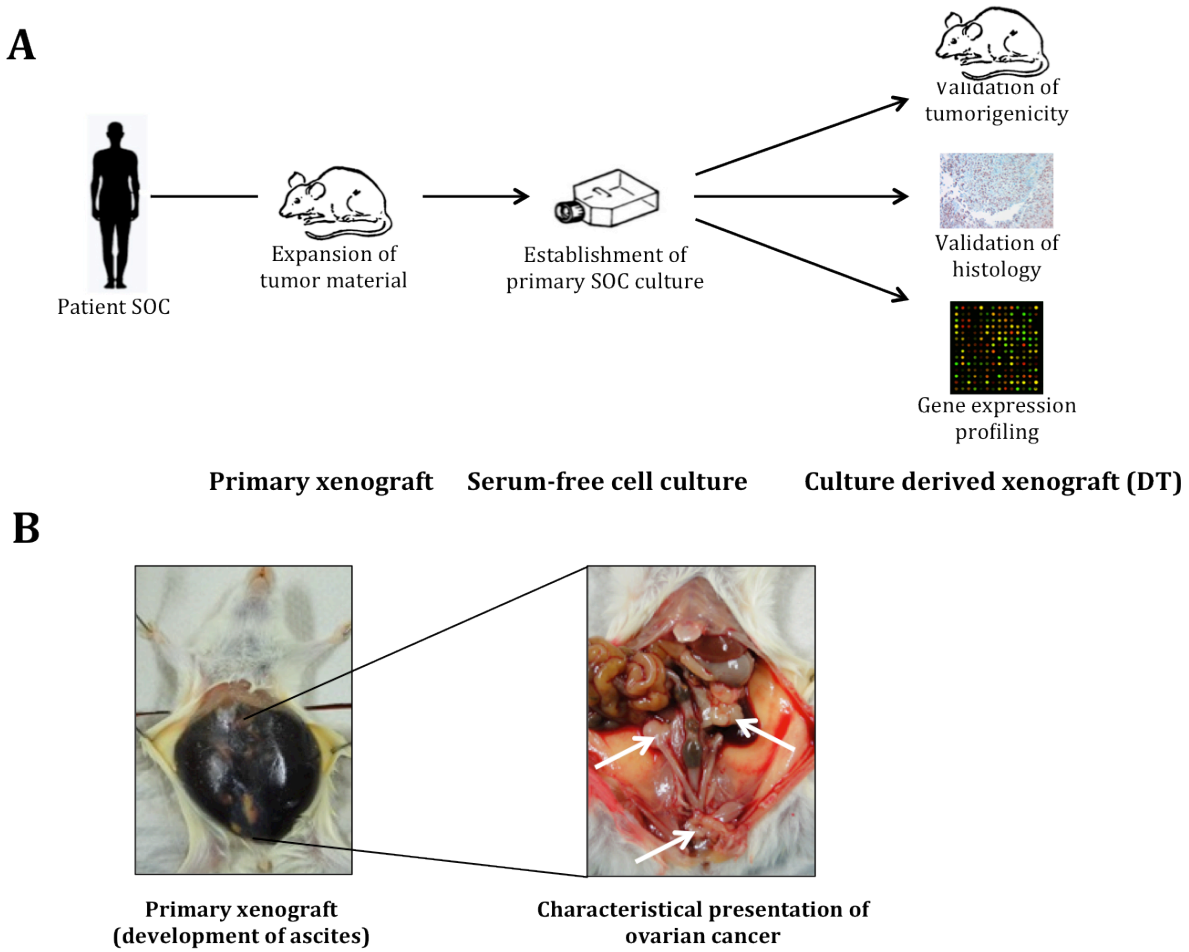

Figure 9 – (A) Schematic overview of the experimental workflow for the generation of xenograft and primary ovarian cancer cell lines. (B) Primary xenograft models established by injection of primary human specimen into the peritoneal cavity faithfully mimic the human disease with development of ascites (left), tumor growth at ovary and abdomen as well as distant sites (right, white arrows).

As soon as any palpable tumor or any ascites development could be detected, tumors were surgically removed and further processed. In general, the volume of excised tumors ranged between 1 – 1,5 cm^3 and the median latency of xenograft tumor growth was 114 (+/-49) days. We detected tumor growth at the ovaries and into the abdomen of xenograft mice. Metastatic deposits could be detected at the abdominal wall, the liver and the diaphragm **(Figure 9B)**. All xenografts were serially transplantable in mice.

The comparison of xenografted tumors with the appropriate primary patient tumor revealed that morphological features and the expression of specific histopathological markers for SOC were well conserved. Importantly, all the xenografted tumors obtained

from patient samples showed strong positive stainings for both of the two clinically used markers for the diagnosis of SOC, CA125 and WT1 **(Figure 10)**. We also observed the appearance of stromal compartments especially in the first *in vivo* passage of the xenografts. However, compared to the original patient tumor we found relative an enrichment in tumor cell content versus stroma content in our xenografted models.

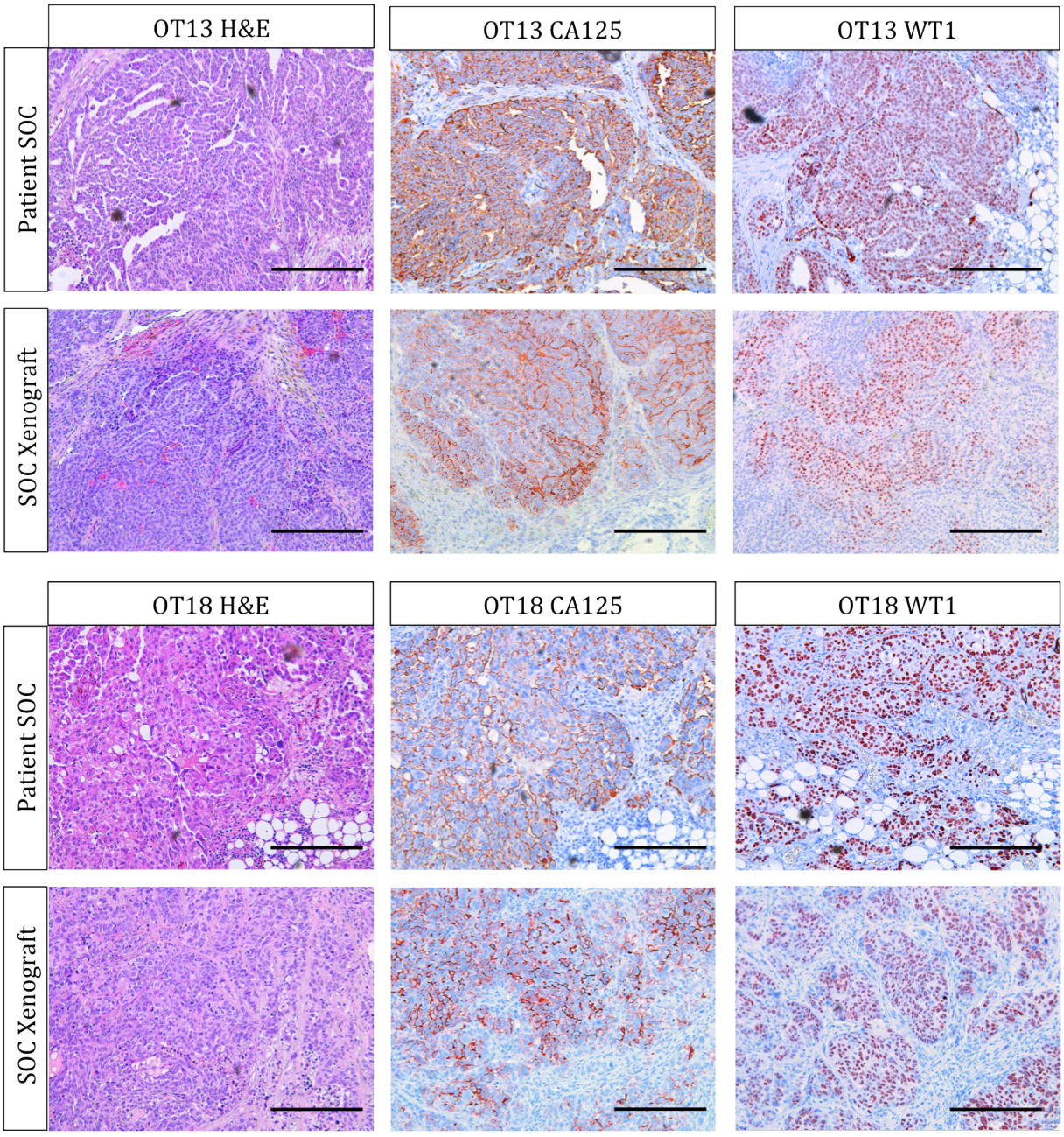

Figure 10 – Representative immunhistochemical stainings of two patient tumors (first row) and their corresponding primary xenografts (second row) for Hematoxylin & Eosin (H&E), CA125 and WT1. Note that all xenograft tumors retained the characteristic morphological features and expression of SOC specific markers of the corresponding primary tumor (scale bar 100 µm).

Establishment of a primary *in vitro* culture system for Serous ovarian carcinoma

Despite many advantages of primary xenograft models, an *in vitro* model is crucial for the manipulation of cells and a more detailed study of cellular mechanisms. Therefore, we tried to set up low passage primary cell cultures out of our successful established primary xenografts. Freshly excised xenograft tumors as well as ascites were enzymatically disaggregated to obtain a single cell suspension. Single cells were subsequently plated at a density of 0,5 - 1 x 10^5 cells per 25 cm^2 flask and cultured in a serum-free media formulation [180] **(Figure 9A)**. In order to define culture conditions, able to lead to a maximum outgrowth of epithelial ovarian cancer cells, we tested different combinations of various growth factors and substrates additionally to the basic stem cell media (SCM) **(Figure 11)**.

Already between 7 to 14 days, we observed growth of a mixed culture consisting of epithelial cell clusters as well as fibroblast-like cells. These mixed populations of cells showed adherent growth on every substrate verified. However, the amount of proliferating cells varied between different settings. We observed that most of the cells attached to Primaria and FCS-coated flasks, whereas cells seeded on Collagen-coated flasks displayed less attachment **(Figure 11A)**. Taken together, these experiments revealed that a larger fraction of cells, including fibroblast-like cells, was able to grow on FCS-coated flasks, indicating that this substrate supports adhesion in general. Furthermore, we analysed the cultivation of primary human ovarian cancer cells in spheroids as this approach has been described in several studies for the successful establishment of primary cultures for ovarian cancer [182,183].

A comparison of the two above mentioned procedures, cultivation as spheroids on ultra-low attachment flasks with the adherent culture on Primaria flasks, revealed that the adherent culture setting promoted a significantly faster growth of cells and a lower amount of dead cells **(Figure 11A**, data not shown). This might be due to the fact that in adherent cultures every cell has an optimal supply of nutrients and growth factors, whereas in sphere cultures only the cells on the sphere surface do so as well. In FCS- and Collagen- coated flasks we noted a higher proportion of fibroblast-like cells attached to the substrate. Especially coating with FCS promoted outgrowth of these type of cells **(Figure 11A)**. While in Primaria flasks, fibroblast-like cells could be removed by sequential treatment with accutase, these cells were able to endure in FCS-coated flasks.

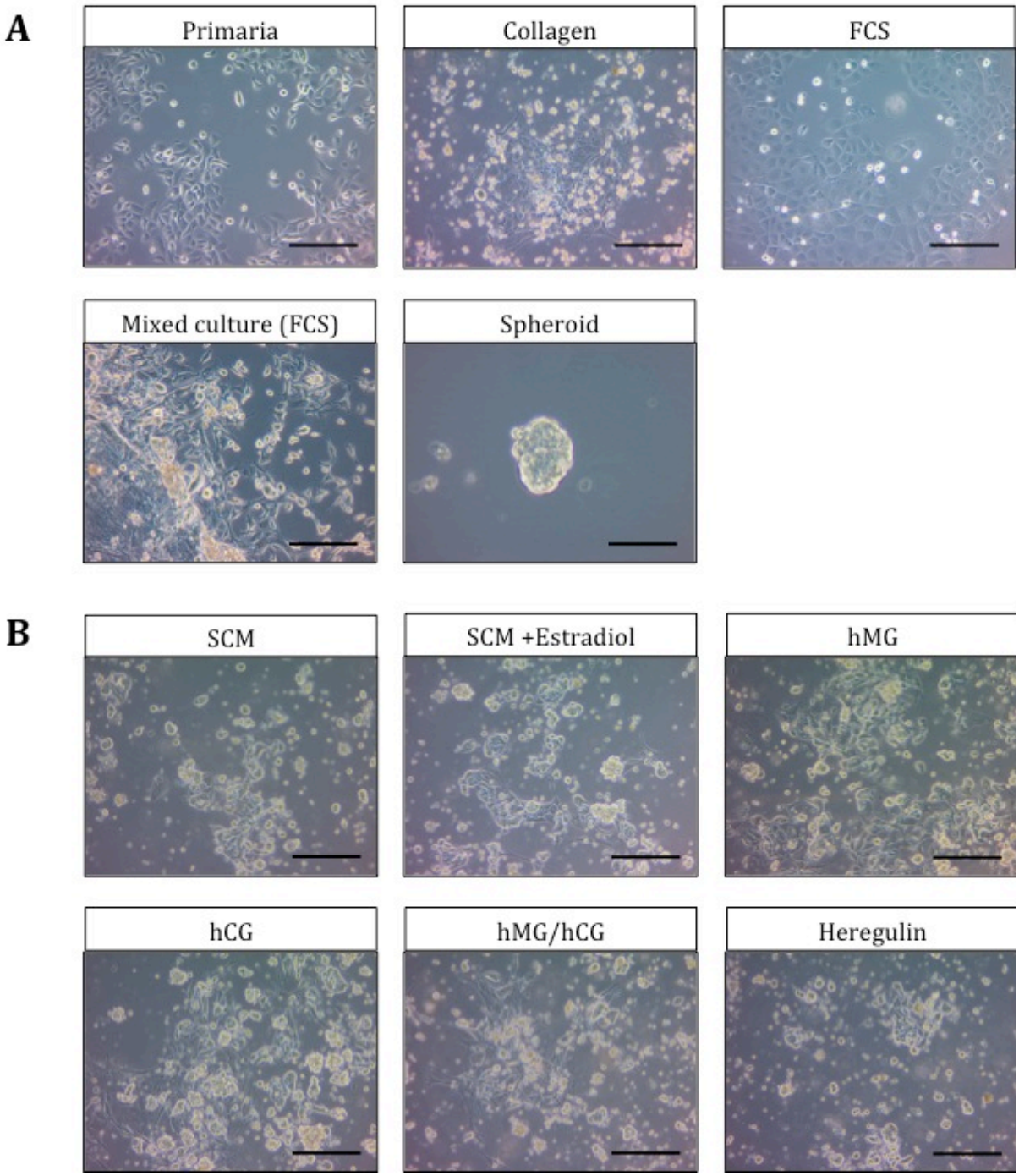

Figure 11 – (A) Exemplary images of cells derived from a primary SOC xenograft (OT12) cultured on different substrates. (B) Exemplary images of cells derived from a primary SOC xenograft (OT13) cultured with several combinations of hormones and growth factors in addition to the basic stem cell media (scale bar 100 µm)

To determine the optimal conditions for the growth and expansion of primary ovarian cancer cells, we tested several hormones and growth factors additionally to the factors bFGF, EGF and IGFR3, which are included in the basic stem cell media. According to previous reports about the cultivation of primary ovarian cells and their dependency on hormones [184] and growth factors [185], we focused on female sex hormones such as human

menopausal gonadotropin, human chorionic gonadotropin and estradiol. They were described to stimulate proliferation of human primary ovarian tumor cells. We also included the growth factor heregulin, which was reported to be effective in stimulating the outgrowth of ovarian tumor cells [183].

However, we observed only in combination with estradiol a significant increase in the number of outgrowing cells. In parallel, we noted in the plates treated with hMG, hCG and hMG/hCG a higher number of differentiated cells, indicating that these hormones drive differentiation of primary ovarian cancer cells **(Figure 11B)**. The results of experiments for the definition of the optimal growth conditions for primary ovarian cancer cells are summarized in **Table 3**.

Table 3 – Summary and results of the different combinations of substrates and growth factors tested to establish a primary culture of ovarian cancer cells

Substrate	Basic SCM	+Estradiol	+menopausal Gonadotropin (hMG)	+chorionic Gonadotropin (hCG)	+hMG/hCG	+He-regulin
Primaria	++	+++	++	++	++	++
Ultra-low attachment	+	++	+	+	+	+
3% FCS	++F	++F	++F	++F	++F	++F
10µg/ml Collagen	+F	+F	+F	+F	+F	+F

+++ High amount of growing epithelial tumor cells
++ Medium amount of growing epithelial tumor cells
+ Low amount of growing epithelial tumor cells
F Significant outgrowth of fibroblast-like cells

According to these results, we supplemented the basic SCM with estradiol and used Primaria flasks for the establishment of primary human SOC cultures in all subsequent studies. By utilizing these conditions, we were able to establish 8 stable cell lines out of 15 primary SOC xenografts.

Interestingly, when we compared the different SOC cell lines, we observed a broad heterogeneity in morphological features. Moreover, the individual SOC cell lines also showed discrepancies in growth behaviour. The cell lines OC18, OC19, OC20 and OC21 grew in clusters of cells and showed an epithelial cell like growth **(Figure 12)**. These cell lines displayed a quite differentiated morphology. The remaining group of cell lines (OC12, OC14 and OC15) reflected the rather undifferentiated histology of their primary tumors. In these lines we observed a loss of epithelial characteristics and a spindle-shaped morphology **(Figure 12)**.

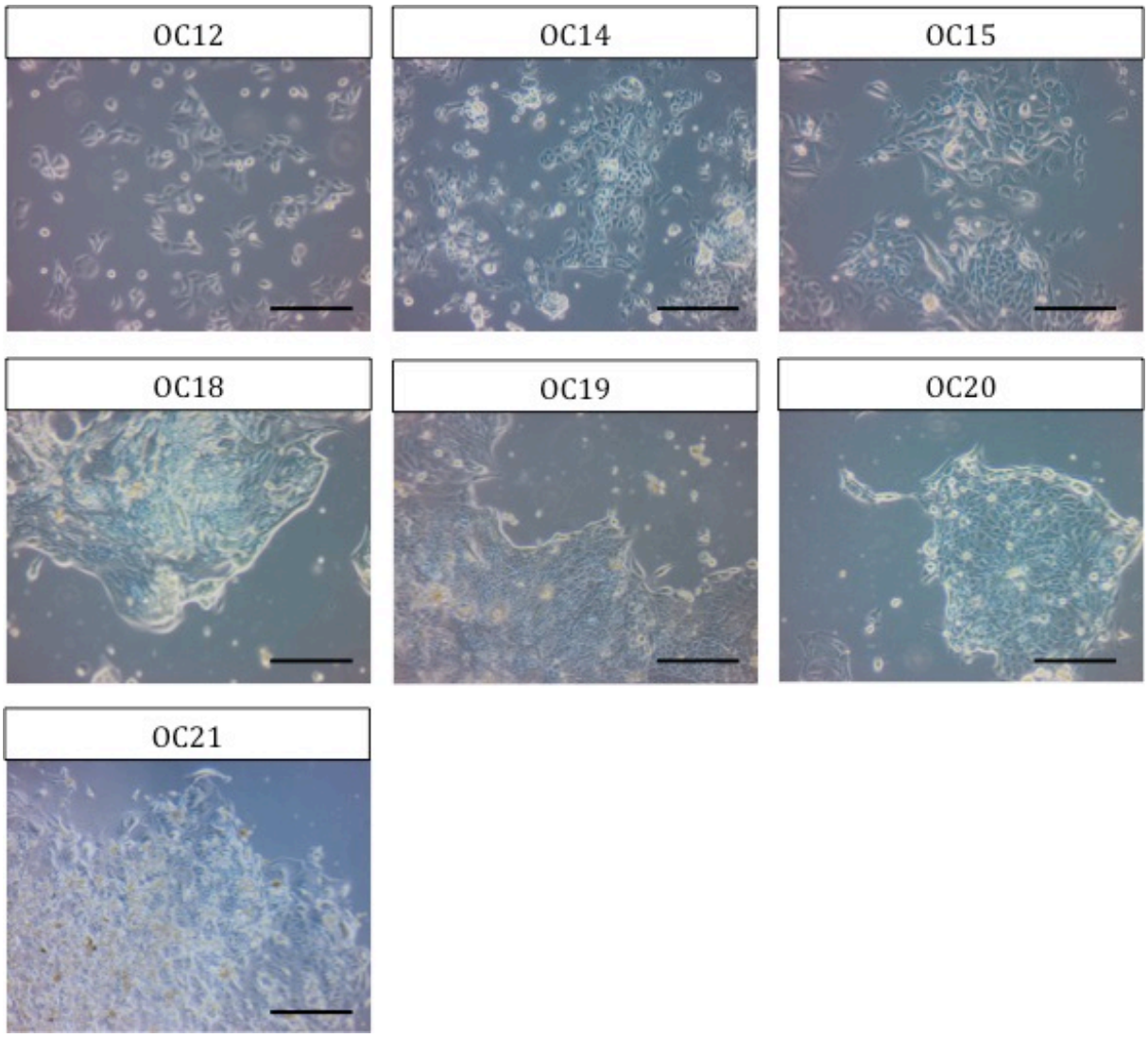

Figure 12 – Representative images of different primary SOC cell lines established in this study (scale bar 100 µm).

A more precise analysis of the growth behaviour confirmed our previous observation and revealed significant differences in the *in vitro* growth between the individual cell lines. While the majority of cell lines with a rather undifferentiated morphology (OC12,

OC14, OC15) were highly proliferative, the remaining SOC cell lines (OC18, OC19, OC20, OC21) displayed a lower growth rate **(Figure 13A)**. To further investigate the growth pattern of the different cell lines, we performed additional cell cycle and proliferation analysis by nucleotide analogue uptake assay. However, we did not observe any significant differences between the individual cell lines in cell cycle stage distribution. We only realized a tendency pointing towards two groups of different cycling cell lines. SOC cell lines, which showed significantly slower growth rates (OC18 and OC20), also contained less active cycling cells (cells in S and G2/M phase) compared to faster cycling cell lines (OC12 and OC14) **(Figure 13B/C)**.

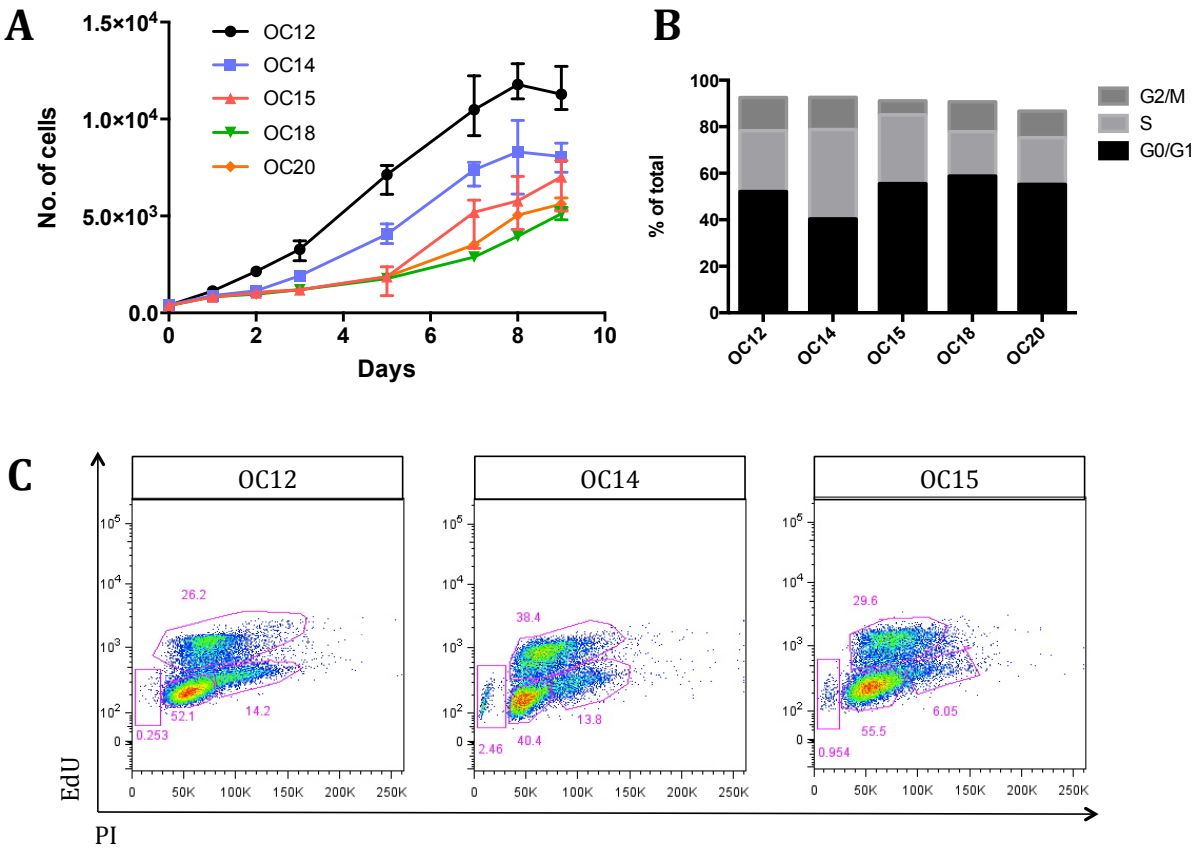

Figure 13 – (A) Analysis of the growth behaviour of different SOC lines revealed that they differ in their proliferation index *in vitro.* (B-C) Cell cycle analysis of different SOC cell lines confirmed the differences in growth behaviour.

To investigate if the differential growth patterns are also linked to differences in the capacity of clonal outgrowth, we analysed the *in vitro* clonogenicity of the individual SOC cell lines **(Figure 14)**. Interestingly, we found that SOC cells that showed a higher proliferation index also exhibited an increased clonogenic potential. Cell lines with a more differentiated morphology consistently had the lowest repopulation frequency.

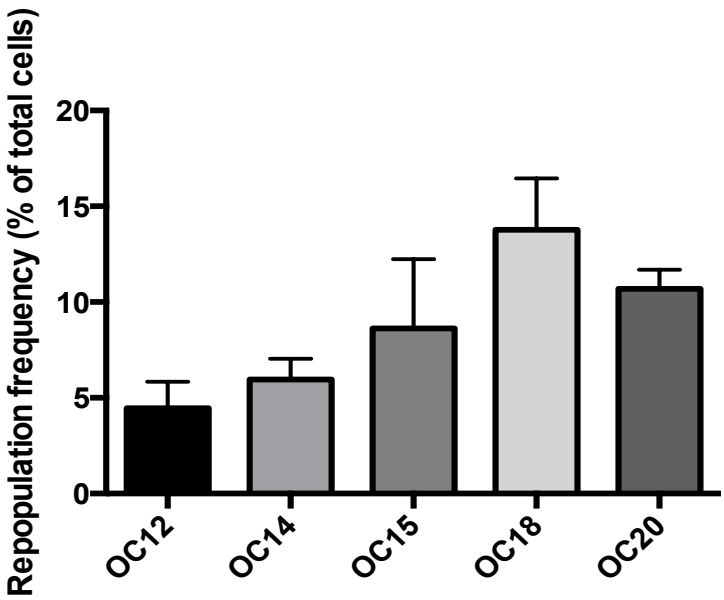

Figure 14 – *In vitro* repopulation frequency of different SOC cell lines

We next investigated whether the observed differences in growth behaviour and clonogenicity between the individual primary SOC lines, could be explained by a diverse expression of tumor initiating cells (TICs). Therefore we analysed all cell lines for the expression of described TIC markers. For ovarian cancer cells CD44 and CD44/CD117, CD133 and CD24 positivity have been associated with tumor initiating capacity [140,141,143,144]. We observed a broad heterogeneity in the expression of CD24 and CD44 in our primary cell lines (CD24 range 83-11%; CD44 range 100-35%). This heterogeneous expression of TIC markers could not been observed in conventional serum-cultured cell lines established *in vitro* **(Figure 15A)**. Remarkably, a high expression of CD24 and CD44 like seen for OC12 and OC14 **(Figure 15B)** correlated also with a high proliferation index and increased clonogenicity *in vitro*. The stem cell factor receptor (CD117) was expressed only at low levels or not at all on the primary SOC cell lines. None of the cell lines assayed showed expression of CD133 **(Table 4)**.

In summary, we were able to establish a novel culture system for primary serous ovarian carcinoma cells under serum-free conditions. Xenograft tumors derived from these cell lines express serous ovarian carcinoma specific markers and faithfully mimic the patients´ disease *in vivo*. According to our data, individual SOC cell lines show besides a broad intrinsic heterogeneity, while marked differences in morphology, proliferation and clonogenicity were evident between different cell lines. In addition, we observed a correlation between the expression of described TIC markers and the features outlined before.

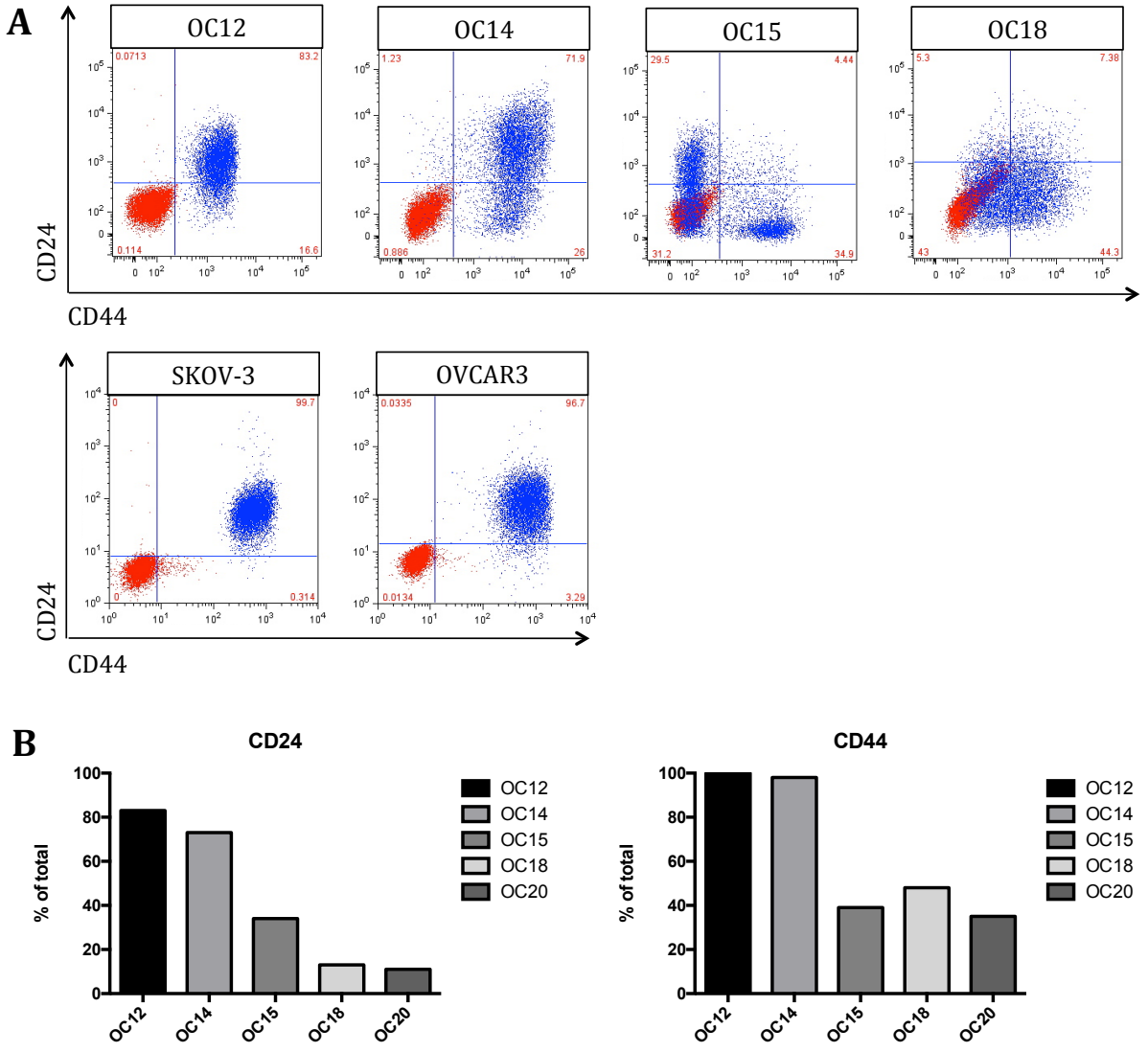

Figure 15 – (A) Representative FACS analysis of different primary SOC cell lines (OC12, OC14, OC15, OC18 and OC20) revealed a strong heterogeneity in the expression of CD24/CD44 compared to conventional cell lines (SKOV-3 and OVCAR3). (B) Frequency of CD24 and CD44 for individual SOC cell lines.

Table 4 – Frequencies of described TIC markers for individual SOC cell lines as determined by FACS

Cell line	CD24⁺	CD44⁺	CD133⁺	CD44⁺/ CD117⁺
OC12	83%	100%	0%	2%
OC14	73%	98%	0%	0%
OC15	34%	39%	0%	5%
OC18	13%	48%	0%	0%
OC20	11%	35%	0%	0%

Primary SOC cell lines are tumorigenic *in vivo* and preserve the original tumor heterogeneity upon xenotransplantation

In order to further investigate the previous established primary SOC cell lines concerning tumorigenicity and stability *in vivo*, we set up transplantation experiments in secondary recipient mice. We were especially interested in the repopulation frequency of the different cell lines and possible correlations with the expression of certain TIC markers. In addition, we wanted verify whether the histopathology of the original primary xenograft was conserved **(Figure 9A)**.

In order to investigate if the significant differences in the clonogenicity between the different SOC lines were also reflected *in vivo*, we set up a limiting dilution assay. Therefore we injected different concentrations of cells, ranging from $1x10^2$ to $1x10^4$, intraperitoneal into NSG mice. For non-invasive monitoring of tumor growth in mice, tumor cells were transduced with a lentiviral reporter expressing luciferase and the fluorescent protein Venus. After successful transduction, Venus-positive cells were sorted by FACS in order to obtain cells which are completely positive for the two reporters. *In vivo* growth of the tumors was monitored every two weeks via bioluminescence imaging using the Xenogen system (IVIS® 200 series, Caliper) **(Figure 16A)**. As for the *in vitro* cultures, we observed significant differences in growth behaviour and clonogenicity between the SOC xenografts. In general, a first appearance of signal was detected between 4 and 7 weeks post injection, and the timeframe of tumor growth ranged between 68 and 189 days. We detected no significant differences in growth between tumors originating from serous effusions or directly from the tumor. Within the groups injected with the highest number of cells ($1x10^4$) all mice of each cell line developed tumors. First differences in *in vivo* clonogenicity became apparent between different SOC lines in groups injected with $1x10^3$ tumor cells. In these groups, only mice injected with the cell lines OC12 and OC14 showed tumor appearance with 100% frequency. We observed an overall agreement between the *in vitro* determined clonogenicity and the tumor initiating potential *in vivo* for the tested SOC cell lines. Mice injected with the lowest cell number ($1x10^2$) developed no tumors in the same time frame **(Table 5)**. Noteworthy, tumor growth for mice injected with $1x10^2$ tumor cells could be observed beyond the time frame shown in **Figure 15A**, e.g. after 77 days (OC12).

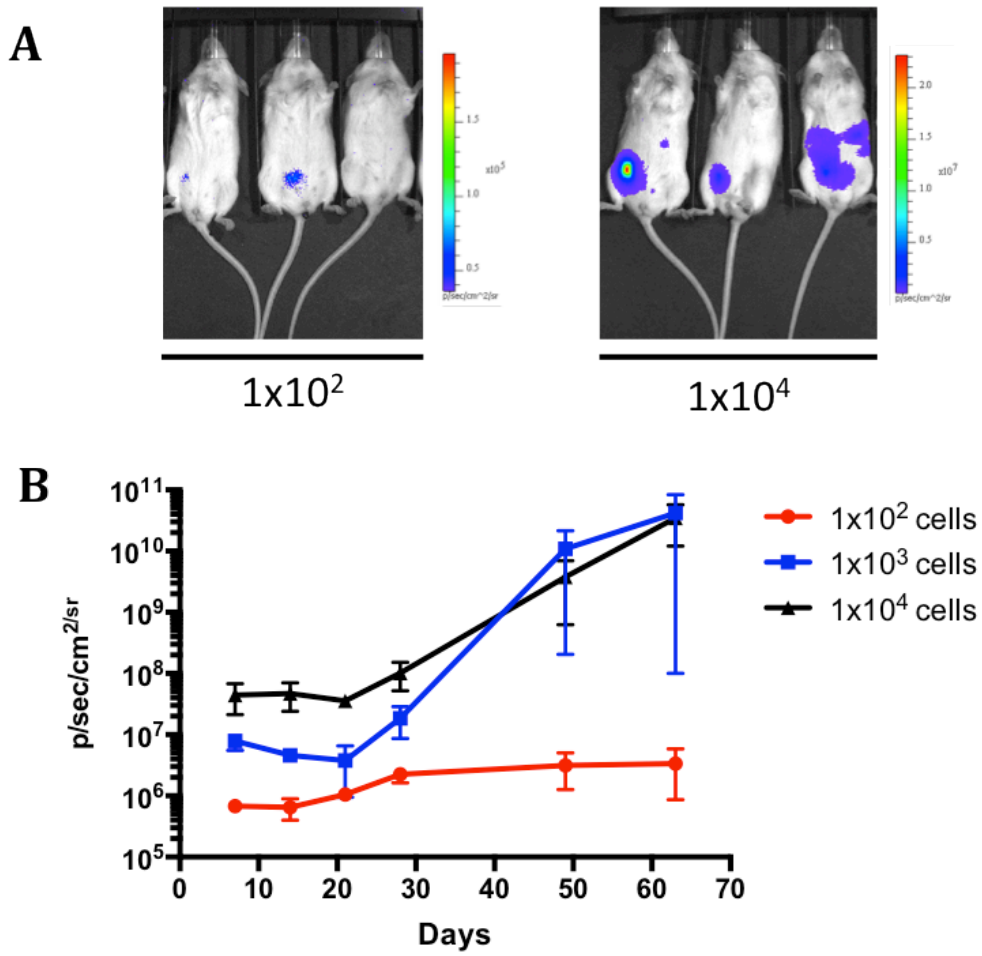

Figure 15 – Representative tumor growth curves of the OC12 cell line. (A) *In vivo* bioluminescence measurement of 2 groups of mice injected with different cell numbers using the Xenogen system. (B) Growth curve according to bioluminescence signal of intraperitoneal injected mice (n=3 per group).

All SOC cell lines we generated retained the capacity to form xenograft tumors in NSG mice. In addition, in every cell-line derived tumors (DT) we observed a strikingly robust development of the stromal compartments. These morphological properties were barely seen in xenografts derived from conventional cell lines **(Figure 17B).** Intriguingly, each SOC cell line DT could also reveal a characteristic metastatic potential. Spontaneous metastasis formation could be observed for 3 out of 7 different primary SOC cell lines. Intraperitoneal injection of both OC14 and OC20 led to the remarkable appearance of distant metastases in the lungs while OC18 developed both liver and lung metastases **(Table 5) (Figure 17C)**. Furthermore, all the mice injected with SOC cell lines developed ascites and showed typical collateral hallmarks of SOC, such as metastatic deposits at the abdominal wall, the liver and the diaphragm. We observed significant correlations between the metastatic capacity of the derived xenograft tumors and the origin of the primary tumor material. Primary cell lines that were derived from serous

effusions such as ascites or pleural effusions exhibited an increased capability for the metastatic colonization of lungs or liver **(Table 5) (Appendix,Table 1)**.

Table 5 – *In vivo* tumorigenictiy of the primary SOC lines

Cell line ID	Cell dose	Tumor incidence	Metastases	Latency (days)	Repopulation frequency)
OC12	$1x10^4$	3/3	-	70	1/417
	$1x10^3$	3/3	-		
	$1x10^2$	0/3	-		
OC14	$1x10^4$	3/3	Lung	91	1/417
	$1x10^3$	3/3	-		
	$1x10^2$	0/3	-		
OC15	$1x10^4$	3/3	-	112	1/2340
	$1x10^3$	1/3	-		
	$1x10^2$	0/3	-		
OC18	$1x10^4$	3/3	Lung, Liver	68	1/1072
	$1x10^3$	2/3	Lung/Liver		
	$1x10^2$	0/3	-		
OC19	$1x10^4$	3/3	-	135	1/2340
	$1x10^3$	1/3	-		
OC20	$1x10^4$	3/3	Lung	75	1/1072
	$1x10^3$	2/3	Lung		
	$1x10^2$	0/3	-		
OC21	$1x10^4$	3/3	-	189	ND

Finally, we found similarities in the morphological heterogeneity and the expression of the SOC specific markers CA125 and WT1 in the SOC cell lines derived tumors (DT) **(Figure 17 A)**. The comparison of the histopathological characteristics between the original patient´s tumor, the corresponding primary xenograft and cell line derived tumors, revealed that the overall features were well conserved along with the model system **(Figure 17A)**. Taken together, our primary SOC cell line derived tumors show several hallmarks of human SOC, which are often lost in xenografts from conventional cell lines.

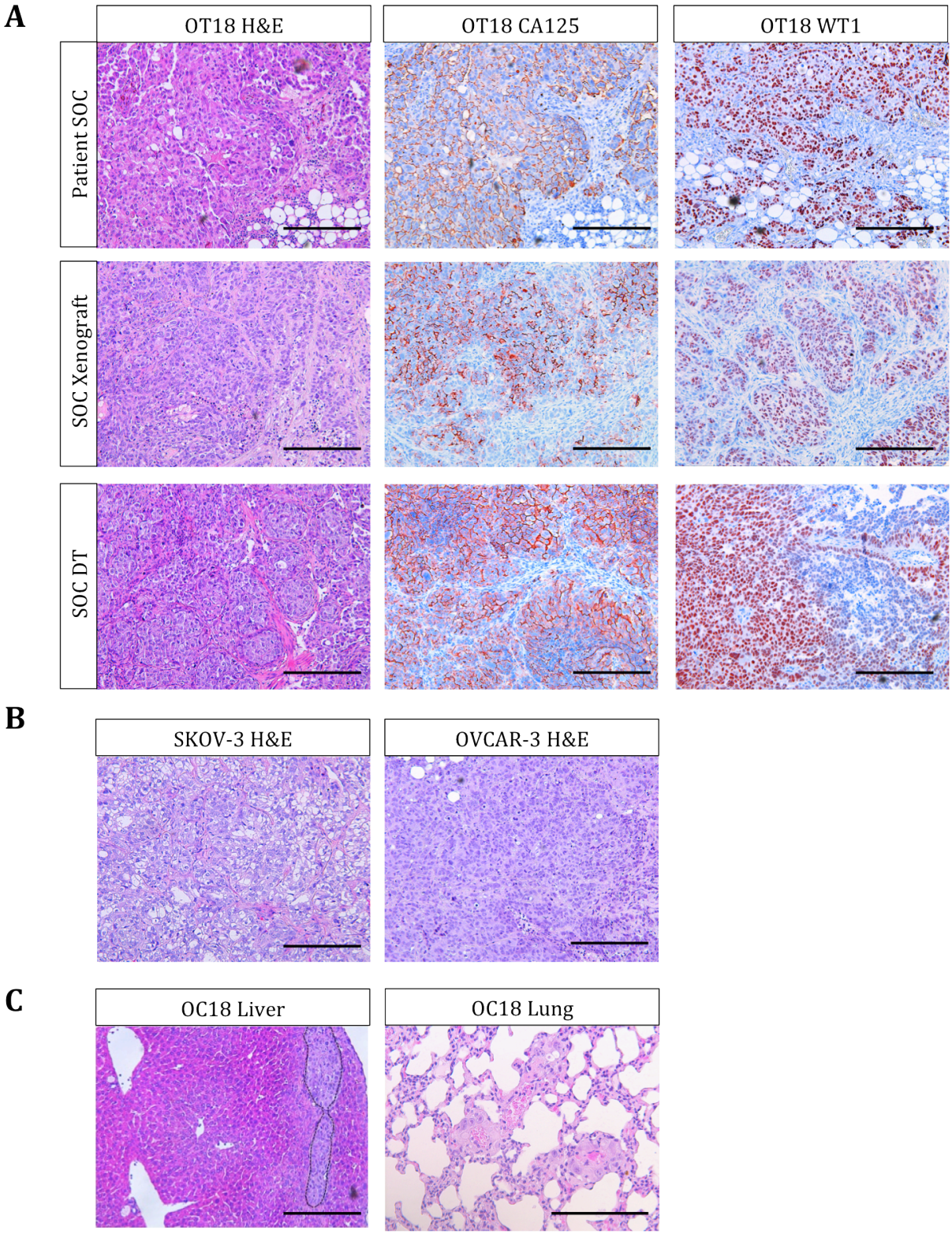

Figures 17 – (A) Morphological characteristics as well as the expression of SOC specific markers CA125 and WT1 observed in of the original ovarian cancer patient tumor (top) and the corresponding primary xenograft (middle) are well conserved in the SOC cell line derived tumors (DT). (B) Xenograft tumors established from conventional cell lines do not display morphological features of SOC. (C) Spontaneous metastases to liver (top) and lung (bottom) detected in derived tumors (scale bar 100 µm)

We next wanted to investigate if the SOC cell line derived tumors retain their ability to form tumors in secondary and tertiary recipient mice. Therefore we injected single cell suspensions derived from the respective tumors into further mice. We found that all SOC cell line derived tumors were able to form tumors for at least three serial passages *in vivo*. Once again, these tumors maintained their histopathology and the expression of serous ovarian carcinoma specific markers **(Figure 18)**.

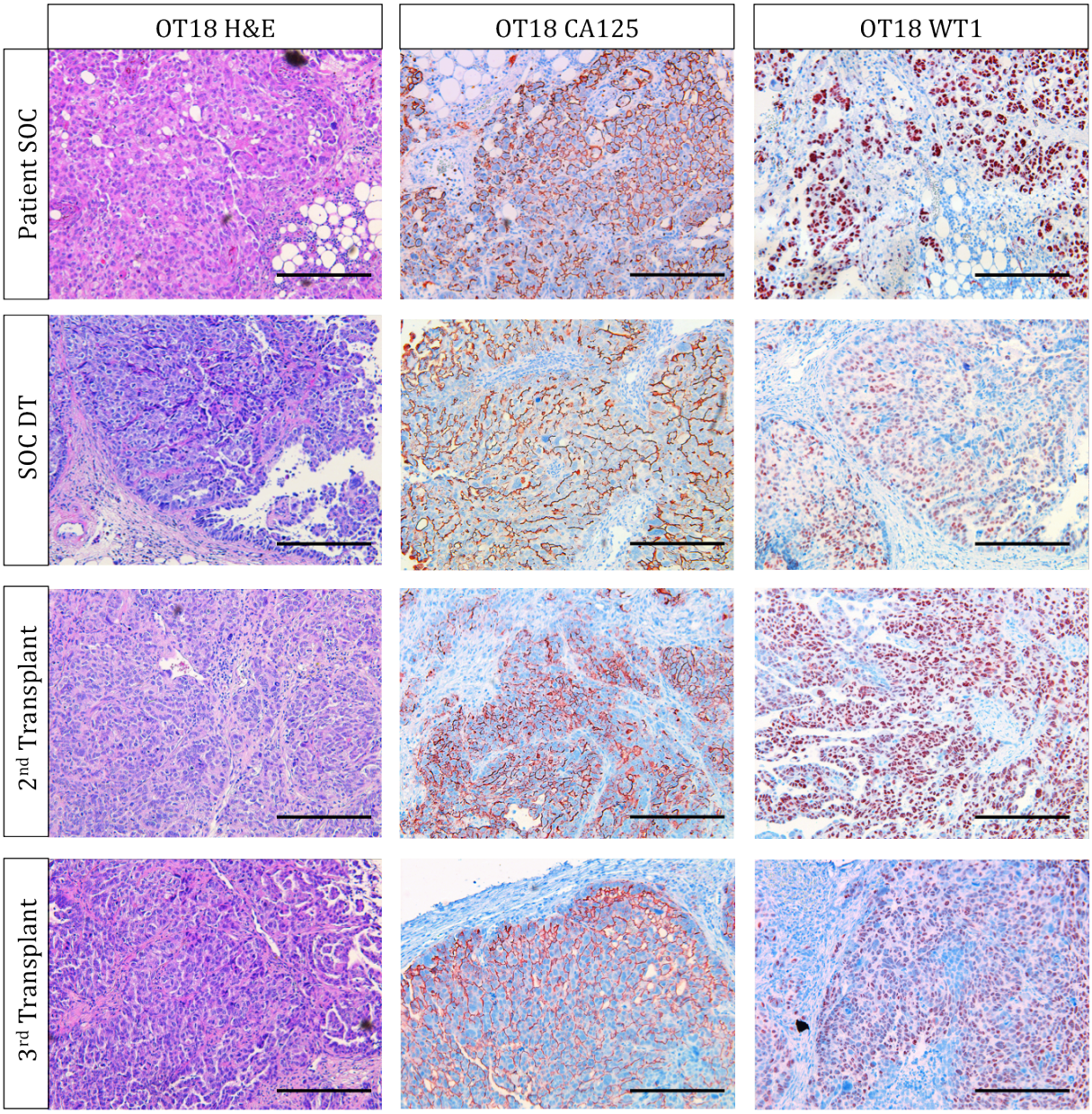

Figure 18 – (A) SOC cell line derived tumors maintain their ability to form tumors for at least three passages *in vivo*. Shown are representative images from a primary SOC line. Importantly, the expression of CA125 and WT1 is retained throughout all serial passages (2nd to 4th row)(scale bar 100 µm).

According to the results, we obtained from the determination of the clongenicity *in vivo*, we wondered if the differences between the cell lines might be explained by the frequency of TIC markers, which are described for ovarian cancer. As we observed for the *in vitro* cultures, also the corresponding DTs showed significant differences in their TIC marker profile as assessed by FACS analysis **(Figure 19)**. Importantly, the specific marker profile of every SOC line was relatively stable between primary xenograft and SOC cell line derived tumor **(Table 6)** and consistently with the *in vitro* data, we found no significant correlation between the TIC frequency *in vivo* and the clonogenic capacity of the SOC line derived tumors.

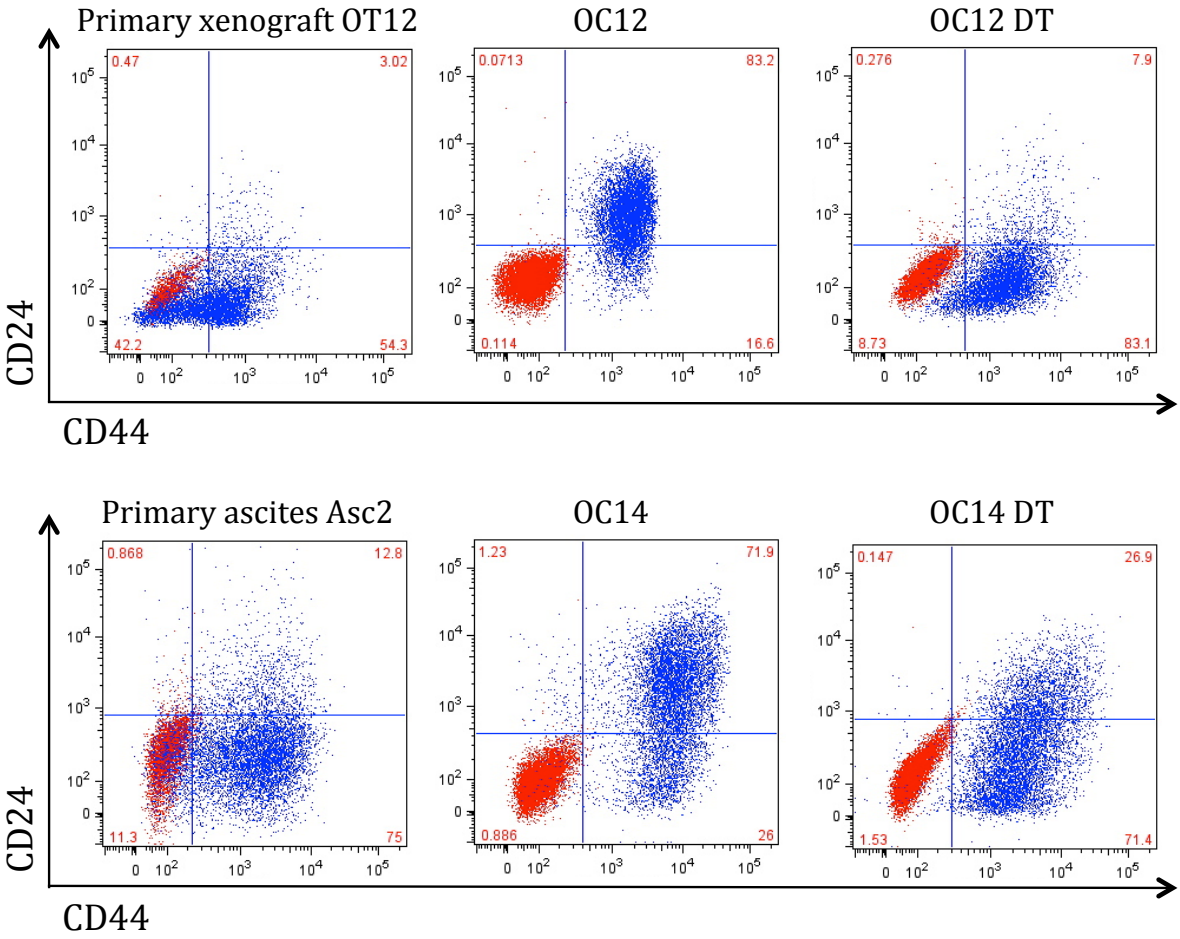

Figure 19 – FACS analysis of described TIC markers CD24/CD44 of primary SOC xenograft (first column), corresponding SOC culture (second column) and derived xenograft (third column). Interestingly, serum-free culture enriches for cells expressing TIC markers. In contrast, SOC culture derived xenograft tumors express markers at levels, comparable to primary xenograft.

More in details, the comparison of expression levels of CD24/CD44 in primary xenograft tumors with the levels observed in the cell line derived tumors revealed no significant

differences **(Figure 19)**. Similar results also were gained for the markers CD133 and CD117 **(Table 6)**.

In conclusion, we could show that our approach leads to the generation of cell lines that remarkably recall the patient's disease upon experimental transplantation *in vivo*. We could observe a huge heterogeneity in morphology and marker expression between different patient tumors and that these features were maintained by our culture model.

Table 6 – Frequencies of described TIC markers for selected primary SOC xenografts and derived tumors as determined by FACS

Cell line	CD24+		CD44+		CD44+/ CD117+	
	Primary xenograft	Derived tumor	Primary xenograft	Derived tumor	Primary xenograft	Derived tumor
OC12	3.49%	8.2%	57.3 %	91%	5.3%	7.8%
OC14	13.7%	27.1%	87.8%	98.3%	3%	6%
OC15	11.9%	26.4%	23.7%	32.5%	0%	0%
OC18	13.4%	19.4%	21.9%	39.4%	0%	0%
OC20	11.4%	21.3%	20.8%	32.2%	0%	0%

Gene expression profiling on the SOC model

Altered pathways in primary SOC lines

In order to identify molecular alterations that influence pathophysiology, histology and constitute possible therapeutic targets, we performed gene expression analyses on the SOC lines. For the generation of mRNA expression profiles we applied the Illumina Human HT12 v4 bead chip technology at the Genomics Proteomics Core Facility of the German Cancer Research Center. We integrated the gene expression profiles of our primary SOC cell lines, the corresponding derived xenograft tumors and a described human ovarian surface epithelial cell line (Hosepic) [186] in our analyses. A comparison of our primary culture models and their derived tumors with ovarian surface epithelium might allow the identification of pathways that specifically altered in ovarian cancer.

Hence, our first focus was the analysis of differentially expressed genes between our SOC models and the human ovarian surface epithelium. Gene expression datasets of seven SOC cell lines and their corresponding xenografts were compared with gene expression data of human ovarian surface epithelial cells using Gene Set Enrichment Analysis (GSEA). The obtained results delivered insights into the expression of genes involved in the maintenance of serous ovarian carcinoma. We found that the majority of the genes most strongly upregulated in the SOC model compared to normal human ovarian surface epithelium were associated with the regulation of mitosis, cell division, cell cycle processes and proliferation **(Figure 20A)**. Furthermore, several members of the *FOXM1* transcription network such as *AURA, CCNB1, BIRC5* and *CDC25* were overexpressed in the SOC cell lines.

With the help of further gene network analysis using GeneMANIA, we were able to link single identified genes to global networks and existing functional contexts. GeneMANIA, an interactive database analysis system, integrated the individual strongest upregulated genes into several hundreds of genomic and proteomic datasets, assembled from GEO, BioGRID, Pathway Commons and I2D databases [187]. The analysis combined, with the help of described datasets, functional interactions of single genes and expanded the gene lists with known interaction partners. Our network analysis of the most strongly upregulated genes in the SOC models postulated a significant functional involvement of genes implicated in cell division, the regulation of cell cycle and spindle apparatus, mitosis and cell cycle **(Figure 20B)**.

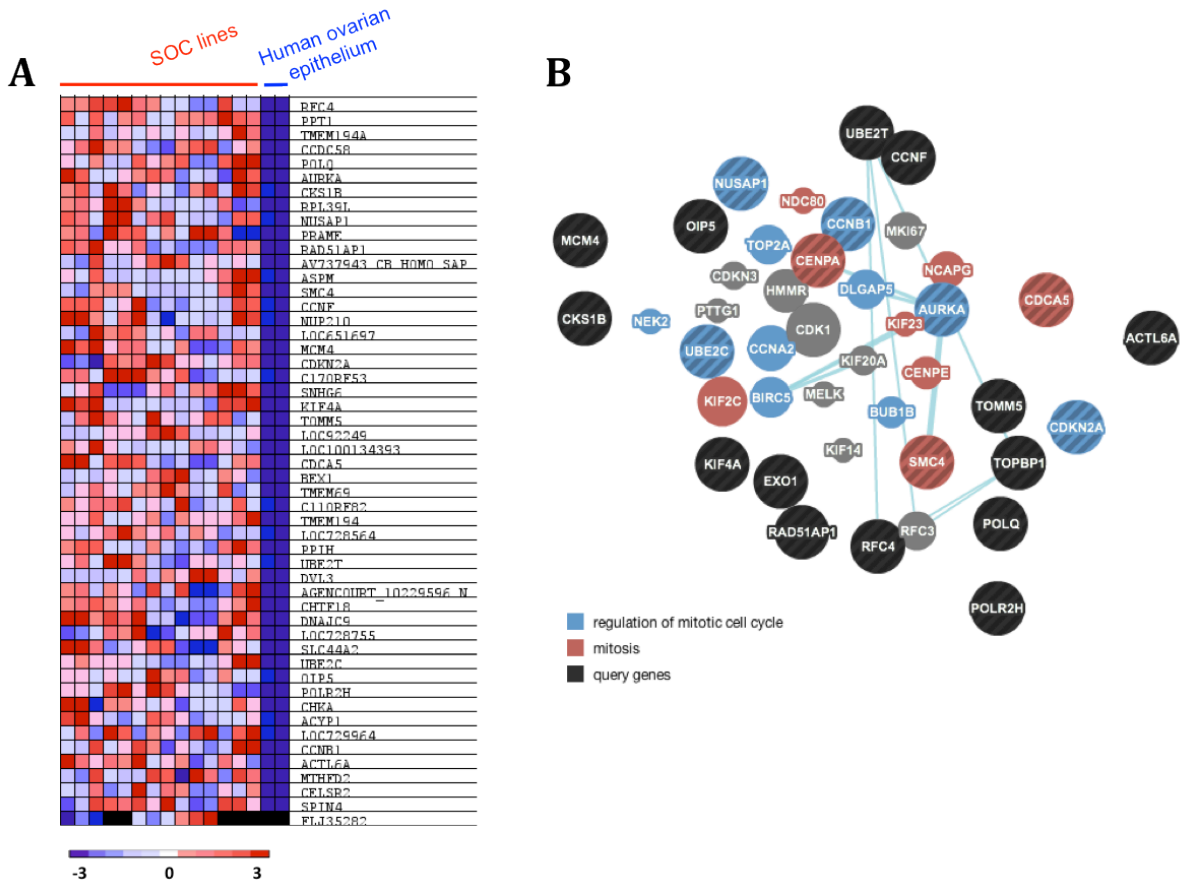

Figure 20 – (A) Heatmap generated by GSEA depicting the strongest upregulated expressed genes in the SOC models compared to human ovarian epithelial cells. (B) Global gene-network analysis of the strongest upregelated genes expressed in the SOC models compared to human ovarian epithelial cells (www.genemania.org).

To gain further insights into pathways driving SOC, we performed gene set enrichment analysis using the MSig database of the Broad Institute (3.82, 10/2011) with our gene expression datasets. This database allowed us the correlation of our gene expression profiles with more than 6770 published gene expression datasets [179] **(Figure 21A)**. We identified 308 gene sets to be positively correlated with a nominal p-value < 0.01 with the gene expression profiles of the SOC model (primary SOC cell lines and derived xenografts). A more precise analysis revealed a strong enrichment of multiple gene signatures associated with alterations in DNA repair pathways and an increased proliferation. Interestingly, also signatures that point to an activation of the IL-6- and the Notch pathway were highly enriched in the gene expression profiles of the SOC model **(Figure 21B,C)**. These results are in line with recent publications describing pathways driving high-grade serous ovarian carcinoma on the basis of gene expression data [66,188].

A

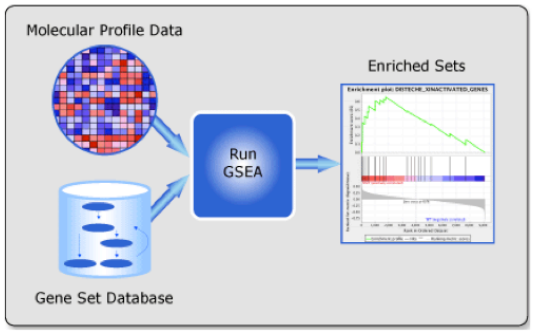

B

C

MSig DB SETS	ES	NES	p-value	FDR
PUJANA_XPRSS_INT_NETWORK	0.77	2.76	0.000	0.000
CROONQUIST_IL6_DEPRIVATION_DN	0.84	2.72	0.000	0.000
BENPORATH_PROLIFERATION	0.74	2.56	0.000	0.000
PUJANA_BRCA2_PCC_NETWORK	0.68	2.66	0.000	0.000
MISSIAGLIA_REGULATED_BY_METHYLATION_DN	0.82	2.70	0.000	0.000
KEGG_NOTCH_SIGNALING_PATHWAY	0.58	1.72	0.002	0.006

Figure 21 – (A) Schematic overview of Gene Set Enrichment Analysis using the MSig database (Broad Institute). (B,C) Overview of differentially enriched pathway signatures as predicted by GSEA for expression data from SOC cell lines and derived xenografts compared to ovarian surface epithelium (statistics calculated by GSEA).

The SOC model reflects four distinct molecular subtypes of SOC

The researchers of The Cancer Genome Atlas (TCGA) recently identified four distinct molecular subtypes of SOC by combined gene expression analysis and non-negative matrix factorization consensus clustering of a set of 489 human serous ovarian tumors. They defined gene panel's specific for every subtype that allow the allocation of individual tumor samples into one of the four subtypes. The subtypes were termed: 'differentiated', 'immunoreactive', 'mesenchymal' and 'proliferative' on the basis of gene content in the clusters [66].

As no xenograft or *in vitro* models were included in this study, we were interested to verify whether these four subtypes are also present in our SOC model. The presence of different subtypes within our model system might serve as an explanation for the observed heterogeneity in growth behaviour and clonogenicity. The described subtype-

specific gene panels were used together with the expression data of SOC cell line derived xenografts for Gene Set Enrichment Analysis (GSEA) to evaluate the subtype affiliation of each SOC line. We were able to clearly match every SOC derived xenograft to a specific subtype with a significant enrichment score (FDR q< 0.2). According to the subtype specific gene panels defined by The Cancer Genome Atlas (TCGA) we were able to determine individual gene expression profiles for every subtype. Out of the gene expression data of seven different derived SOC xenograft tumors we could classify two tumors as differentiated (OC18DT, OC21DT), two as mesenchymal (OC12DT, OC14 DT), two as proliferative (OC19DT, OC20DT) and one as immunoreactive subtype (OC15DT). After the classification of the xenograft models we wondered if also our cell lines would match to the individual subtypes. Therefore, we applied the same analysis sequence to the gene expression data of the *in vitro* cultured cell lines and could confirm the previous subtype affiliation **(Figure 22A-D) (Table 7)**.

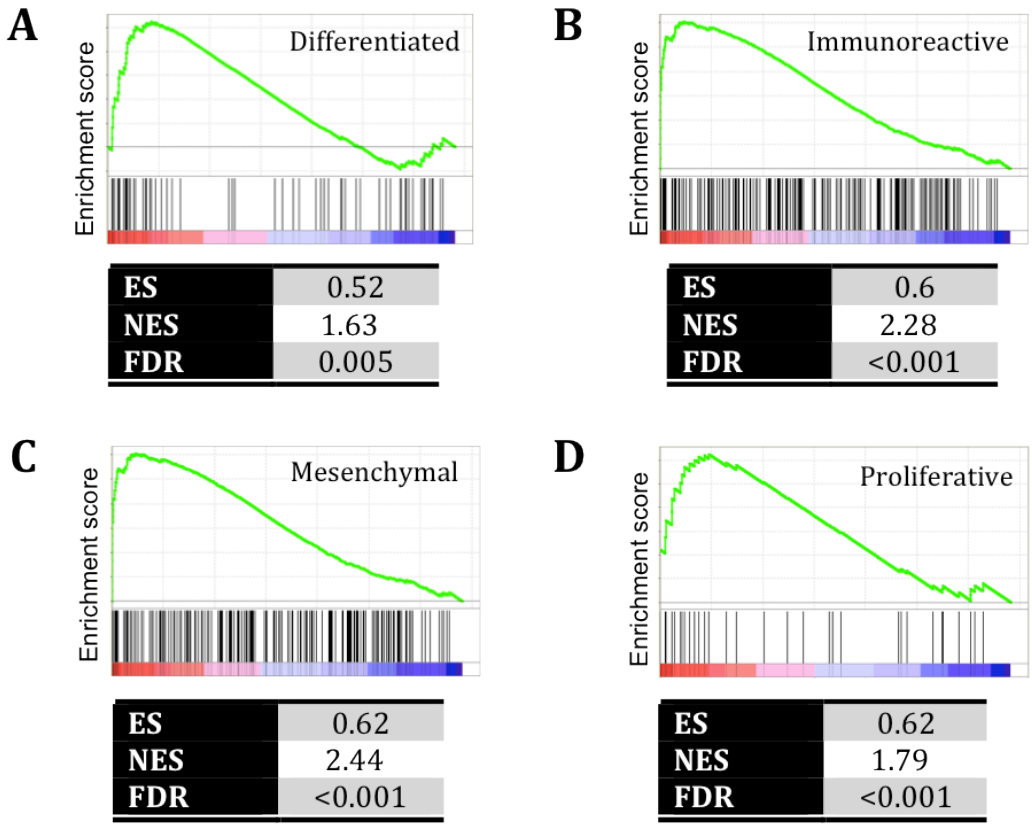

Figure 22 – (A-D) Enrichment plots and corresponding statistics generated by GSEA using subtype specific signatures [66] on expression datasets of SOC cell lines and derived tumors. Shown are Enrichment score (ES), Normalized Enrichment Score (NES) and False Discovery Rate (FDR). (A) – differentiated subtype, (B) – immunoreactive subtype, (C) – mesenchymal subtype, (D) – proliferative subtype.

Importantly, as shown in **Table 7**, the four subtypes were stably maintained *in vitro* and *in vivo*. Our previous results revealed significant differences in morphology, growth and clonogenicity between the individual primary SOC cell lines. We suggested the existence of at least two groups of cell lines showing different growth behaviour and clonogenicity present in our model system. This observation raised the question if they might belong to distinct molecular subtypes. Indeed, we found that the rather undifferentiated tumors (OC12DT and OC14DT) were classified as mesenchymal subtypes, whereas the morphological group of well-differentiated tumors consisted exclusively of the other three subtypes. We were not able to further subclassify this group of tumors according to molecular properties such as growth behaviour or clonogenicity.

Furthermore, as we were able to establish *in vitro* cultures for all four subtypes, we concluded that there is no tendency for one subtype to prevail nor being excluded under conditions provided by our model system.

Table 7– Subtype classification of SOC cell lines and corresponding derived xenografts (NES – Normalized enrichment score, FDR – False discovery rate; statistics calculated by GSEA)

Cell line	Subtype	NES	p-value	FDR
OC18	Differentiated	1.60	0.011	0.018
OC18 DT	Differentiated	2.13	<0.001	<0.001
OC15	Immunoreactive	1.66	<0.001	0.004
OC15 DT	Immunoreactive	2.44	<0.001	<0.001
OC12	Mesenchymal	1.14	0.149	0.2
OC12 DT	Mesenchymal	2.47	<0.001	<0.001
OC14	Mesenchymal	2.17	<0.001	<0.001
OC14 DT	Mesenchymal	2.43	<0.001	<0.001
OC19	Proliferative	1.46	0.002	0.028
OC19 DT	Proliferative	1.62	0.004	0.002
OC20	Proliferative	1.44	0.049	0.017
OC20 DT	Proliferative	1.65	0.016	0.017

In summary, we showed that our SOC culture contains all four described subtypes and that their characteristic gene expression signatures are retained. Moreover, xenograft tumors established from SOC cell lines maintain their subtype affiliation *in vivo* and recapitulate tumors of all the four subtypes. We were not able to find an enrichment of a certain subtype in our culture suggesting that all subtypes have similar abilities to grow in our model.

Identification of tumor initiating cells in Serous ovarian carcinoma

Large scale surface marker profiling identifies differentially expressed cell populations

After the investigation of the intertumoral heterogeneity between our SOC models, we next wanted to analyse the expression of different cell populations on the SOC lines. Therefore, we performed a large scale surface marker screen using the BD Lyoplate Cell Surface Screening Panel, consisting of monoclonal antibodies against 242 different known cell surface proteins. The analysis of the screen confirmed several previous gained results like for the expression of CD24 and CD44, but even more important, we identified multiple differentially expressed markers **(Figure 23)**. These heterogeneously expressed markers are of particular interest as they may lead to the identification of functional subpopulations such as drug resistant cells or even a CSC subpopulation. In addition, we could show that our *in vitro* model preserves the heterogeneity of cell populations within the SOC cell lines.

As stated above, we identified several already described markers for cancer initiating cells in ovarian cancer such as CD24 or CD44. However, our aim was to discover and characterize novel surface markers for subpopulations, which show properties of cancer initiating cells. Therefore, we focused on markers that have not been implicated in tumor initiation in ovarian cancer before. One of these molecules, which were also highly differential expressed, was CD151 (Tetraspanin 24, PETA-3) **(Figure 23, Plate2)**. CD151 is a member of the transmembrane 4 superfamily, also known as the tetraspanin family. Tetraspanins are characterized by four transmembrane domains and play an important role in a variety of cellular functions, including cell proliferation, differentiation, and cancer cell invasion and metastasis [189,190]. CD151 in particular has been shown to interact directly with the α subunit of several integrins [191] and mediates their function by the regulation of cytoplasmic signaling. Specifically, CD151 is involved in the adhesion dependent activation of Ras, RAC1, and integrin-associated Cdc42 signaling [192]. In addition, the expression of CD151 correlates with a poor prognosis, advanced disease stage and enhanced metastatic spread in several cancer entities [193-196]. CD151 has also been described as a marker for tumor initiating cells in prostate cancer [197]. As we wanted to investigate if CD151 plays a likewise role in ovarian cancer, we went on with further analysis on this transmembrane protein.

Remarkably, when we analysed the results obtained from the Lyoplate Cell Surface Screen, we also found several markers implicated in stemness and pluripotency such as SSEA-1, SSEA-3, SSEA-4 and TRA -1-81 to be differentially expressed on our primary ovarian cancer cell lines **(Figure 23 Plate3)**.

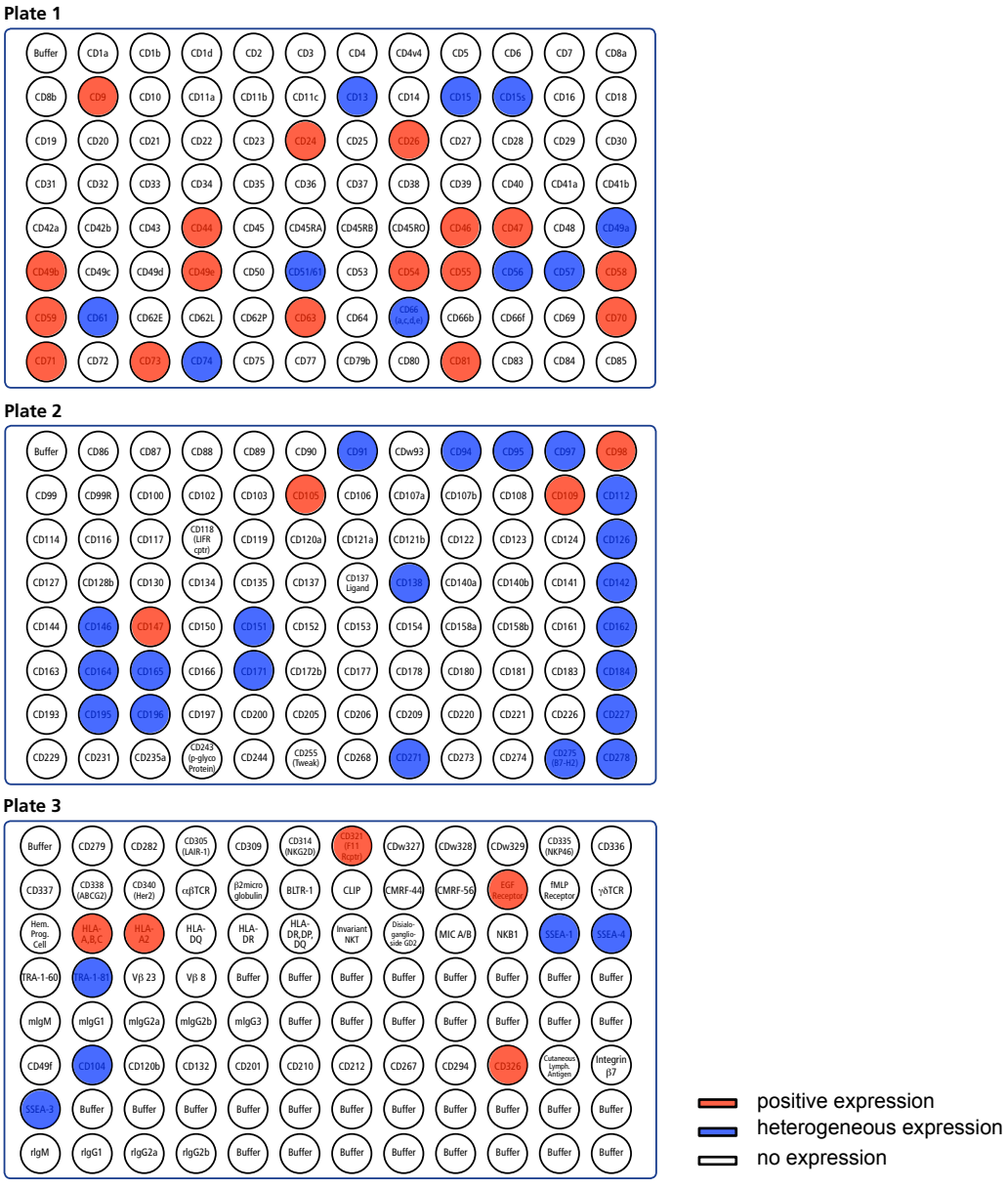

Figure 23 – Analysis of the cell surface marker screen performed using the BD Lyoplate Cell Surface Screening Panel on the OC12 cell line. Red – positive expression, blue – heterogeneous expression, white – no expression of the surface marker

A large scale surface marker screen revealed the transmembrane protein CD151 to be differentially expressed on primary SOC cell lines. These results were further validated via flow cytometry on several primary SOC cell lines as depicted in **Figure 24A**. We found that CD151 was heterogeneously expressed on all tested cell lines and that the

total expression level was very variable between the cell lines, ranging between 17.8% (OC12) and 86.2% (OC15).

Interestingly, the expression level of CD151 correlated with an advanced disease stage. SOC cell lines that were derived from serous effusions such as ascites or pleural effusion showed a significant higher expression of CD151 compared to cell lines derived directly from tumor material.

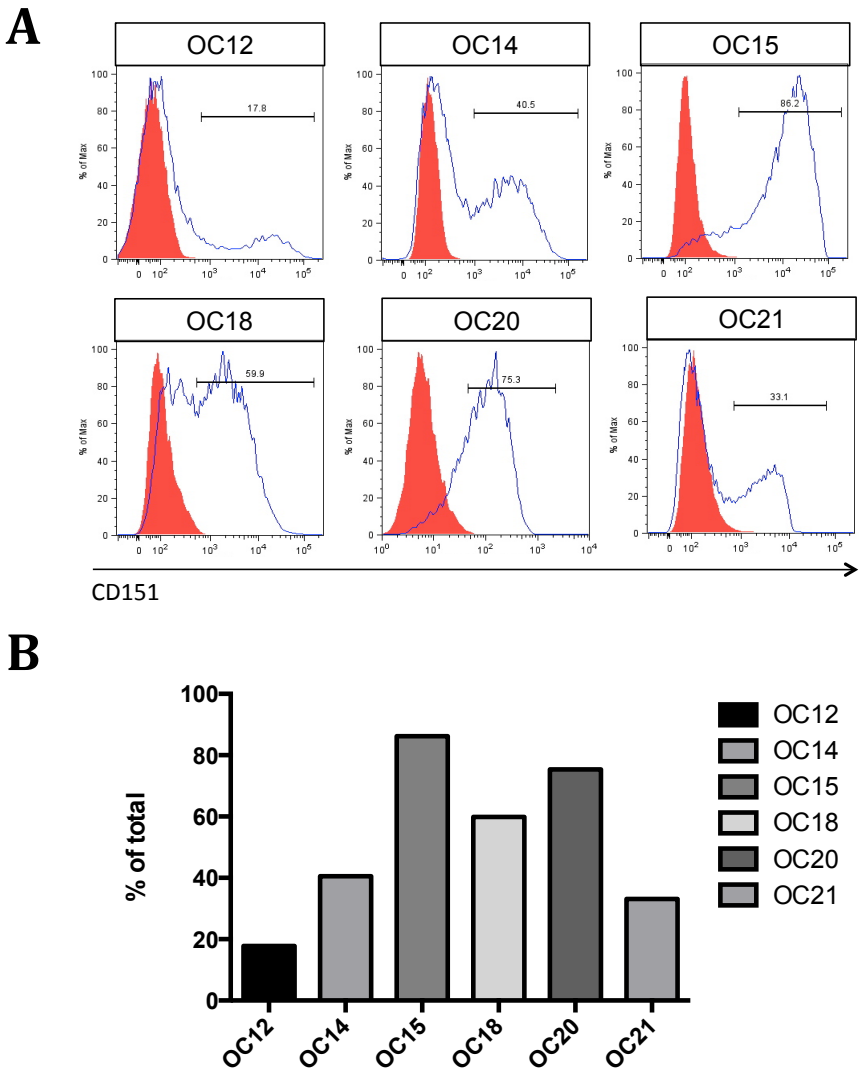

Figure 24 – (A) CD151 is heterogeneously expressed on all tested SOC lines. (B) The expression levels of CD151 show a high variability throughout the SOC lines ranging from 17.8% to 86.2%.

Having proved that CD151 is heterogeneously expressed on all established cell lines, we wanted to evaluate the expression pattern on the corresponding cell line derived tumors by immunohistochemistry. The analysis of the immunohistochemical stainings revealed a specific membrane associated expression pattern of CD151. Additionally, we observed that expression levels of the SOC cell lines are reflected by their corresponding derived

tumors. Cell lines showing a low expression of CD151 also gave rise to tumors with a low expression level and vice versa **(Figure 25)**. This observation also confirmed our previous findings that the phenotype of the tumor cells is conserved in derived tumors.

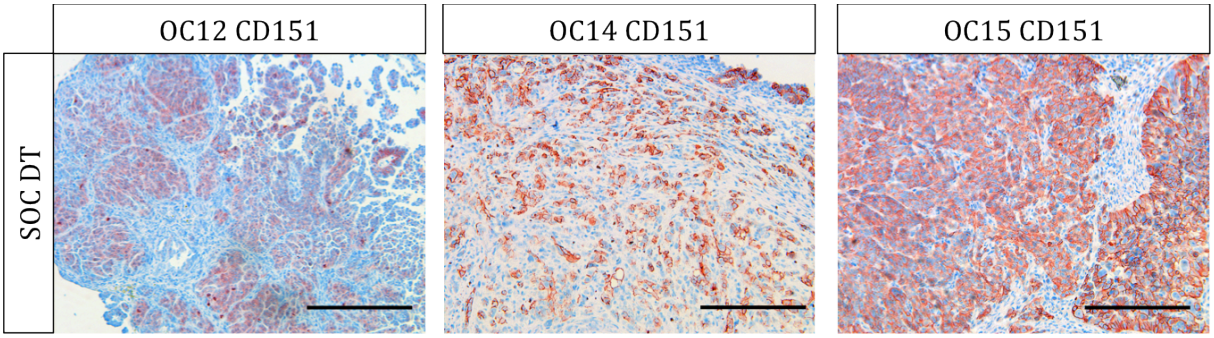

Figure 25 – Immunhistochemical stainings for CD151 on SOC cell line derived tumors reveals that expression levels are conserved in the tumors (scale bar 100 µm).

In summary, we could show that our SOC models can be utilized for large scale screening approaches, which might lead to the identification of functional subpopulations that play a role in drug resistance or tumor initiation. Here, we applied a surface marker screen to get an overview of the main surface markers expressed on our SOC models. We successfully identified several interesting targets that were described to be involved in metastatic processes, tumor initiating as well as stemness. These surface markers could be confirmed by additional FACS analysis. Furthermore, we focused on the transmembrane protein CD151, which has been implicated in cancer cell invasion and metastasis and correlates with a poor prognosis in several cancer entities. CD151 is heterogeneously expressed on all our SOC cell lines and the expression level is conserved between SOC cell lines and corresponding xenograft tumor.

Growth characteristics of CD151$^+$ and CD151$^-$ subpopulations *in vitro*

CD151 showed a heterogeneous expression throughout all tested SOC cell lines *in vitro* as well as for the corresponding xenograft tumors resulting in a CD151 positive and a CD151 negative subpopulation. In order to investigate the capacity for self-renewal and differentiation in the observed phenotypes, we sorted Venus$^+$/CD151$^+$ and Venus$^-$/CD151$^-$ cells from the primary SOC cell line OC12 (transduced with a lentiviral reporter containing the Venus fluorochrome), mixed them in the same ratio and cultured them under regular conditions. The additional labelling of the CD151$^+$ subpopulation with a reporter construct allowed the discrimination between the two originally populations. Expression of Venus and CD151 was monitored for 17 days by flow cytometry **(Figure 26A)**. We found that the proportion of CD151$^+$ cells dramatically declined over time in the purified Venus$^+$/CD151$^+$ population, and reached almost the original distribution of CD151 expression. As expected, the expression of the Venus fluorchrome did not change in the monitored time frame **(Figure 26B)**. In contrast, the purified Venus$^-$/CD151$^-$ population retained their phenotype and we observed no Venus$^-$ cells expressing CD151 **(Figure 26C)**.

We concluded from this experiment that CD151$^+$ tumor cells arose only from the CD151$^+$ population, which is also able to give rise to CD151$^-$ cells. CD151$^-$ cells gave rise exclusively to CD151$^-$ progeny. In parallel, we analysed the ratio of the two purified populations by measuring the expression of the Venus fluorchrome. At the beginning of the experiment equal proportions of Venus$^+$/CD151$^+$ and Venus$^-$/CD151$^-$ were seeded **(Figure 26D)**. The determination of Venus positive cells over time allowed us the evaluation of the growth of both populations under exactly the conditions. An increase of Venus$^+$ cells in the culture indicated that the originally Venus$^+$/CD151$^+$ subpopulation had a stronger ability to grow compared to the Venus$^-$/CD151$^-$ subpopulation **(Figure 26E)**.

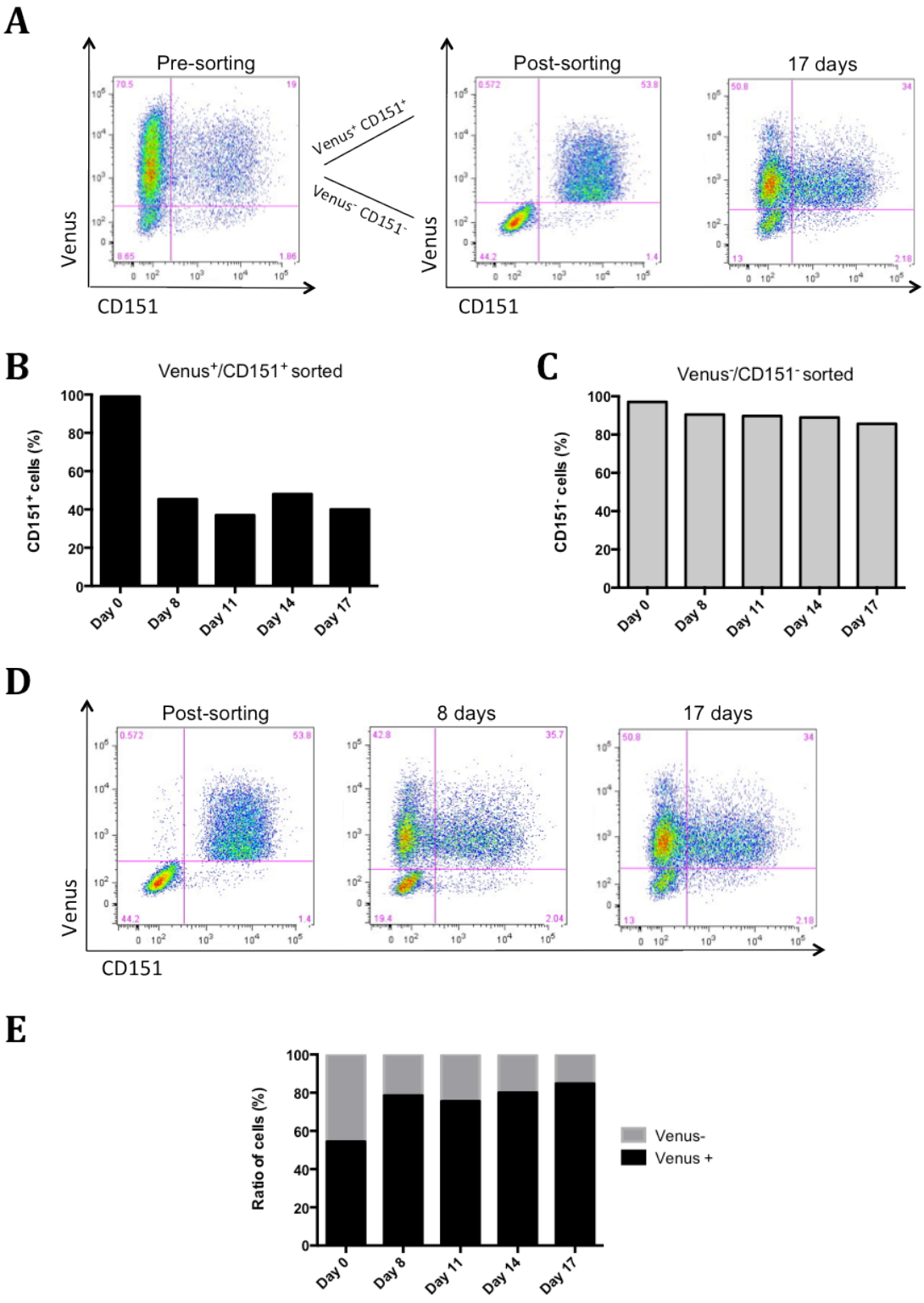

Figure 26 – Differentiation of purified CD151⁺ and CD151⁻ cells *in vitro* (A) FACS analysis of Venus and CD151 expression before sorting, right after sorting and splitting, and after 17 days in culture. Directly after sorting Venus⁺/CD151⁺ and Venus⁻/CD151⁻ cells were mixed in equal amounts. (B) Bar diagrams summarizing obtained expression values. The purified Venus⁺/CD151⁺ population generated both Venus⁺/CD151⁺ and Venus⁺/CD151⁻ cells, (C) whereas Venus⁻/CD151⁻ remained unchanged. (D) Venus⁺/CD151⁺ and Venus⁻/CD151⁻ cells were seeded in a 50:50 ratio and Venus expression was monitored over 17 days. (E) Summary of the change in Venus expression.

Given the observed discrepancies in the growth of the purified CD151 positive subpopulation in comparison with the purified CD151 negative population, we asked whether this could be explained by differences in the proliferative capacity of the two subpopulations. Therefore we performed an EdU proliferation assay and compared the cell cycle status of the different subpopulations. The proliferation of cells was measured by the incorporation of the modified nucleoside EdU (5-ethynyl-2´-deoxyuridine) into newly synthesized DNA **(Figure 27A)**. We tested three representative SOC cell lines that showed various levels in the expression of CD151. In the cell line OC12, we detected differences in the amount of active cycling cells of 48.9% in the $CD151^+$ subpopulation compared to 38.5% in the CD151 negative cells. OC15 showed only a minor variation in cells in S-phase between the two populations. The biggest difference in cell cycle status between $CD151^+$ and $CD151^-$ cells was observed in the cell line OC18. Whereas only 57% of cells expressing CD151 could be assigned to the $G_{0/1}$ phase, 86% of the $CD151^-$ cells were found to be in this phase. In parallel, the amount of active cycling cells was significantly higher in the CD151 positive subpopulation **(Figure 27B)**.

In summary, we were able to show that purified $CD151^+$ cells were gave rise to $CD151^+$ and $CD151^-$ cells, whereas purified $CD151^-$ cells did not. In a competition assay, the amount of the originally $CD151^+$ cells increased from 54% at the beginnining of the experiment to 84% at the end, meaning that the originally $CD151^-$ cells were outcompeted. In all tested cell lines, the $CD151^+$ cells exhibited a higher proliferative capacity compared to the $CD151^-$ cells. This difference between the two subpopulations was displayed to variable extents in the cell lines.

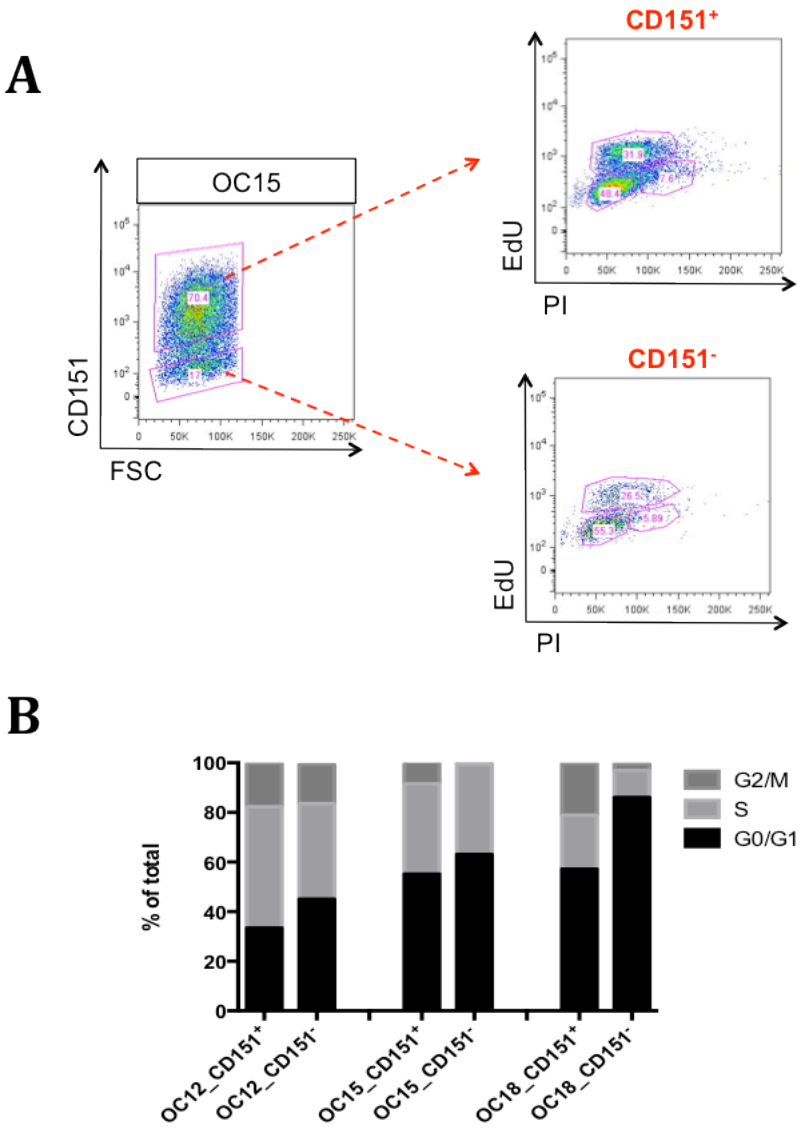

Figure 27 – Cell cycle analysis of CD151⁺ and CD151⁻ subpopulations of SOC cell lines *in vitro.* (A) Gating scheme of the analysis, (B) Comparison of cell cycle phases between CD151 subpopulations confirms observed differences in growth behaviour.

CD151 defines a tumor initiating subpopulation in serous ovarian carcinoma

In order to further explore the functional differences between CD151⁺ and CD151⁻ cells, we set up a xenotransplantation assay comparing the two purified CD151 subpopulations. Therefore, Venus⁺ /CD151⁺ and Venus⁺ /CD151⁻ cells were sorted by flow cytometry. Purity of these sorted populations as assessed by post sort flow cytometry was >90% for the CD151⁺ fraction and >75% for the CD151⁻ fraction **(Figure 28A).**

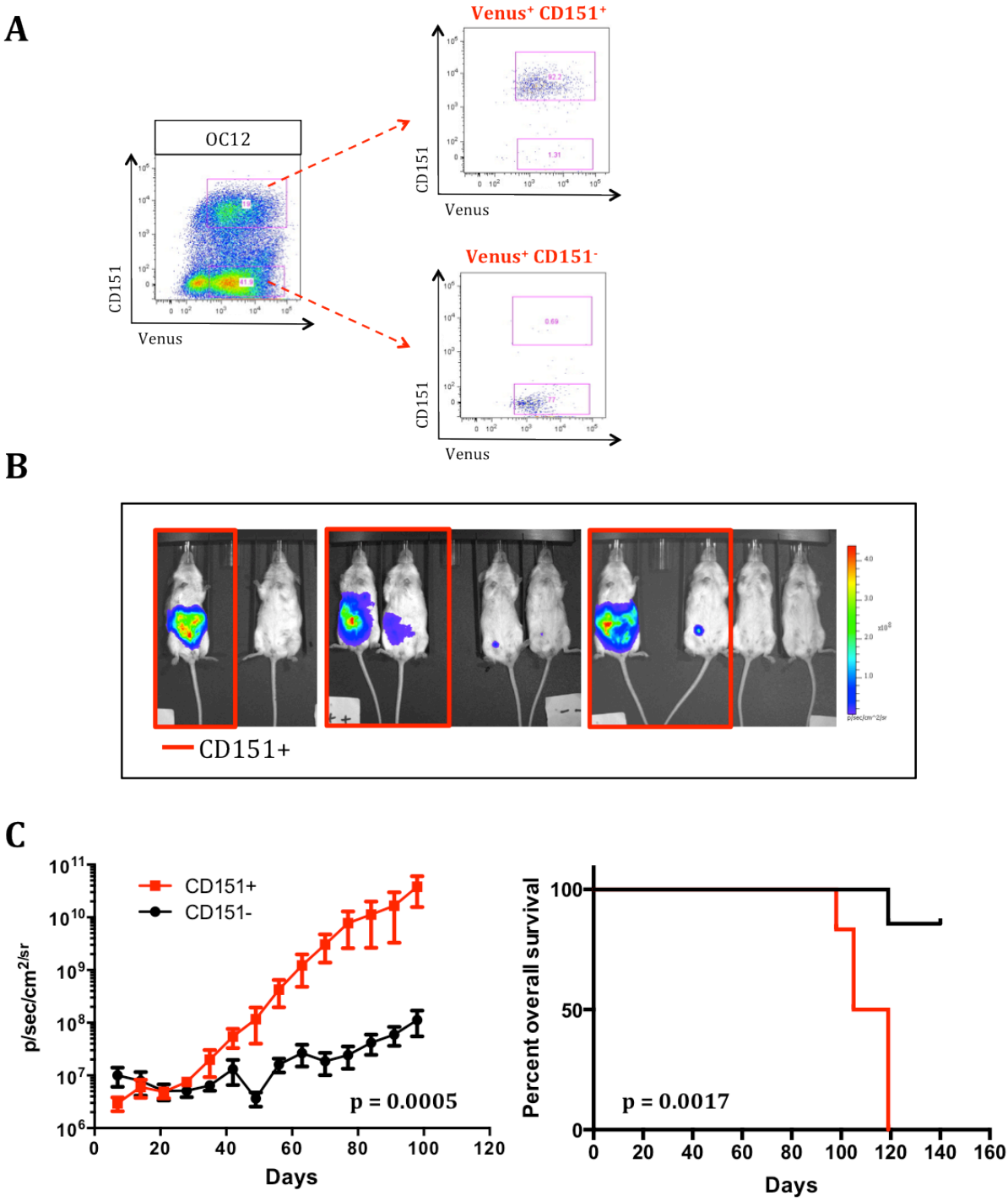

Figure 28 – (A) Gating scheme used for FACS purification of Venus$^+$ /CD151$^+$ and Venus$^+$ /CD151$^-$ cells (doublet- and dead cell exclusion were performed before). Note the high purity of both fractions. (B) Representative bioluminescence images of mice injected with purified CD151$^+$ cells (red boxes) and mice injected with CD151$^-$ cells. (C) Growth curve according to bioluminescence signal (left) and Kaplan-Meier plots (right) of mice injected with the respective subpopulation.

We injected 1x10^4 cells of each purified subpopulation from the OC12 cell line intraperitoneal into immunocompromised mice. In this experimental setting, we used seven mice for the CD151- cohort, six mice for CD151+ cohort and one mouse as a

control for Luciferase background. Hence, 13 mice were injected in total. Constant monitoring of tumor growth *in vivo* was performed by weekly bioluminescence imaging using the Xenogen system as described before. The first measurement was conducted one week after injection of tumor cells. Tumor growth was monitored until termination conditions for animals were reached. We observed tumor growth and development of ascites in six out of six mice in the group injected with purified $CD151^+$ cells. The tumor latency ranged between 98 and 119 days **(Figure 28C)**. In contrast, in the group of mice injected with $CD151^-$ cells, only one mouse showed an increase in bioluminescent signal. A comparison of the tumor growth curves, which were determined by bioluminescence measurement, of the two groups resulted in a significant difference between mice injected with purified $CD151^+$ cells compared to mice injected with purified $CD151^-$ cells **(Figure 28B)**. FACS analysis of tumor material dissected from the single mouse with an increased bioluminescence signal revealed a contamination with $CD151^+$ cells. 140 days post injection remaining mice from this group were analysed for tumor development. We were not able to detect any tumor growth in the mice injected with $CD151^-$ cells. Therefore, we assumed that tumor initiating cells are enriched in the CD151 positive subpopulation of the OC12 cell line. Subsequent analyses of generated tumors by flow cytometry revealed a heterogeneous expression pattern of CD151 suggesting that the diverse tumor phenotype was recapitulated following injection of a highly purified fraction of CD151 expressing cells (data not shown).

Importantly, immunhistochemical analysis of dissected tumors from mice injected with purified $CD151^+$ cells confirmed that they originated from injected cells by expression of Venus fluorochrome. Additionally, we analysed the expression of CD151 in these tumors and found an enrichment for $CD151^+$ cells compared to the original OC12 cell line derived tumor. However, the tested tumors displayed a heterogeneous expression of CD151 containing $CD151^+$ and $CD151^-$ cells. Investigation of the organs that were dissected from mice of this experiment revealed metastatic spread of purified $CD151^+$ cells to the lungs. Tumor cells in the lungs of the mice expressed CD151 and stained positive for the proliferation marker Ki67, pointing to the fact that these cells did proliferate in the lungs of the mice. In contrast, we observed no tumor cells in the lungs of mice injected with $CD151^-$ cells **(Figure 29)**.

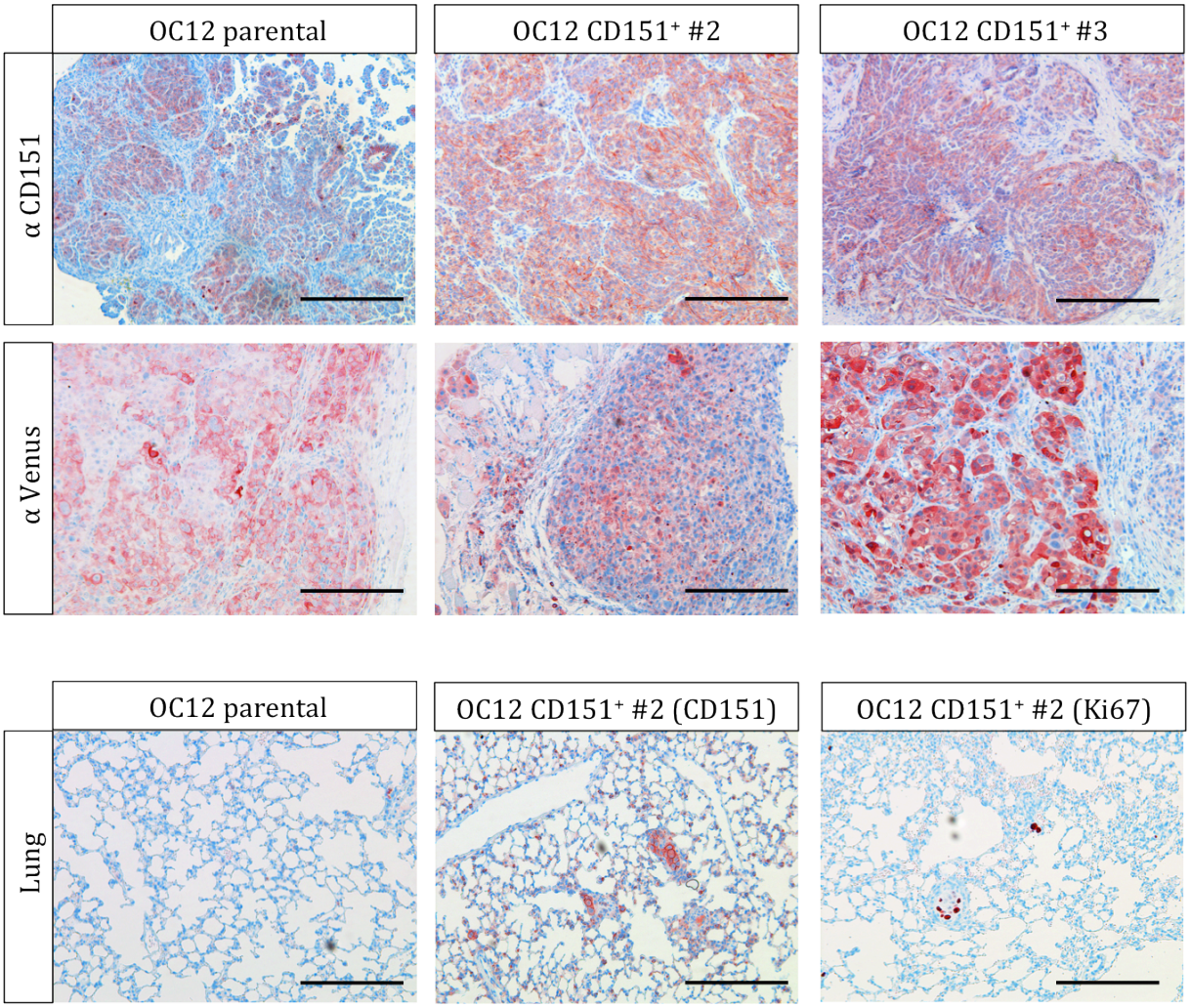

Figure 29 – Immunohistochemical stainings of tumors and lungs dissected from mice injected with the parental OC12 cell line (left column) or purified CD151+ cells (middle and right column). CD151 enriched tumors show an increased expression of membraneous CD151 compared to the parental tumor (top row). Verification of the used reporter construct by detection of cytoplasmatic Venus fluorochrome (middle row). Metastasis in the lung of mice injected with CD151+ cells express CD151 and Ki67 (bottom row). (scale bar 100 µm).

In order to validate these results, the same experiment was carried out using two further primary SOC cell lines. CD151+ and CD151- cells from the cell lines OC14 and OC15 were purified by flow cytometry. Every group consisted of six mice that were injected intraperitoneal with a concentration of $1x10^4$ cells of the respective subpopulation. For non-invasive monitoring also these cells had been transduced with a lentiviral reporter containing luciferase and the Venus fluorochrome. Again, similar to the results gained from the experiment using the OC12 cell line, we observed a higher tumorigenic potential in the purified CD151+ cells compared to the CD151- cells. Mice injected with purified CD151+ cells from the cell line OC14 showed a significant increase in the bioluminescence signal compared to mice injected with purified CD151- cells from

the same cell line over time **(Figure 30A, left)**. Injection of CD151⁺ cells led to tumor and ascites development in six out of six mice with tumor latency between 119 and 147 days. Immunhistochemistry was used to additionally investigate the expression pattern of CD151 in the individual tumors and to detect possible metastatic spread to the lungs of the mice **(Figure 31)**.

Conversely, in the group injected with CD151⁻ cells, none of the mice showed tumor development. Analysis of luminescence signals from this group revealed only a slight increase in signal intensity compared to the group injected with CD151⁺ cells. Remaining mice injected with CD151⁻ cells were monitored for 161 days until endpoint analysis, but we were not able to detect tumor growth in these mice **(Figure 30A, right)**.

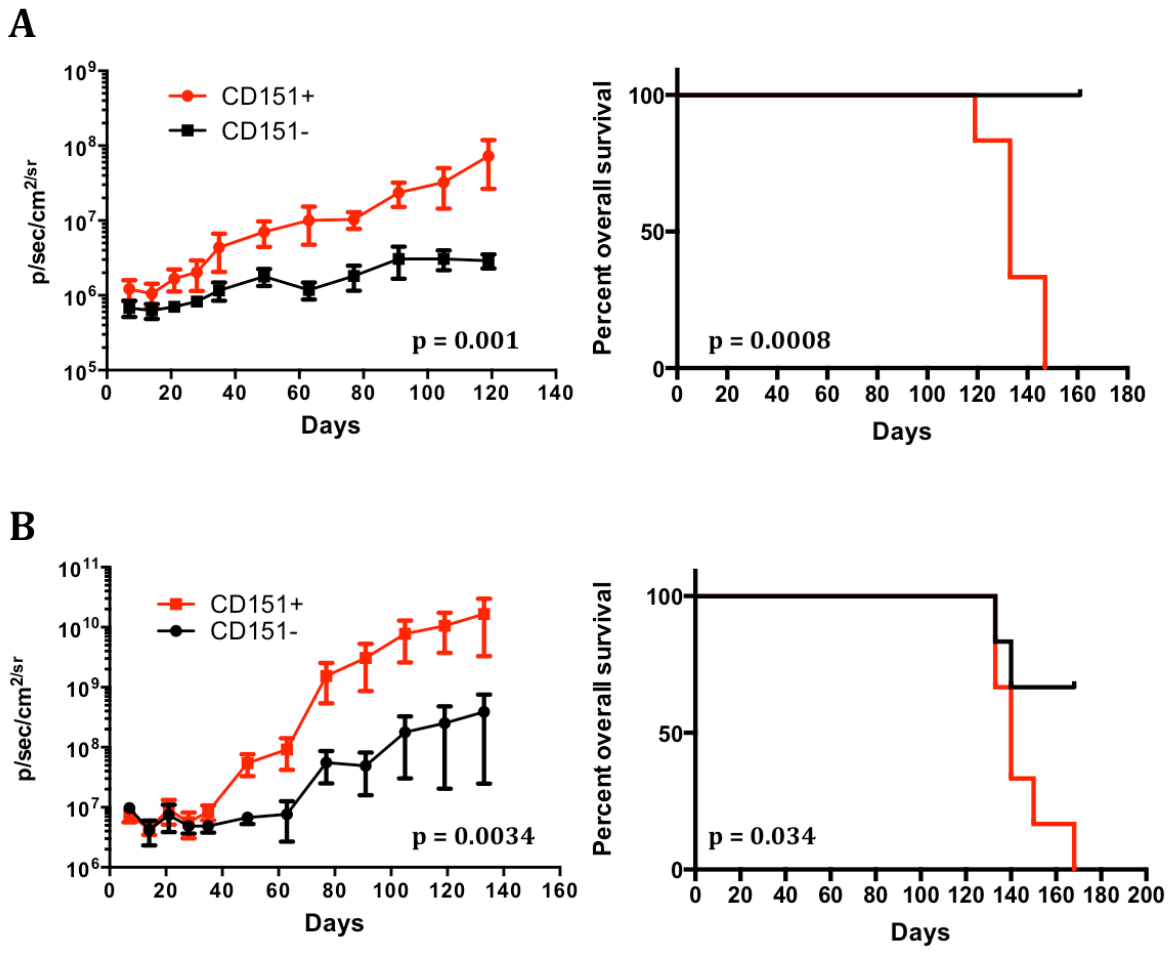

Figure 30 – Growth curves calculated based on bioluminescence signals (left) as well as Kaplan-Meier plots (right) for mice mice which were injected with purified CD151⁺ as well as CD151⁻ cells from the cell line OC14 (A) and OC15 (B).

For purified subpopulations originating from the cell line OC15, we observed similar results as seen for the cell lines OC12 and OC14. Also for this cell line, purified CD151⁺

showed a significant increased tumorigenic capacity compared to the CD151$^-$ cell fraction. Remarkably, we detected growth of tumors in two mice of the group injected with purified CD151$^-$ cells **(Figure 30B, left)**. Subsequent end point analysis of the individual tumors by flow cytometry revealed the presence of CD151$^+$ cells in these tumors (data not shown). This observation was also confirmed by immunohistochemistry **(Figure 31, OC15 CD151$^-$#3).**

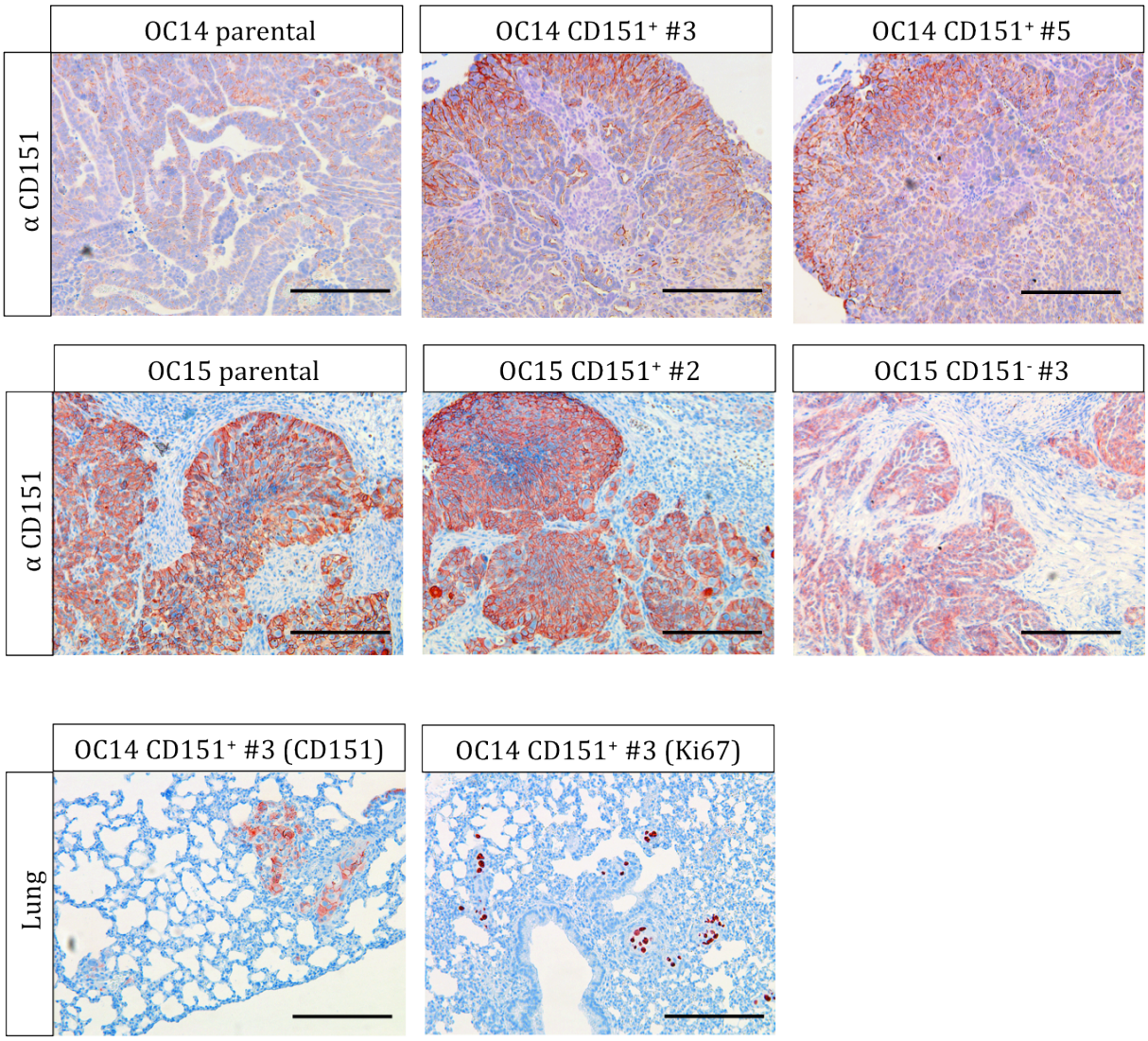

Figure 31 – Immunohistochemical analyses of CD151 expression in tumors and lungs dissected from mice injected with either parental OC14 /OC15 cell lines or their purified subpopulations. CD151 staining is predominantly membraneous. The staining intensity is slightly increasing from parental to purified CD151$^+$ cells. Note, OC15 CD151$^-$#3 showed expression of CD151$^+$ cells, probably due to contamination with CD151$^+$ cells during FACS sorting. Mice injected with CD151$^+$ cells (OC14) developed lung metastasis that stain positive for CD151 and Ki67 (scale bar 100 µm).

Given the mostly unidirectional repopulation dynamics we showed *in vitro*, this retrospective observation strongly suggests an initial contamination of the CD151$^-$ cell input with CD151$^+$ cells during enrichment by flow cytometry.

To further investigate the possible mechanisms behind the obtained results, we examined the expression of CD151 in association with described markers for tumor initiating cells in ovarian carcinoma. Therefore, we analysed if CD151 is coexpressed with CD24 and/or CD44 on the surface of our cell lines. The enrichment of described cancer stem cell markers in the CD151$^+$ subpopulation might be a possible explanation for the enhanced tumorigenic potential of these cells. Interestingly, only in one cell line we found a significant upregulation of a putative TIC marker in the CD151$^+$ subpopulation (OC15) **(Figure 32)**. In none of the other cell lines we found a correlation of the expression of CD151 with CD24 or CD44. Hence, we concluded that other factors might contribute to the differences observed in the subpopulations of CD151.

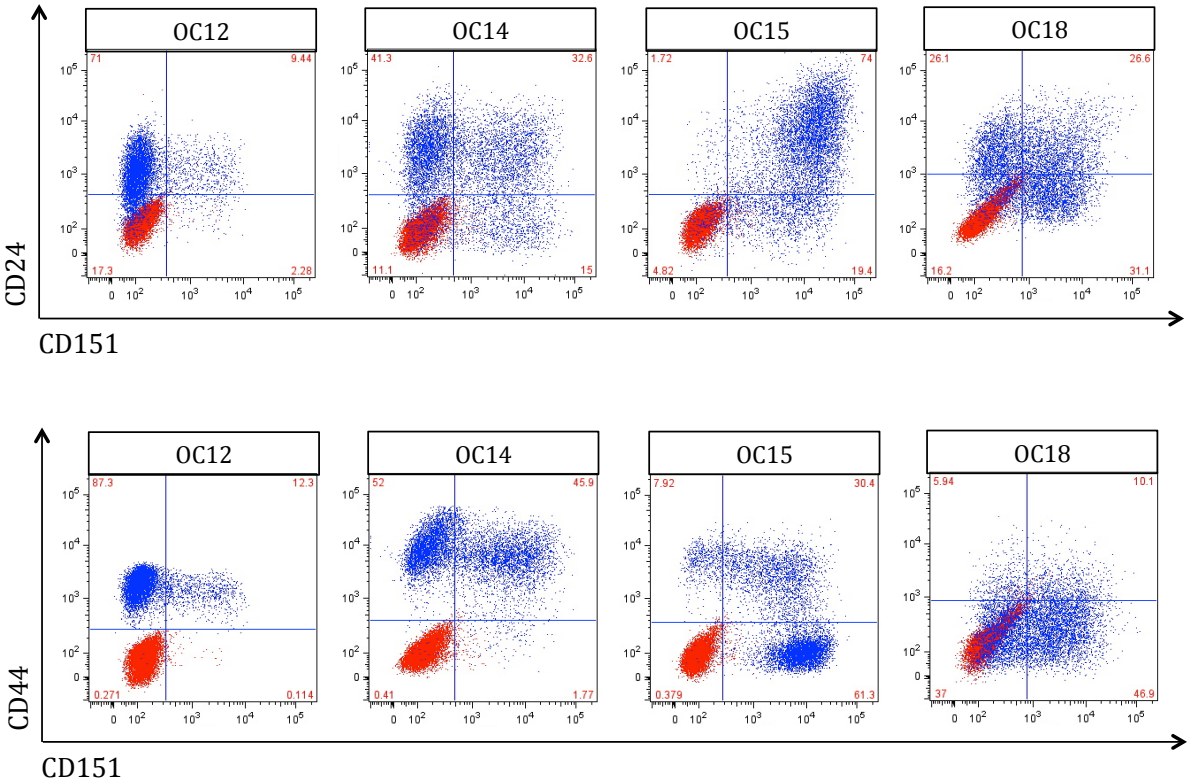

Figure 32 – FACS Analysis of described TIC markers in ovarian cancer in correlation to the expression of CD151 in the surface of primary SOC cell lines. Note, only for the cell line OC15 an enrichment of a TIC marker (CD24) in the CD151$^+$ subpopulation was observed.

Taken together, these data indicate that the CD151$^+$ cells of our primary SOC cell lines have an increased tumorigenic capacity compared to their CD151$^-$ counterparts. In the tested cell lines OC12 and OC14, the CD151$^+$ fraction was capable of generating tumors following injection of 1x10^4 cells whereas CD151$^-$ cells generated only one tumor in the same time period. Importantly, this tumor displayed a high expression of CD151$^+$ cells indicating a contamination and subsequent outgrowth of CD151$^+$ cells. Additionally, we observed the metastatic colonization of the lungs in mice injected with the CD151$^+$ cell fraction **(Table 8)**. These metastatic cells expressed CD151 and stained positive for the proliferation marker Ki67. In further investigations, we have been able to show that CD151 is not enriching for already described TIC markers in ovarian cancer, indicating that CD151 is functionally independent of these markers. These results strongly suggest that the CD151$^+$ cell fraction of serous ovarian tumor cells is enriched for TICs.

Table 8– Tumorigenic capacity as well as induction of lung metastases of CD151$^+$ and CD151$^-$ subpopulations

Cell line	Subpopulation	Tumor formation	Lung metastasis
OC12	CD151$^+$	6/6	2/6
	CD151$^-$	1/7	0/7
OC14	CD151$^+$	6/6	3/6
	CD151$^-$	0/6	0/6
OC15	CD151$^+$	6/6	0/6
	CD151$^-$	2/6	0/6

Analysis of CD151 mediated signaling

Gene expression analysis on CD151 predicts differences in pathway activity

Given the observed differences in growth and tumorigenicity between purified $CD151^+$ and $CD151^-$ cells, we hypothesized that more complex molecular differences might underlie these discrepancies. To uncover these mechanisms, we generated gene expression profiles of purified CD151 positive and –negative subpopulations from the cell lines OC12, OC14, OC15 and OC18 using the Illumina BeadChip Technology (HumanHT-12v4) **(Figure 33A)**. These gene expression profiles were applied for gene set enrichment analysis (GSEA) and correlated to described gene expression datasets. This analysis revealed a strong positive enrichment of distinct proliferation associated signatures such as the JNK/MAPK signaling pathway- or the EGFR signaling signature in the $CD151^+$ cells **(Figure 33B)**. One of the main activators of the JNK/MAPK pathway are integrins that signal through the recruitment and activation of Src family kinases (SFKs). These kinases activate Rac, which is upstream of PAK, NF-κB and the Jun amino-terminal kinase, JNK. A major JNK target is the transcription factor AP1, which is composed of Fos and Jun. The JNK/JUN pathway regulates a plethora of target genes, which are involved in cell cycle as well as survival and apoptosis [198]. Intriguingly, CD151 has been shown to directly interact with integrins and thereby regulating their signaling [191,192]. In parallel, CD151 has been proposed to be a molecular linker between integrins and growth factor receptors such as epidermal growth factor receptor (EGFR) [199]. Upon activation, EGF receptors recruit signaling proteins, such as Shc, Grb7, Grb2, Crk, Nck, the phospholipase Cγ (PLCγ), the intracellular kinases Src and PI3K, the protein tyrosine phosphatases SHP1 and SHP2 and the Cbl E3 ubiquitin ligase. This leads to the subsequent activation of the RAF/MAPK pathway, the phosphoinositide 3-kinase (PI3K) and the STAT signaling pathway, which induce cell proliferation, angiogenesis, migration, survival, and adhesion [200]. A distinct activation of these pathways in the $CD151^+$ subpopulation might explain the previous observations of a higher proliferation and an increased tumorigenic capacity of these cells. Importantly, the identified gene sets were exclusively enriched in the $CD151^+$ subpopulation.

We also found signatures that point to an activation of the Wnt pathway in the CD151⁺ subpopulation. An important pathway for non-canonical Wnt signal transduction is in turn the activation of JNK [201].

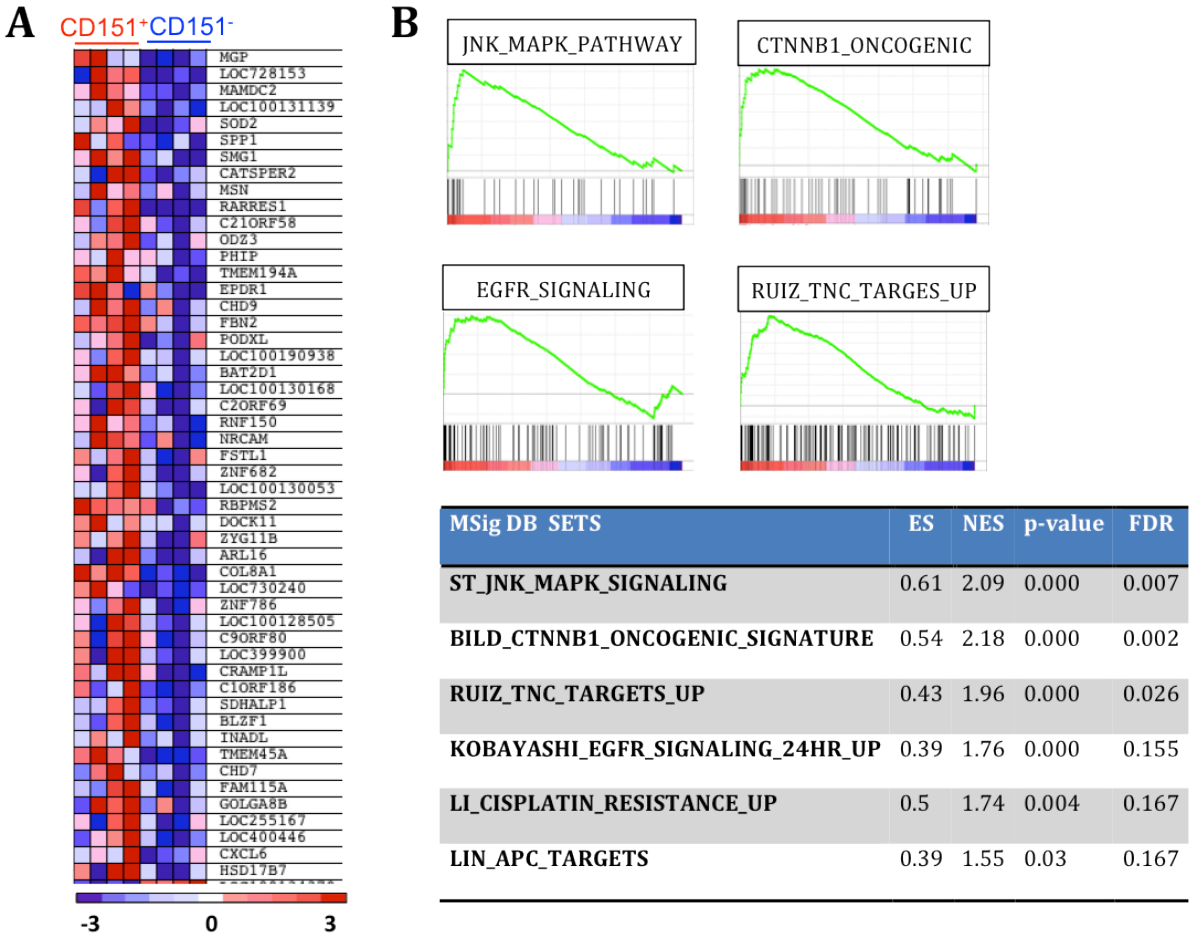

MSig DB SETS	ES	NES	p-value	FDR
ST_JNK_MAPK_SIGNALING	0.61	2.09	0.000	0.007
BILD_CTNNB1_ONCOGENIC_SIGNATURE	0.54	2.18	0.000	0.002
RUIZ_TNC_TARGETS_UP	0.43	1.96	0.000	0.026
KOBAYASHI_EGFR_SIGNALING_24HR_UP	0.39	1.76	0.000	0.155
LI_CISPLATIN_RESISTANCE_UP	0.5	1.74	0.004	0.167
LIN_APC_TARGETS	0.39	1.55	0.03	0.167

Figure 33 – Gene expression analysis on purified CD151⁺ and CD151⁻ cells from the cell lines OC12, OC14, OC15 and OC18. (A) Heatmap generated by GSEA depicting strongest upregulated genes in CD151⁺ subpopulation compared to CD151⁻ cells. (B) Overview of differentially enriched pathway signatures in CD151⁺ cells (statistics calculated by GSEA).

We next wanted to investigate whether the predicted activation of pathways in the specific subpopulation was also displayed on protein level. Therefore, we prepared protein lysates of the parental OC12 cell line as well as purified CD151⁺ - and CD151⁻ cells and tested the total expression level as well as the phosphorylation status of key proteins of respective pathway by Western blotting. As gene set enrichment analysis predicted a positive correlation of the purified CD151⁺ cells and an activation of the JNK/MAPK signaling pathway, we wanted to further investigate this pathway. The JNK/MAPK pathway comprises of a core signaling unit that is composed of a MAPKKK, typically MEKK1-MEKK4, which phosphorylate MKK4/7. These MKKs in turn activate

JNK [202]. Small GTPases of the Rho family (Rac, Rho, Cdc42) are the major activators of this pathway. Upon activation JNK dimerises and translocates to the nucleus to where it mediates the stimulation of the transcription factor AP-1 [203].

Moreover, to prove the direct connection between integrin signaling and CD151 as a modulator and activator of these, we included the determination of the activity of the Src family kinases (SFKs). As stated above, integrins signal predominantly through the recruitment and activation of SFKs [198]. Furthermore, SFKs can be stimulated by EGFR. The SFK members are activated by the phosphorylation of a tyrosine at (Tyr^{416}) that can be detected by Western blotting.

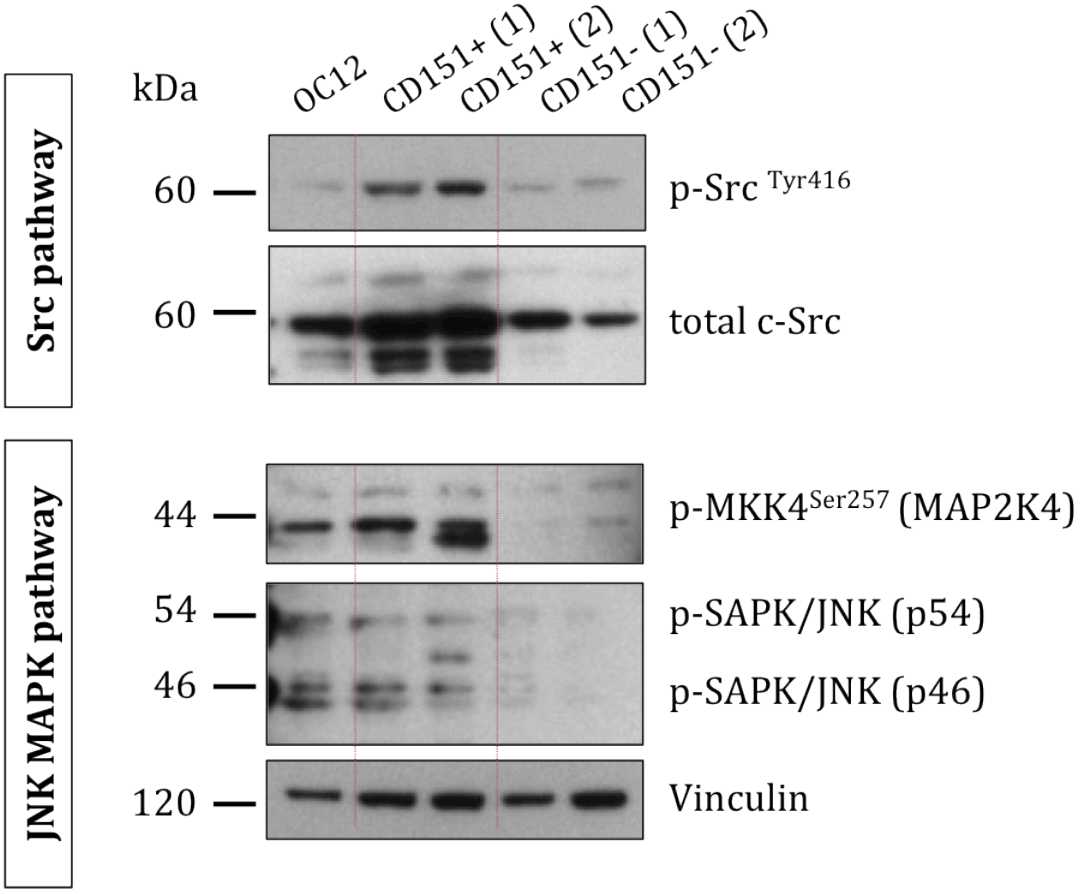

Figure 34 –Western blot analysis of pathway activation as predicted by gene set enrichment analysis. Protein lysates of two independent FACS sorting experiments were analysed for the expression and phosphorylation status of members of the oncogenic Src family kinases (top) as well as the JNK/MAPK pathway (bottom). Vinculin was used as a loading control.

Western blot analysis revealed a significantly increased phosphorylation at Tyr^{416} for the purified $CD151^+$ cells compared to the parental cell line or the $CD151^-$ cells **(Figure 34)**. Additionally, we observed an increased expression of the total Src protein in the

CD151 positive fraction. MKK4, a member of JNK/MAPK pathway, showed a similar phosphorylation as Src. The activation of this protein was significantly stronger in the $CD151^+$ cells than in the $CD151^-$ cells, but only slightly compared to the parental cells. Also the two isoforms of JNK itself displayed a stronger phosphorylation in the $CD151^+$ subpopulation than in the $CD151^-$ cells **(Figure 34)**. Altogether, these results confirmed our assumption that the $CD151^+$ subpopulation shows an increased activity of the JNK/MAPK pathway. We found an exclusive activating phosphorylation of MKK4 and JNK itself in the $CD151^+$ cells. Furthermore, we observed a significantly stronger phosphorylation of SFKs, an important signaling node between integrins, growth factor receptors and downstream pathways such as JNK/MAPK, RAF/MAPK and PI3K, which promote survival, angiogenesis, proliferation and invasion.

CD151 ablation directly affects cell signaling

The results shown above suggested CD151 to play an important role in the modulation and activation of integrin and EGFR signaling leading to an increased proliferation and tumorgenicity *in vivo*. To further prove that CD151 directly affects signaling pathways and thus influences the proliferation of tumor cells, we performed a stable silencing of CD151 by the lentiviral-mediated expression of shRNA specifically targeting the CD151 transcript in the cell lines OC12, OC14 and OC15. A scrambled shRNA (con) was used as a control and also introduced in the different cell lines. The constructs contained a GFP reporter cassette, which allowed the purification of transduced cells by flow cytometry. For further experiments, we went on with two different shRNA´s targeting CD151 (sh_RNA1/sh_RNA2), which have been selected by their efficiency in silencing CD151. The knockdown of CD151 was demonstrated by the flow cytometric measurement of the surface protein. For the cell line OC12, we reached a silencing of >95%, whereas for OC14 and OC15 the knockdown amounted between 60 and 70% **(Figure 35A)**.

Previous results indicated differences in growth behaviour between purified $CD151^+$ and $CD151^-$ cells. Therefore, we performed an analysis of the *in vitro* growth comparing control cells of the respective cell line with the corresponding CD151 silenced cells. We observed minor discrepancies in the growth behaviour between konockdown- and control shRNA transduced cell lines, that where more distinct in the cell lines OC14 and OC15 **(Figure 35B)**.

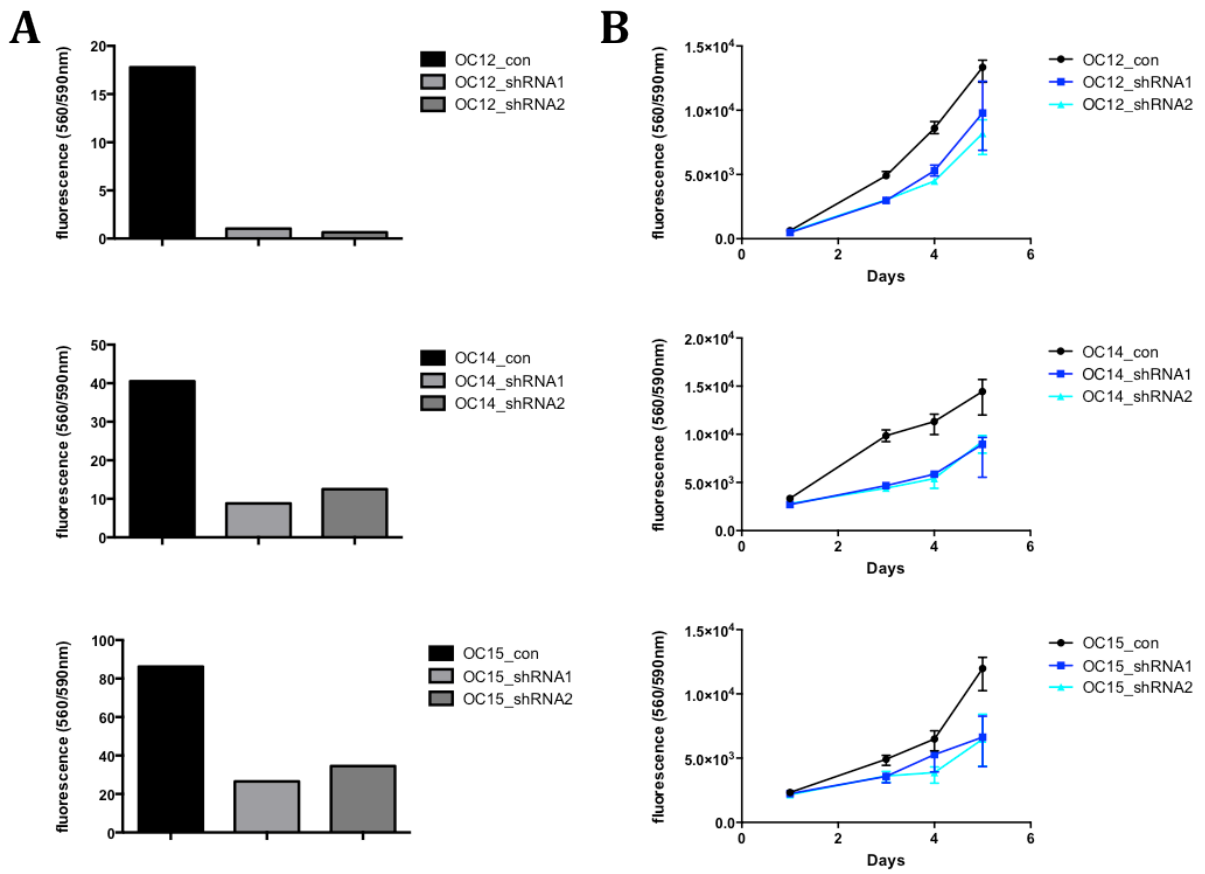

Figure 35 – (A) Lentiviral mediated shRNA knockdown of CD151 in the cell lines OC12, OC14 and OC15. Depicted are expression levels of CD151 as determined by flow cytometry on cells transduced with either scrambled control shRNA or two different shRNAs against CD151. (B) *In vitro* growth of SOC cell lines transduced with a scrambled shRNA con) or CD151 targeting shRNAs (shRNA1/2).

As previously shown, CD151 affects the activation of Src and seems to play role in the upregulation of integrin signaling to Src **(Figure 34)**. We next examined whether CD151 directly participates in pathway signaling or if CD151 as a marker indirectly enriches for a subpopulation with a certain pathway activation. To clarify this question, we analysed global changes in gene expression induced by silencing of CD151 by gene expression profiling comparing CD151 knockdown cells with scrambled control shRNA transduced cells. In the subsequent analysis by GSEA, we exclusively focused on gene sets that predict pathways that are deregulated in CD151 silenced cells. Under the top deregulated pathways, we found multiple gene signatures associated with the EGFR signaling pathway, the oncogenic Src pathway and targets of Myc (data not shown).

These data also supported our previous findings that CD151 affects the activation of Src and seems to play role in the upregulation of integrin signaling to Src **(Figure 34)**.

We next wanted to investigate if the predicted activation of pathways could also be detected on protein level. Therefore, we prepared protein lysates of the parental OC12 cell line, the scramled control (con) and the two CD151 silenced cell lines (shRNA1/shRNA2).

Western blot analysis revealed that CD151 ablation almost completely abrogated the activating phosphorylation of Src at Tyr^{416} in the CD151 knockdown cell lines **(Figure 36)**. In parallel, cells transduced with the scrambled shRNA showed similar phosphorylation levels at Tyr^{416} as parental tumor cells. We therefore excluded an indirect effect of the virus transduction.

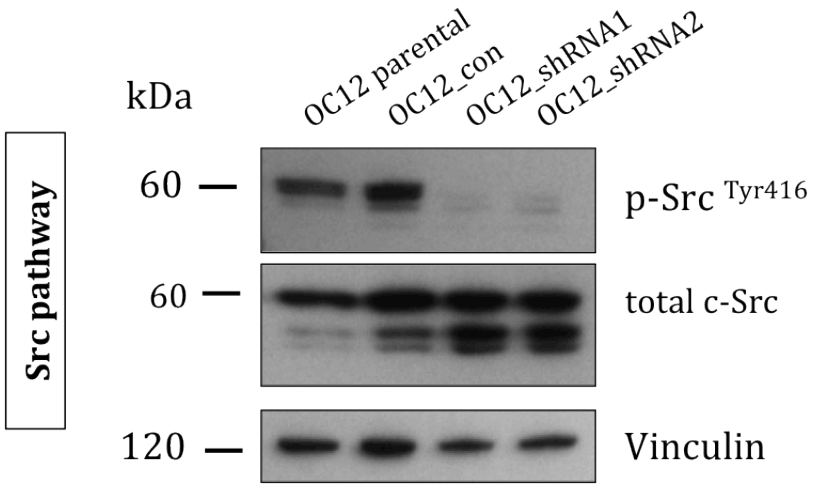

Figure 36 – Lysates of the parental OC12 cell line, scrambled shRNA transduced cells and CD151 silenced cells were analysed by immunoblot for the expression and phosphorylation status of members of the oncogenic Src family kinases.

In summary, we have been able to prove that the predictions of our gene expression approach can be used for the identification of differentially activated signaling pathways. We were able to link the increased tumorigenic capacity, observed in the $CD151^+$ subpopulation of various cell lines, to the activation of distinct signaling pathways. With the help of pathway predictions based on gene expression data, we identified several proliferative pathways such as the JNK/MAPK signaling pathway, the EGFR signaling pathway as well as the oncogenic Src pathway to be activated in $CD151^+$ cells. Furthermore, we were able to show CD151 ablation directly impacts Src family kinase activation.

Correlation of CD151 expression with clinical outcome in serous ovarian carcinoma

Our previous results strongly suggested that the CD151^{+} subpopulation is enriched for a tumor initiating subpopulation in serous ovarian carcinoma. In our xenograft studies, we have been able to show that purified CD151^{+} cells have a significant increased tumorigenic capacity compared to their CD151^{-} counterparts. However, we wanted to translate these findings to a larger cohort of patients and validate our previous gained results. We investigated whether differences in CD151 expression levels in primary tumors were associated with progression-free and overall survival in SOC. To this end, we analysed a representative pooled cohort of 489 patients for which transcriptomic profiles and clinical follow up were publicly available [66].

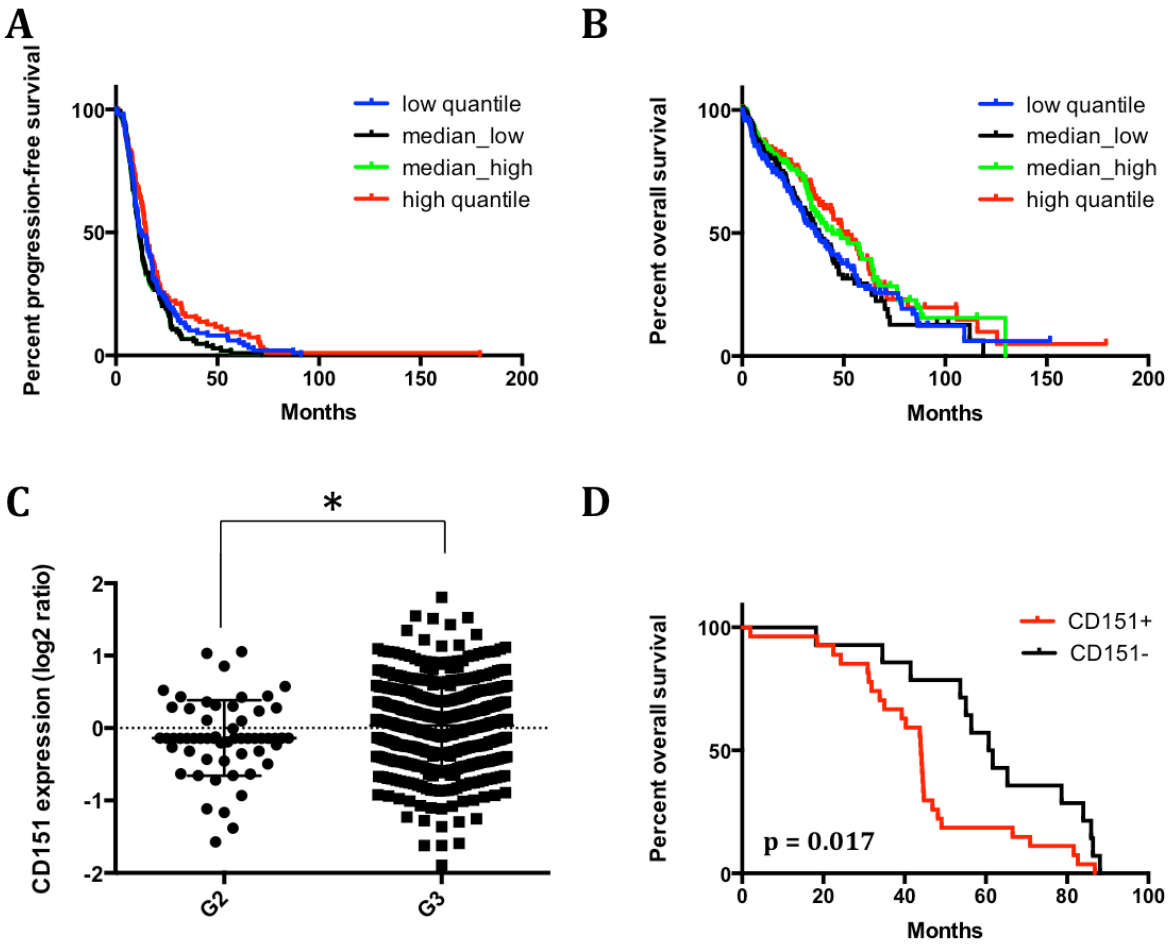

Figure 37 – Kaplan-Meier plots displaying overall survival (A) and progression-free survival (B) for four groups defined according to CD151 expression. (C) CD151 expression increases with tumor grade. (D) Overall survival is significant decreased for patients with a high expression of CD151 compared to patients with a low expression of CD151 in grade 2 tumors.

According to their expression of CD151, the patient cohort was divided into four groups (group 1:0-25%, group 2: 25-50%, group 3: 50-75%, group 4: 75-100% expression of CD151). Based on these groups, we investigated the correlation of CD151 expression with progression-free and overall survival. This comparison did not reach statistical significance neither for progression-free survival nor for overall survival SOC patients **(Figure 37A/B)**. We next wondered if this might be attributed to the characteristics of our patient cohort and included further parameters in our analysis. We observed that the expression of CD151 significantly correlated with grading of the tumor, meaning patients with an advanced disease exhibit elevated expression levels of CD151 **(Figure 37C)**. We analysed the two grading's provided in out patient cohort separately. Interestingly, patients with a low-grade tumor (G2) showing a high expression of CD151 had a significant shorter overall survival compared to patients with a low expression of CD151 and a tumor of this grading **(Figure 37D)**. These observations would suggest a selection for $CD151^{+}$ cells during tumor development. Furthermore, patients showing a high expression of CD151 have a significant poorer prognosis than patients with a low expression of CD151 in low-grade tumors.

6 Discussion

Ovarian cancer represents the fifth-leading cause of cancer related death among women in the United States and Europe [204]. Among ovarian cancer, high grade serous ovarian carcinoma (SOC) represents the most aggressive subtype accounting for approximately 70% of all deaths [66]. The overall five-year survival probability is only 30% [205]. Despite improvements in diagnosis and therapy, the survival rate did not virtually change in the last three decades. A major obstacle in SOC is disease recurrence after therapy, which prohibits the cure of this cancer [206].

Disease recurrence is believed to b by small numbers of persisting cells that have been able to escape standard treatment by platinum-taxane based chemotherapy, raising the possibility that intrinsically resistant cancer cells account for re-growth of the tumor, treatment failure and relapse. In the CSC model, treatment failure is reflected by the fact that conventional chemotherapies are rather unspecific and mainly eradicate the tumor bulk sparing the cancer stem cell compartment. Therefore, it is of highest importance to identify targets, which would enable the treatment of these cells. In order to do so, these cells need to be purified and characterized, which requires CSC specific markers.

In this study, we present the establishment and first characterization of a novel model for serous ovarian carcinoma, which fully recapitulates the human disease. Importantly, we showed that xenograft tumors formed upon injection of our primary SOC cell lines display histopathological features of the patient tumor and express the two clinically used SOC specific markers CA125 and WT1. By the help of this model we were able to demonstrate that the four SOC subtypes, recently described by the researchers of The Cancer Genome Atlas (TCGA), are also present in *in vitro* cultivated cells and that respective subtype is maintained in their corresponding xenograft tumors.

Furthermore, we describe a novel surface marker (CD151) identifying a functionally different subpopulation within the tumor, which displays properties of tumor initiating cells. Cells that have been purified for the expression of CD151 exhibits an increased tumorigenic potential compared to their $CD151^-$ counterparts in xenoraft mouse models. Moreover, these cells show a distinct activation of pathways implicated in proliferation, migration and invasion. We proved that the expression of CD151 correlates with an advanced disease stage and defines patients with a significant decreased overall survival

in low-grade tumors of serous ovarian carcinoma. Taken together, our model is perfectly suited for the evaluation of molecular subtypes within SOC, drug screens and the study of tumor initiating cells in SOC.

Establishment and characterization of a novel patient matched model system for serous ovarian carcinoma

In order to study serous ovarian carcinoma more precisely we established a novel model system, which combines serum-free cultivation of primary cell lines with xenotransplantation. This advanced model faithfully recapitulates histolopathological features of the patient tumor and reflects recently described molecular subtypes of serous ovarian carcinoma. Additionally, we showed that our model preserves the heterogeneous nature of each individual patient tumor. After the enrichment of tumor cell content using a xenograft mouse model, we were able to directly establish primary cell lines out of the patient specimen. Previous studies proved that primary and low passage xenografts recapitulate the histology of the primary tumor in ovarian cancer [141-143], but they also showed that after a certain passage in the xenograft nuclear and morphological changes were apparent, highlighting the importance of a careful histological evaluation [142]. A comparison of the original patient tumors and their corresponding primary xenograft tumors revealed that all histological features of the primary tumor are well preserved in our model. These observations are in line with other studies [141-143]. In addition, our established primary xenograft tumors express the two clinically used serous ovarian carcinoma specific markers CA125 and WT1.

Xenograft mouse models are well accepted tools for the identification of tumor initiating cells [141-143] and drug screenings in ovarian cancer [207]. Usually, highly immunocompromised mice are used in these studies, which have been genetically modified and therefore harbour defects in important parts of the immune system. This immunodeficiency inhibits the rejection of the graft by the host immune system and the extent influences the success rate of transplantations [208]. However, these xenotransplantation assays have certain limitations. Major problems are nuclear and morphological changes in the xenograft tumors, which occur already after a few passages. Furthermore, hamper the strong differences between individual tumor specimen, e.g. variable tumor cell contents, the reproducibility of such assays.

Additionally, because of the high degree of immunodeficiency, the influence of the immune system on tumor development cannot be considered. This is especially problematic for immunotherapeutic approaches, which aim to engage the immune system against tumor cells.

To circumvent these problems genetic engineered mouse models for ovarian cancer have been developed, which should mimic the human disease more faithfully. These models possess a complete functional immune system and thus allow the study of interactions between tumor cells and the host immune system. Furthermore, they are indispensable for the realistic investigation of the role of the microenvironment in tumor progression. However, the development of genetically engineered mouse models for ovarian cancer has been hindered due to the lack of ovary specific promoters that drive transgene expression exclusively in the ovarian surface epithelium. Nowadays, several GEMs for ovarian cancer exist, which differ in the histological tumor subtype that is induced **(Table 2)**. These models improved our understanding regarding gene dysfunction necessary for tumorigenesis such as the deletion of *p53* and *Rb* or the overexpression of the known oncogenes *c-myc*, *Kras* and *Akt* . In order to completely understand the complexity of ovarian cancer and to use them as pre-clinical models for drug screening approaches, mouse models representing each subtype of ovarian cancer are needed.

Despite the mentioned advantages of these models, they also have certain limitations. Induction of ovarian tumors by the inactivation of the two major tumor suppressor genes *p53* and *Rb* using the Cre-loxP system is fairly costly and labor-intesive and therefore inappropriate for high-throughput compound screens. In this regard, the lack of an ovarian epithelium specific promoter remains a major problem for the development of GEM models for ovarian cancer. Furthermore, several studies already showed that findings acquired by the use of these mouse models have to be considered carefully and cannot be translated per se to the human situation. There is no direct correlation between drug responses observed in mouse models and the success of a therapy in the clinic [181].

Even though xenograft- as well as genetically engineered mouse models represent useful tools for the study of ovarian cancer, *in vitro* cell culture systems are indispensible for the investigation of cellular processes in a defined environment. Cell culture systems allow various manipulations of the cells and enable testing of hypotheses in a less complex system compared to the *in vivo* setting. By the help of *in*

vitro culture systems major insights has been gained into the biology of several cancers. In this respect, it has been shown that the culture conditions have a great impact on the genetic stability of the cells. Since development of the first *in vitro* cultures fetal calf serum (FCS) was usually added to the media as a source of nutrients and growth factors [209]. However, FCS-cultured cell lines often fail to recapitulate the morphological and histopathological characteristics of the original patient tumor upon xenotransplantation [167]. The loss of the stromal compartments within the xenograft tumor is one example for changes that were observed for FCS-cultured cells. Indeed, when we investigated the morphology of xenograft tumors induced by two of the most prominent ovarian cancer cell lines, SKOV-3 and OVCAR-3, it became clearly evident that SKOV-3 tumors completely lacked stromal parts and OVCAR-3 tumors showed only a minor presence of them **(Figure 17B)**. Furthermore, Lee and colleagues show that cells serially passaged in medium containing FCS acquire secondary mutations over time, which are not found in the original primary tumor. Additionally, cultivation with FCS promotes the outgrowth of subclones and the original heterogeneity of the patient tumor is lost over time [210].

In order to improve currently used culture systems for ovarian cancer cells, we applied serum-free cultivation techniques for the establishment of primary SOC cell lines. These serum-free cultures have been shown to preserve the genotypic and phenotypic features of several tumor entities [137,167,180]. For the establishment of the adherent *in vitro* culture system, we used primary xenograft tumors. Xenograft derived SOC cell lines were further investigated for their ability to form tumors in secondary recipient mice and the resulting tumors were evaluated for their histopathology. According to histological characteristics ovarian cancer is clinically classified into five distinct histotypes, which have significant different prognoses as well as sensitivities to platinum- and taxane based chemotherapies [12]. Therefore, the histopathological classification and verification of xenograft tumors is of highest importance. For instance, several commonly used ovarian cancer cell lines have been reported to not resemble the tumor subtype they are originated from [211]. To ensure that all primary cell lines, which have been established in this study, still recapitulate the histopathological features of their corresponding patient tumor, they were pathologically classified at the Department of Pathology of the University of Heidelberg. The direct comparison of patient tumor and corresponding cell line derived tumor revealed that morphological characteristics and the expression of histotype specific markers was very well retained in our model **(Figure 17A)**.

A total of 15 human SOC xenografts were established following intraperitoneal injection of $1x10^5$ – $1x10^6$ CD45 depleted ovarian tumor cells with an engraftment success rate of 65%. The tumor formation rate of the initial xenograft was mainly depending on the FIGO stage of the tumor and overall quality of the tumor sample. Whereas primary tumors with FIGO stages III and IV grafted with a success rate of 68%, we were not able to expand any tumor with the FIGO stage I.

A further parameter, which was identified to influence the engraftment success rate was the general quality of the primary specimen, particularly the quantity of cancer cells within the received tumor piece. Before preparation of primary tumor material for intraperitoneal injection, a part of the tumor was used for immunohistochemical analysis. Based on the results of immunohistochemistry we assessed the quantity of tumor cells within the received tumor piece and retrospectively link to engraftment success. However, we cannot exclude further factors, which might have influenced tumor growth. As described before, many tumors contain phenotypically and functionally heterogeneous cell populations [124], which might exhibit different abilities to grow in the xenograft model. Furthermore, the normal ovary is a complex tissue containing several distinct cell types and the cell of origin for SOC has not been fully defined yet [26]. For that reasons, we cannot ensure that the heterogeneous nature of the original patient tumor is completely reflected by the corresponding xenograft.

For the establishment of a primary serum-free culture system for SOC, we tested several substrates and growth factors to define the optimal conditions for the cultivation and expansion of primary human ovarian cancer cells. First, we determined a substrate, which yielded a maximal outgrowth of primary epithelial ovarian cancer cells. Therefore, we compared the growth of tumor cells on Primaria flasks to the expansion on flasks with different coatings (3% FCS and Collagen) as well as the cultivation in suspension. We detected the proliferation of adherent cells on every tested substrate. However, we observed no significant growth advantage of any kind of coating **(Figure 11A)**. Spheroid cultures have been described for the cultivation of several primary tumor cells [180], including ovarian cancer cells [143]. In serous effusions of ovarian cancer patients, similar structures have been observed [212]. We confirmed these results by our observations on ascites originating from patients as well as our xenograft models.

However, when we compared the adherent cultivation of our primary tumor cells on Primaria flasks with the spheroid culture on ultra-low attachment flasks **(Figure 11A)**, we noticed significant faster outgrowth in the adherent culture. Moreover, we detected

also a lower amount of dead cells using Primaria flasks instead of ultra-low attachment flasks. We explained these results with the fact that the adherent culture provides an optimal supply of nutrients and growth factors for nearly all cells. In contrast, we detected especially in larger spheroids the appearance of dead cells in the core of the spheroid, which might be due to a worse supply with nutrients for these cells. Additionally, several studies reported that the insufficient access to growth factors leads to differentiation of the cells [167,176].

According to previous reports, we selected a panel of growth factors and hormones for further experiments on the optimal cultivation of primary ovarian cancer cells [183-185]. Female sex hormones such as human menopausal gonadotropin, human chorionic gonadotropin and estrogen have been described to stimulate the growth of primary ovarian tumor cells. Therefore, we included these substances in our cultivation experiments. However in our hands, only the combination of our basic SCM with estradiol led to significant increase in the number of outgrowing cells. In the cultures supplemented with hMG and/or hCG, we could only detect a higher number of differentiated cells **(Figure 11B)**. Furthermore, we tested the supplement of the growth factor heregulin to our basic media. As we observed a significant enhancement in growth of primary ovarian cancer cells only estradiol, we decided to use hormone together with our basic SCM and Primaria flasks for all further experiments **(Table 3)**. Even though, we cannot exclude that tumor cells, which were not tested in this initial experiment, would need these hormones/growth factors to proliferate *in vitro*.

We were able to establish 8 stable primary SOC cell lines, which show a broad heterogeneity in morphology, *in vitro* growth, clongenicity as well as the expression of markers for putative tumor initiating cells. Out of four described TIC markers for ovarian cancer, we found three of these markers, CD24, CD44 and CD117, expressed at different levels on our SOC models. CD117 was not expressed on every cell line, which is in line with previous reports [142]. However, none of the tested cell lines showed the expression of CD133 **(Table 4)**. Stewart *et al.* reported that the expression of CD133 on tumorigenic cells changed during passaging, suggesting that CD133 is not stably expressed on ovarian cancer cells.

Taken together, we cannot exclude the introduction of a certain selection pressure by our *in vitro* culture, and the subsequent outgrowth of distinct clones. On the other hand, tumors that were derived from our primary SOC cell lines represent several hallmarks of human serous ovarian carcinoma, including the stable expression of SOC specific clinical

markers (CA125 and WT1). Additionally, we observed a broad heterogeneity in the morphology of the cell lines as well as in their expression of putative TIC markers, indicating the presence of a certain repertoire of different cells.

The combination of serum-free cultures with advanced xenograft models enables the dissection of the biology of SOC at a molecular level as well as the functional validation in xenograft tumors. Therefore, our system has the potential to significantly improve existing models.

Gene expression profiling on the SOC model reveals signaling pathways activated in ovarian cancer and the presence of all four SOC subtypes

To identify molecular pathways that contribute to SOC and subsequent new therapeutic approaches, we analysed the gene expression profiles of our primary SOC cell lines and their corresponding derived tumors. The analysis of differential gene expression between our SOC models and normal human ovarian surface epithelium revealed pathways specifically altered in ovarian cancer.

Interestingly, we found that the vast majority of upregulated genes in the SOC model compared to human ovarian surface epithelium are associated with the regulation of mitosis, cell division, cell cycle processes and proliferation. In particular, we identified several members of the *FOXM1* transcription network such as *AURA, CCNB1, BIRC5* and *CDC25* **(Figure 20A).** In non-neoplastic cells, *FOXM1* is regulated by *TP53* and repressed upon DNA damage [213]. The overexpression of *FOXM1* and its proliferation-related target genes suggests a high frequency of *TP53* mutations in the SOC models. Several other studies also described a significant activation of this network when they compared tumors with normal epithelial tissue in SOC [66].

Furthermore, using gene set enrichment analysis (GSEA) we found multiple gene signatures related to alterations in DNA repair pathways positively enriched in the SOC specific gene expression datasets **(Figure 21B,C)**. Defects in DNA repair pathways are very common in SOC, especially mutations in *BRCA1* and *BRCA2*. These proteins are required for DNA double strand break repair by homologous recombination. Cells without functional BRCA1 or BRCA2 perform DNA repair by non-homologous end joining which leads to chromosomal rearrangements and genomic instability [26]. It has been shown that cells with a mutated or methylated *BRCA1* or mutated *BRCA2* are highly

responsive to PARP inhibitors [66], indicating the use of our model system for preclinical trials.

In line with other studies [26], also signatures that point to an activation of the IL-6 pathway were positive correlated with the gene expression datasets of the SOC model **(Figure 21B,C)**. The vast majority of ovarian cancers show an overexpression of IL-6 leading to an autocrine stimulation of the IL-6 receptor. This in turn facilitates the nuclear translocation of STAT3 and upregulation of target genes, which drive proliferation, inhibit apoptosis and induce angiogenesis.

The analysis of the gene expression profiles in our model system revealed the activation of several described key pathways of SOC. We confirmed that in addition to morphological- and histopathological features, our primary SOC cell lines also reflect genetic hallmarks of ovarian cancer. Furthermore, our model might serve as basis for molecular studies on the identified pathways and provide the opportunity for preclinical drug screening.

Combined efforts by the researchers of The Cancer Genome Atlas Research Network (TCGA) led to the identification of at least four distinct transcriptional subtypes of SOC. These subtypes were based on gene expression analyses on a set of 489 human serous ovarian tumors. The subtypes were termed 'differentiated', 'immunoreactive', 'mesenchymal' and 'proliferative' on the basis of gene content in the clusters [66]. The study by the TCGA did not include any xenograft or *in vitro* cell line models, thus we were interested if the described subtypes are also present in our SOC model.

Indeed, we were able to clearly assign every SOC cell line as well as their corresponding xenograft tumor to one of the described subtypes **(Table 7)**. As we were able to establish *in vitro* cultures for every of the four subtypes, we concluded that none of the subtypes has significant lower potential to grow *in vitro* or in the xenograft model under the given conditions. However, at the moment our data are based on quite a low number of cell lines per subtype. Further investigations are necessary to enable significant conclusions on the molecular features of these subtypes. Anyhow, as the TCGA study did not include any subtype specific pathway analysis or researches on drug sensitivities of the different subtypes in e.g. available human ovarian cancer cell lines, our model might serve as basis for first pathway analysis and subsequent subtype-specific therapies.

CD151 enriches for tumor initiating cells in serous ovarian carcinoma

So far, several groups have claimed to identify tumor initiating cells in ovarian cancer. Described markers for the enrichment of tumorigenic cells in ovarian cancer are CD24 [144], CD44 [140], CD117/CD44 [143], and CD133 [141]. However, the distinct phenotype of the TIC population in ovarian cancer has not been defined satisfying. Stewart *et al.* investigated a cohort of 138 SOC patient samples and tried to confirm the previous mentioned TIC markers. They reported that most of the ovarian cancers in their study showed no expression of a $CD44^{+}CD117^{+}$ subpopulation. We gained similar results for our primary SOC cell lines. Whereas CD44 was expressed at medium or high levels, CD117 showed only a very low or no expression **(Table 4)**. Furthermore, this study could not confirm an increased tumorigenic potential in the described subpopulation [142]. In order to identify novel differentially expressed surface markers on our primary SOC cell lines, which might lead to the identification of functional subpopulations, we performed a large scale surface marker screen. In addition to previous identified surface molecules such as CD24 and CD44, the screen revealed multiple heterogeneous expressed markers **(Figure 23)**. As our aim was to discover and characterize novel surface markers that define TIC populations in ovarian cancer, we focused on molecules that have not been implicated in tumor initiation in ovarian cancer before. One of the molecules, which attracted our attention, was CD151 **(Figure 23, Plate2)**. Interestingly, CD151 was highly differential expressed among all our primary SOC cell lines **(Figure 24A)**. This marker was not yet described to enrich for TICs in ovarian cancer but has been proposed for prostate cancer [197]. Furthermore, the expression of CD151 has been shown to correlate with a poor prognosis, advanced disease stage and metastasis in several types of cancer [193-196]. Indeed, we gained similar results by comparing the expression level of CD151 to the origin of the tumor cells. Cell lines that were established from serous effusions such as ascites or pleural effusion expressed significant higher levels of CD151 than cell lines derived directly from tumor material. For instance, the cell lines OC12 and OC21 that were directly derived from tumor show a significant lower expression of CD151 compared to cell lines originating from ascites (OC15) or pleural effusion (OC20) **(Figure 24B)**.

Next we were interested if the expression levels of CD151 are retained in xenograft tumors derived from the corresponding SOC cell line. The analysis of

immunhistochemical stainings of different SOC cell line derived xenograft tumors confirmed that the CD151 is expressed in the corresponding tumors and that the expression level is reflected by the corresponding tumor **(Figure 25)**. Moreover, we observed a specific membrane associated expression pattern of CD151 in the xenograft tumors, which is line with previous reports describing CD151 to be mainly expressed on the cell membrane and to interact directly with several integrins [191]. Particularly, CD151 is a member of the transmembrane 4 superfamily whose members play a role in various cellular functions such as proliferation, differentiation as well as cancer cell invasion and metastasis [189,190].

Having confirmed that the heterogeneous phenotype of CD151 is stable between primary SOC cell lines and corresponding xenograft tumor, we wondered whether the $CD151^+$ subpopulation has different capacities concerning self-renewal and differentiation compared to the $CD151^-$ subpopulation. Keeping in mind that the expression of the molecule correlates with a poor prognosis as well as metastasis and CD151 was shown to be involved in the adhesion dependent activation of RAS, RAC1 and CDC42 [192].

To investigate if the two populations show different characteristics, we purified $Venus^+/CD151^+$ and $Venus^-/CD151^-$ cells from the SOC cell line OC12. To note, this cell line has been transduced before with a lentiviral reporter containing the Venus fluorochrome. The purified populations were mixed together in the same ratio and analysed in regular intervals. By the help of this experiment, we clearly showed that $CD151^+$ cells give rise to $CD151^+$ and $CD151^-$ cells, whereas $CD151^-$ cells were not able to repopulate the $CD151^+$ cell fraction **(Figure 26A/B)**. Furthermore, we noticed that the total amount of cells originating from the $Venus^-/CD151^-$ cell population declined over time in our culture **(Figure 26D)**. These results led to the assumption that $CD151^+$ cells might have an increased proliferative ability and that $CD151^-$ cells represent a more differentiated state exhibiting a lower potential to differentiate. Interestingly, Ang and colleagues described in a study on prostate cancer that the expression of CD151 inversely correlates with the differentiation status of the tumor, meaning well-differentiated tumors show no or only a weak expression of CD151.

Given the observed discrepancies in self-renewal and differentiation between the $CD151^+$ subpopulation and the $CD151^-$ counterpart, we wondered whether this might be explained by a differential proliferative capacity. The analysis of the proliferation of both

subpopulations revealed a higher proliferation of the CD151$^+$ cell population in general. However, these differences did not reach statistical significance in all tested cell lines **(Figure 27)**. At this point it has to be admitted that the short term application of EdU, used in this assay, could lead to the incorporation into cells, which will arrest posterior to the EdU pulse [214]. Thus, a significant difference for all cell lines between the subpopulations might be masked due to the selection of an inadequate pulse period.

In order to further investigate functional differences between CD151$^+$ and CD151$^-$ cells, we performed a xenotransplantation assay comparing the two purified CD151 subpopulations. We assessed the ability of both purified populations to form tumors in immunocompromised mice for three different SOC cell lines. In all three experiments CD151$^+$ cells were able to induce growth of tumors, whereas CD151$^-$ could not **(Table 8)**. In some cases, we observed tumor growth in mice injected with CD151$^-$ cells, but have been able to show that this was due to a contamination with CD151$^+$ cells. CD151$^+$ cells in these tumors were detected by flow cytometry as well as immunohistochemistry **(Figure 31)**. Mice injected with CD151$^-$ cells were further monitored for appearance to tumor growth for at least 140 days or more. *In vivo* growth curves determined by bioluminescence imaging as well as overall survival of mice was highly significant **(Figure 28/30)**. According to these data, we assume that CD151 defines a tumor initiating subpopulation in SOC. Per definition, TICs are able to adjust better to changing environmental conditions and thus able to induce tumor growth [124]. Interestingly, CD151 has been reported previously to enrich TICs in prostate cancer together with further markers confirming our data [197]. Consistent with the CSC model, CD151$^+$ TICs yield tumors containing both CD151$^+$ and CD151$^-$ cells **(Figure 29/31)**. In line with our data, several studies described that the ablation of CD151 notably delays tumor progression in various mouse xenograft models [199].

Additionally, we observed metastatic spread to the lungs in the mice injected with purified CD151$^+$ cells for two of the three cell lines tested. Metastatic colonies in the lung stained positive for CD151 as well as Ki67, indicating that are also proliferative. To note, we did not detect occurrence of lung metastasis in the parental OC 12 cell line indicating an enrichment of for more metastatic cells by purification for CD151 positivity **(Figure 29)**. As stated above, CD151 has been implicated several times to promote metastatic growth to the lung [192,215,216]. These reports strongly support our findings.

To investigate if the CD151$^+$ subpopulation enriches for already described TIC markers, we analysed the expression of CD151 in association with CD24 and CD44 in several primary SOC lines. According to these results, we excluded an enrichment for known TIC markers and concluded that other factors might contribute to the observed phenotype.

In summary, we showed that our primary SOC cell lines heterogeneously express various surface molecules. These markers can lead to the identification of functional subpopulations. Our data strongly suggest that CD151 enriches for tumor initiating subpopulation in SOC. Additionally, CD151 has been shown to promote metastatic spread to the lungs in our xenograft model. Previous reports support these results. Moreover, CD151 is functionally independent of described TIC markers in SOC.

CD151$^+$ cells show a distinct pathway activity and ablation of CD151 directly impacts signaling

CD151 has been reported to be involved in the adhesion dependent activation of Ras, Rac1 and Cdc42 [192]. This activation is mediated by the direct interaction of several integrins with CD151 [191]. Further studies described CD151 as a linker between integrins and growth factor receptors such as EGFR and c-MET [199].

However, to uncover possible pathways regulated by CD151 specifically in SOC, we performed gene expression profiling on purified CD151$^+$ cells of four different SOC cell lines and compared them to the profiles of CD151$^-$ cells. Gene set enrichment analysis revealed a strong positive correlation of the CD151$^+$ cells with distinct proliferation associated signatures such as the JNK/MAPK signaling pathway and EGFR signaling **(Figure 33B)**. Integrins, which directly interact with CD151, have been described to be main activators of the JNK/MAPK signaling pathway [198]. According to these results, CD151 activates integrin signaling via the JNK/MAPK pathway. This activation occurs by the recruitment and activation of Src family kinases (SFKs).

When we analysed the activation of SFKs and members of the JNK pathway on protein level, we indeed detected a specific activation only in the CD151$^+$ subpopulation. In detail, Western Blot analysis revealed a significantly increased activating phosphorylation of SFKs at Tyr^{416}. Furthermore, MKK4, which is upstream of JNK, and the two isoforms of JNK itself were activated by phosphorylation **(Figure 34)**. An increased kinase activity of JNK has been shown to control tumor initiation and promotion by affecting proliferation of tumor cells [217,218]. SFKs have been identified to

be overexpressed and activated in more than 50% of ovarian cancers [26]. These kinases are involved in a variety of cell signalling events, regulating cell proliferation and differentiation [219]. Our data reveal an increased activity of SFKs and members of the JNK pathway in the CD151$^+$ cell fraction compared to CD151$^-$ cells or parental cells. As the JNK pathway regulates multiple target genes, which are involved in cell cycle, survival and apoptosis [198], this might be an explanation for the observed differences between CD151$^+$ and CD151$^-$ cells.

Interestingly, JNK and Jun have been proposed to be essential mediators of oncogenic ß-catenin signaling [220,221], a signature that was also enriched in our analysis on CD151 **(Figure 33B)**. Additionally, we identified a signature predicting APC targets genes to be expressed in the gene expression profiles of the CD151$^+$ subpopulation, indicating an activation of the Wnt pathway in CD151$^+$ cells.

To directly investigate the effects of CD151 on growth and signaling in our SOC models, we stably silenced CD151 in several SOC cell lines by the lentiviral-mediated expression of shRNAs specifically targeting the CD151 transcript. Previous results suggested a differential growth of CD151$^+$ and CD151$^-$ cells. Therefore, we compared the growth behaviour SOC cell lines transduced with a scrambled shRNA to cells with a CD151 knockdown. This analysis yielded only minor discrepancies in *in vitro* growth between control- and CD151 silenced cell lines **(Figure 35B)**. A possible explanation might be that CD151 is *in vitro* not critical for the growth of the tumor cells. The cells are supplemented with various growth factors and nutrients and the cell culture is designed to ensure an optimal growth of cells. In contrast, the situation *in vivo* is completely different. There, cells have to adapt to a certain environment, growth factors and nutrients are limited and cells have to adhere. This hypothesis is supported by several reports, which found a significant the ablation of CD151 at least significantly delayed tumor progression [199].

To clarify the question if the ablation of CD151 induces global in gene expression, we compared the gene expression data of SOC cell lines transduced with the scrambled control shRNA to CD151 knockdown cells. Intriguingly, we found several gene signatures associated with EGFR signaling, oncogenic Src signaling and targets Myc significant deregulated supporting our previous data on the purified CD151$^+$ subpopulation **(Figure 34)**. In order to validate the predicted pathway activation, we compared the phosphorylation status of parental cells to cells transduced with control

vector and CD151 silenced cells. Indeed, Western blot analysis revealed an almost complete abrogation of the activating phosphorylation of Src at Tyr^{416} **(Figure 36)**.

Taken together, we showed that molecular analyses on our advanced SOC model system can be used for the identification of subpopulation-specific pathway activities. By this approach, we were able associate an increased tumorigenic capacity, observed in for CD151^{+} cells of various cell lines, by the activation of distinct pathways. We identified several pathways driving proliferation, survival and metastasis such as the JNK/MAPK signaling pathway, the EGFR signaling pathway as well as the oncogenic Src pathway to be induced by the interaction of integrins and CD151. Moreover, we found that the ablation of CD151 directly abrogates SFK activation.

Interestingly, SFK inhibitors are already under evaluation in several clinical trials for ovarian cancer. The Src inhibitor Saracatinib is been investigated in combination with Paclitaxel against Platinum-resistant ovarian cancer in a phase II study (NCT01196741). Dasatinib, a further small molecule kinase inhibitor targeting Src, is currently evaluated in a phase I clinical trial in combination with Caboplatin and Paclitaxel (NCT00672295). Furthermore, several studies described the usage of CD151 blocking antibodies in different animal models resulting in an inhibition of metastatic spread of tumor cells and an increased survival of treated mice compared to non-treated mice [199]. They are increasing efforts in the development of antibodies targeting CD151, which effect tumor dissemination as well as proliferation. Currently, these antibodies are under evaluation [199].

CD151 correlates with an advanced disease stage and predicts outcome in low-grade serous ovarian carcinoma

In humans, an increased expression of CD151 is indicative of an advanced disease stage and a poor prognosis in multiple cancer entities [199]. However, the association of CD151 with clinical outcome, disease stage as well as prognostic factor in ovarian cancer is unclear. Moreover, the incidence of CD151 expression and the significance of CD151 on clinical outcome in ovarian cancer have not been investigated so far.

Our previous findings revealed that CD151^{+} cells have a significant increased tumorigenic capacity compared to their CD151^{-} counterparts in our xenograft mouse model. Furthermore, we showed that tumor cells originating from an advanced disease

stage express significant higher levels of CD151 indicating a selection process for CD151^{+} cells during tumor progression.

In order to prove our results in a larger cohort of patients, we investigated the transcriptomic profiles as well as clinical follow up data of a representative group of 489 SOC patients, which were publicly available [66]. Indeed, our analysis revealed a significant correlation of the expression of CD151 with an advanced disease stage. Patients diagnosed with a lower tumor grading (G2) showed a significant lower expression of CD151 compared to patients with an advanced tumor grade (G3) **(Figure 37 C)**. Hence, we were able to confirm findings made for lung-, colorectal-, prostate-, pancreatic- and breast cancer on the expression of CD151 also for ovarian cancer [199].

Next, we were interested if the expression of CD151 also predicts a shorter progression-free- or overall survival. Based on retrospective analysis of tissue microarray data CD151 has been shown to correlate with a significant shorter overall survival in various cancer entities [222]. However, when we analysed the expression of CD151 on transcriptional level in association with progression-free- and overall survival, we did not detect significant differences in the two parameters between patients with a high or a low expression of CD151 **(Figure 37 A/B)**. A possible explanation for the gained result might be the characteristic of our patient cohort, which mostly included high-grade SOC patients. As illustrated before, the expression of CD151 increases with disease stage. Therefore, we analysed mainly patients with an already elevated expression of CD151 distorting our results. A further reason might be that CD151 is typically involved in cancer initiation and progression in early disease stages. This hypothesis is supported by findings of Ang and colleagues, which described CD151 as a prognostic indicator of clinical outcome in low-grade prostate cancer [193]. According to these findings, we exclusively analysed patients diagnosed with low-grade tumors. Intriguingly, we detected a significant decrease in overall survival in patients wit a high expression of CD151 supporting the previous hypothesis.

In sum, our observations demonstrate a significant correlation between an increase in the expression of CD151 and disease progression. These data are supported by the findings of several groups in multiple cancer entities [199]. Furthermore, we have been able to demonstrate that the expression of CD151 is predictive a decreased overall survival in patients with low-grade tumors.

Concluding remarks and outlook

In this study, we present the development of an advanced model system combining the advantages of the serum-free culture of primary SOC patient specimen with xenotransplantation techniques. We demonstrate that this model system faithfully recapitulates all hallmarks of the original patient disease. Gene expression analyses based on established primary cell lines as well as corresponding xenograft tumors confirmed the activation of SOC-specific pathways and the presence of recently described subtypes of SOC. Furthermore, we demonstrate the successful application of this model for the identification of tumor initiating cells in SOC and identify molecular mechanisms underlying tumor heterogeneity.

Further analysis will focus on the molecular characterization of identified pathways driving SOC initiation and progression. So far, existing models for SOC have been incapable to accurately mimic the human disease. Drug screens performed using conventional cell lines often yielded targets of limited clinical relevance. Our model system opens up completely new possibilities for drug screening, including subtype-specific treatment. This could finally allow the development of targeted therapies for SOC. Hence, our model system could provide the basis for preclinical studies on inhibitors of these pathways. Furthermore, we confirmed the *FOXM1* transcription network as well as several DNA repair pathways to be significantly altered in our SOC model. Several of therapeutics targeting these pathways are already in clinical trials such as PARP inhibitors.

In the course of this work we identified the heterogeneously expressed surface molecule CD151 defining a TIC subpopulation in our primary SOC model. Furthermore, we were able to assign differential activated pathways to this subpopulation that explain the increased tumorigenic capacity. Thus, these findings might provide the basis for the development of appropriate therapeutics targeting the TIC population in SOC. As we identified JNK/MAPK- and EGFR signaling as well as the Src kinases specifically activated in TICs, inhibitors targeting these pathways in SOC in combination with the standard therapy might increase treatment success. Even though some of the pathway targets that were found in this study are already under evaluation in clinical trials, we suggest novel combinatorial treatments including combinatorial approaches targeting the described pathways. Our system might be instrumental as a pre-clinical model for

combinatorial treatment assessment optimizing treatment efficiency.

Myant and colleagues, recently described RAC1 as a mediator of Wnt-driven proliferation and cancer initiation [223]. JNK as well has been proposed to facilitate oncogenic ß-catenin signaling [221]. As already discussed, we found the JNK/MAPK signaling pathway specifically activated in CD151^{+} cells suggesting CD151 as a mediator of the activation of this pathway. Strikingly, we also found an enrichment of signatures predicting APC target genes as well as oncogenic ß-catenin signaling to be activated in the CD151^{+} cell fraction. It will be interesting to further investigate the role Wnt signaling in the context of tumor initiation in SOC.

Appendix

Patient cohort

Tumor ID	Cell_line	Age	Origin	FIGO	Nodal	Metastasis	Grade	Pathological diagnosis
OT11		76	Tumor	Ia	N0	M0	G2	Adenocarcinoma serous
OT12*	OC12	74	Tumor	IIIc	N1	M1	G3	Adenocarcinoma serous
OT13*		59	Tumor	IIIc	N1	M1	G3	Adenocarcinoma serous
Asc1*	OC14	61	Ascites	IV	N1	M1	G3	Adenocarcinoma serous
Asc2*	OC15	78	Ascites	IIIc	N1	M1	G3	Adenocarcinoma serous
OT15		75	Tumor	IIIb	N1	M1	G2	Adenocarcinoma serous
Asc3*		69	Ascites	IIIc	N1	M1	G3	Adenocarcinoma serous
OT18*	OC18	53	Tumor	IIIc	N1	M1	G3	Adenocarcinoma serous
OT19*	OC19	57	Tumor	IIIc	N1	M1	G3	Adenocarcinoma serous
PE1*	OC20	62	Pleural effusion	IIIc	N1	M1	G3	Adenocarcinoma serous
OT21*	OC21	60	Tumor	IIIc	N1	M1	G3	Adenocarcinoma serous
OT24		70	Tumor	Ic	N0	M0	G2	Adenocarcinoma serous
OT25*	OC25	78	Tumor	IIIc	N1	M1	G3	Adenocarcinoma serous
OT26*		69	Tumor	IIIc	N1	M1	G3	Adenocarcinoma serous
Asc4		66	Ascites	IIIc	N1	M1	G3	Adenocarcinoma serous
OT27*		65	Tumor	IIIc	N1	M1	G3	Adenocarcinoma serous
OT28		63	Tumor	IIIc	Nx	Mx	G2	Adenocarcinoma serous
OT29		60	Tumor	Ia	N0	M0	G2	Adenocarcinoma mucinous
Asc5*		80	Ascites	IIIc	N1	M1	G3	Adenocarcinoma serous
OT30*		72	Tumor	IIIc	N1	M1	G3	Adenocarcinoma serous
Asc6		76	Ascites	IV	N1	M1	G3	Adenocarcinoma serous
Asc7*		69	Ascites	IIIc	N1	M1	G3	Adenocarcinoma serous
OT31		58	Tumor	IIIc	N0	M0	G3	Adenocarcinoma serous
OT32		68	Tumor	IIIc	N1	M1	G3	Adenocarcinoma serous

Vector map pV2Luc2

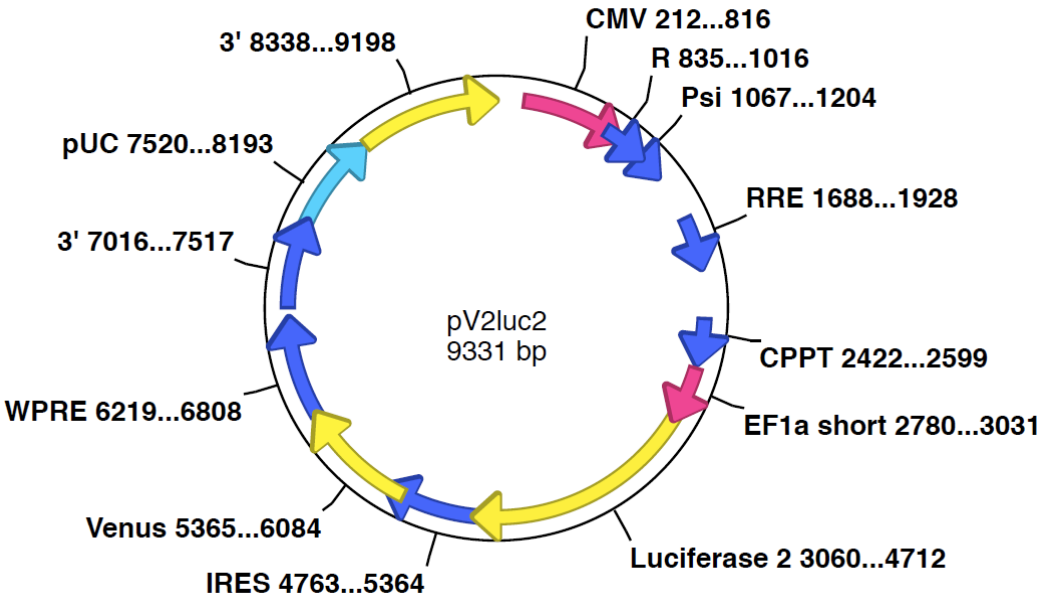

Acknowledgements

I would like to express my sincere gratitude to the following persons, who have supported and helped me during my PhD:

First of all, I would like to thank Prof. Andreas Trumpp for giving me the opportunity of performing my PhD in his lab even though I had to start with a new project. I would like to thank him for his enthusiasm, his encouragement, his discussions and for always having an open door if needed! I would also like to thank him for this great environment in the lab, which could not exist without him as the head of this department!

Dr. Martin Sprick: thank you for all your input, ideas and discussions to help me put my experiments on the right track. Thank you also, for being open-minded and for your humour!

I also want to thank my committee members, Prof. Petra Boukamp for being my second referee as well as Dr. Thomas Hofmann and Prof. Michael Wink to be part of my committee.

I would also like to express my gratitude to our pathologists Prof. Wilko Weichert and Dr. Albrecht Stenzinger. Thank you for your help and support on my work. It has been a real pleasure working with you.

Another big thanks goes to Dr. Thomas Höfner for all the discussions and input he gave on my project.

I am eternally obliged to my whole group, the „METICS“, whose patience and humor have rescued me from peril more times than I can recall: Elisa Noll, Elisa Espinet, Massimo Saini, Christian Eisen, Corinna Klein, Vanessa Vogel, Teresa Watermeier and the former members: Jan Engelhardt, Corinna Köhler, Irene Baccelli. I want to say a special thanks to Nolly, Elisa and Massimo for proof reading my thesis and for joining the group! THANK YOU! Thank you Massimo, if I had the chance, I would always share an office with you again!;) You became a good friend during the past few months. Thank

you Christian, for all your input, ideas and wisdom! You have been a great help throughout my thesis. Thank you Corinna, for helping me out when I needed it with my mice and being there! Thank you Vanessa, for all the work you invested in my project. Thank you Nolly, for all your happiness and being who you are! Thank you Elisa, for joining our group, being a great teacher and thank you for helping me with all of your advise!

Jacob, Camille, Alex, Paul, thanks for joinging the Trumpp lab and for all the good moments!
Wiebke, thank you for taking care of the samples and for being there!
I would also like to thank all other members of the Trumpp Lab for the great environment in this lab. A special thank you goes to Dr. Michael Milsom, who has always supported my project and gave me the opportunity for a great collaboration.

Der meiste Dank gebührt allerdings meinen Eltern, meinen Brüdern und meiner Freundin, ohne deren Unterstützung diese Arbeit niemals möglich gewesen wäre! Vielen Dank, dass Ihr immer für mich da wart - vor allem wenn es mal nicht so gut lief. Ihr habt mich immer unterstützt und an mich geglaubt. Vielen, vielen Dank dafür!

7 References

1 Siegel, R., Naishadham, D. & Jemal, A. Cancer statistics, 2013. *CA: a cancer journal for clinicians* **63**, 11-30, doi:10.3322/caac.21166 (2013).

2 Das, P. M. & Bast, R. C., Jr. Early detection of ovarian cancer. *Biomarkers in medicine* **2**, 291-303, doi:10.2217/17520363.2.3.291 (2008).

3 Nicodemus, C. F. & Berek, J. S. Monoclonal antibody therapy of ovarian cancer. *Expert review of anticancer therapy* **5**, 87-96, doi:10.1586/14737140.5.1.87 (2005).

4 Heintz, A. P. *et al.* Carcinoma of the ovary. FIGO 26th Annual Report on the Results of Treatment in Gynecological Cancer. *International journal of gynaecology and obstetrics: the official organ of the International Federation of Gynaecology and Obstetrics* **95 Suppl 1**, S161-192, doi:10.1016/S0020-7292(06)60033-7 (2006).

5 Narod, S. *et al.* Genetic heterogeneity of breast-ovarian cancer revisited. Breast Cancer Linkage Consortium. *American journal of human genetics* **57**, 957-958 (1995).

6 Frank, T. S. *et al.* Sequence analysis of BRCA1 and BRCA2: correlation of mutations with family history and ovarian cancer risk. *J Clin Oncol* **16**, 2417-2425 (1998).

7 Bewtra, C., Watson, P., Conway, T., Read-Hippee, C. & Lynch, H. T. Hereditary ovarian cancer: a clinicopathological study. *International journal of gynecological pathology : official journal of the International Society of Gynecological Pathologists* **11**, 180-187 (1992).

8 Moynahan, M. E., Cui, T. Y. & Jasin, M. Homology-directed dna repair, mitomycin-c resistance, and chromosome stability is restored with correction of a Brca1 mutation. *Cancer research* **61**, 4842-4850 (2001).

9 Narod, S. A. & Foulkes, W. D. BRCA1 and BRCA2: 1994 and beyond. *Nature reviews. Cancer* **4**, 665-676, doi:10.1038/nrc1431 (2004).

10 Feeley, K. M. & Wells, M. Precursor lesions of ovarian epithelial malignancy. *Histopathology* **38**, 87-95 (2001).

11 Naora, H. & Montell, D. J. Ovarian cancer metastasis: integrating insights from disparate model organisms. *Nature reviews. Cancer* **5**, 355-366, doi:10.1038/nrc1611 (2005).

12 du Bois, A. *et al.* Role of surgical outcome as prognostic factor in advanced epithelial ovarian cancer: a combined exploratory analysis of 3 prospectively randomized phase 3 multicenter trials: by the Arbeitsgemeinschaft Gynaekologische Onkologie Studiengruppe Ovarialkarzinom (AGO-OVAR) and the Groupe d'Investigateurs Nationaux Pour les Etudes des Cancers de l'Ovaire (GINECO). *Cancer* **115**, 1234-1244, doi:10.1002/cncr.24149 (2009).

13 Gilks, C. B. & Prat, J. Ovarian carcinoma pathology and genetics: recent advances. *Human pathology* **40**, 1213-1223, doi:10.1016/j.humpath.2009.04.017 (2009).

14 Goff, B. A. *et al.* Development of an ovarian cancer symptom index: possibilities for earlier detection. *Cancer* **109**, 221-227, doi:10.1002/cncr.22371 (2007).

15 Bast, R. C., Jr. *et al.* A radioimmunoassay using a monoclonal antibody to monitor the course of epithelial ovarian cancer. *The New England journal of medicine* **309**, 883-887, doi:10.1056/NEJM198310133091503 (1983).

16 Clarke, C. H. *et al.* Proteomic biomarkers apolipoprotein A1, truncated transthyretin and connective tissue activating protein III enhance the sensitivity of CA125 for detecting early stage epithelial ovarian cancer. *Gynecologic oncology* **122**, 548-553, doi:10.1016/j.ygyno.2011.06.002 (2011).
17 Salani, R., Axtell, A., Gerardi, M., Holschneider, C. & Bristow, R. E. Limited utility of conventional criteria for predicting unresectable disease in patients with advanced stage epithelial ovarian cancer. *Gynecologic oncology* **108**, 271-275, doi:10.1016/j.ygyno.2007.11.004 (2008).
18 Edge, S. B., American Joint Committee on Cancer. & American Cancer Society. *AJCC cancer staging handbook : from the AJCC cancer staging manual*. 7th edn, (Springer, 2010).
19 Mendelsohn, J. *The molecular basis of cancer*. 3rd edn, (Saunders, 2008).
20 Ahmed, A. A. *et al.* Driver mutations in TP53 are ubiquitous in high grade serous carcinoma of the ovary. *The Journal of pathology* **221**, 49-56, doi:10.1002/path.2696 (2010).
21 Stiewe, T. The p53 family in differentiation and tumorigenesis. *Nature reviews. Cancer* **7**, 165-168, doi:10.1038/nrc2072 (2007).
22 Rubin, S. C. *et al.* BRCA1, BRCA2, and hereditary nonpolyposis colorectal cancer gene mutations in an unselected ovarian cancer population: relationship to family history and implications for genetic testing. *American journal of obstetrics and gynecology* **178**, 670-677 (1998).
23 Lancaster, J. M. *et al.* BRCA2 mutations in primary breast and ovarian cancers. *Nature genetics* **13**, 238-240, doi:10.1038/ng0696-238 (1996).
24 Eder, A. M. *et al.* Atypical PKCiota contributes to poor prognosis through loss of apical-basal polarity and cyclin E overexpression in ovarian cancer. *Proceedings of the National Academy of Sciences of the United States of America* **102**, 12519-12524, doi:10.1073/pnas.0505641102 (2005).
25 Cheng, K. W., Lahad, J. P., Gray, J. W. & Mills, G. B. Emerging role of RAB GTPases in cancer and human disease. *Cancer research* **65**, 2516-2519, doi:10.1158/0008-5472.CAN-05-0573 (2005).
26 Bast, R. C., Jr., Hennessy, B. & Mills, G. B. The biology of ovarian cancer: new opportunities for translation. *Nature reviews. Cancer* **9**, 415-428, doi:10.1038/nrc2644 (2009).
27 Marumoto, T. *et al.* Aurora-A kinase maintains the fidelity of early and late mitotic events in HeLa cells. *The Journal of biological chemistry* **278**, 51786-51795, doi:10.1074/jbc.M306275200 (2003).
28 Singer, G., Kurman, R. J., Chang, H. W., Cho, S. K. & Shih Ie, M. Diverse tumorigenic pathways in ovarian serous carcinoma. *The American journal of pathology* **160**, 1223-1228 (2002).
29 Bell, D. A. Origins and molecular pathology of ovarian cancer. *Modern pathology : an official journal of the United States and Canadian Academy of Pathology, Inc* **18 Suppl 2**, S19-32, doi:10.1038/modpathol.3800306 (2005).
30 McCluskey, L. L. & Dubeau, L. Biology of ovarian cancer. *Current opinion in oncology* **9**, 465-470 (1997).
31 Singer, G. *et al.* Mutations in BRAF and KRAS characterize the development of low-grade ovarian serous carcinoma. *Journal of the National Cancer Institute* **95**, 484-486 (2003).
32 Sieben, N. L. *et al.* In ovarian neoplasms, BRAF, but not KRAS, mutations are restricted to low-grade serous tumours. *The Journal of pathology* **202**, 336-340, doi:10.1002/path.1521 (2004).

33 Rodabaugh, K. J. *et al.* Detailed deletion mapping of chromosome 9p and p16 gene alterations in human borderline and invasive epithelial ovarian tumors. *Oncogene* **11**, 1249-1254 (1995).

34 Berchuck, A. *et al.* Overexpression of p53 is not a feature of benign and early-stage borderline epithelial ovarian tumors. *Gynecologic oncology* **52**, 232-236, doi:10.1006/gyno.1994.1037 (1994).

35 Shih Ie, M. & Kurman, R. J. Ovarian tumorigenesis: a proposed model based on morphological and molecular genetic analysis. *The American journal of pathology* **164**, 1511-1518 (2004).

36 Singer, G. *et al.* Patterns of p53 mutations separate ovarian serous borderline tumors and low- and high-grade carcinomas and provide support for a new model of ovarian carcinogenesis: a mutational analysis with immunohistochemical correlation. *The American journal of surgical pathology* **29**, 218-224 (2005).

37 Russell, S. E. & McCluggage, W. G. A multistep model for ovarian tumorigenesis: the value of mutation analysis in the KRAS and BRAF genes. *The Journal of pathology* **203**, 617-619, doi:10.1002/path.1563 (2004).

38 Rosen, D. G. *et al.* Ovarian cancer: pathology, biology, and disease models. *Frontiers in bioscience : a journal and virtual library* **14**, 2089-2102 (2009).

39 Samuels, Y. *et al.* High frequency of mutations of the PIK3CA gene in human cancers. *Science* **304**, 554, doi:10.1126/science.1096502 (2004).

40 Samuels, Y. & Velculescu, V. E. Oncogenic mutations of PIK3CA in human cancers. *Cell cycle* **3**, 1221-1224 (2004).

41 Shayesteh, L. *et al.* PIK3CA is implicated as an oncogene in ovarian cancer. *Nature genetics* **21**, 99-102, doi:10.1038/5042 (1999).

42 Yuan, T. L. & Cantley, L. C. PI3K pathway alterations in cancer: variations on a theme. *Oncogene* **27**, 5497-5510, doi:10.1038/onc.2008.245 (2008).

43 Shaw, R. J. & Cantley, L. C. Ras, PI(3)K and mTOR signalling controls tumour cell growth. *Nature* **441**, 424-430, doi:10.1038/nature04869 (2006).

44 Katso, R. *et al.* Cellular function of phosphoinositide 3-kinases: implications for development, homeostasis, and cancer. *Annual review of cell and developmental biology* **17**, 615-675, doi:10.1146/annurev.cellbio.17.1.615 (2001).

45 Cantley, L. C. The phosphoinositide 3-kinase pathway. *Science* **296**, 1655-1657, doi:10.1126/science.296.5573.1655 (2002).

46 Duronio, V. The life of a cell: apoptosis regulation by the PI3K/PKB pathway. *The Biochemical journal* **415**, 333-344, doi:10.1042/BJ20081056 (2008).

47 Wendel, H. G. *et al.* Survival signalling by Akt and eIF4E in oncogenesis and cancer therapy. *Nature* **428**, 332-337, doi:10.1038/nature02369 (2004).

48 Schmelzle, T. & Hall, M. N. TOR, a central controller of cell growth. *Cell* **103**, 253-262 (2000).

49 Lazaris-Karatzas, A., Montine, K. S. & Sonenberg, N. Malignant transformation by a eukaryotic initiation factor subunit that binds to mRNA 5' cap. *Nature* **345**, 544-547, doi:10.1038/345544a0 (1990).

50 Polunovsky, V. A. *et al.* Translational control of the antiapoptotic function of Ras. *The Journal of biological chemistry* **275**, 24776-24780, doi:10.1074/jbc.M001938200 (2000).

51 Hu, L., Hofmann, J., Lu, Y., Mills, G. B. & Jaffe, R. B. Inhibition of phosphatidylinositol 3'-kinase increases efficacy of paclitaxel in in vitro and in vivo ovarian cancer models. *Cancer research* **62**, 1087-1092 (2002).

52 Hennessy, B. T., Smith, D. L., Ram, P. T., Lu, Y. & Mills, G. B. Exploiting the PI3K/AKT pathway for cancer drug discovery. *Nature reviews. Drug discovery* **4**, 988-1004, doi:10.1038/nrd1902 (2005).

53 Calo, V. *et al.* STAT proteins: from normal control of cellular events to tumorigenesis. *Journal of cellular physiology* **197**, 157-168, doi:10.1002/jcp.10364 (2003).

54 Rosen, D. G. *et al.* The role of constitutively active signal transducer and activator of transcription 3 in ovarian tumorigenesis and prognosis. *Cancer* **107**, 2730-2740, doi:10.1002/cncr.22293 (2006).

55 Samanta, A. K., Huang, H. J., Bast, R. C., Jr. & Liao, W. S. Overexpression of MEKK3 confers resistance to apoptosis through activation of NFkappaB. *The Journal of biological chemistry* **279**, 7576-7583, doi:10.1074/jbc.M311659200 (2004).

56 Huang, S., DeGuzman, A., Bucana, C. D. & Fidler, I. J. Nuclear factor-kappaB activity correlates with growth, angiogenesis, and metastasis of human melanoma cells in nude mice. *Clinical cancer research : an official journal of the American Association for Cancer Research* **6**, 2573-2581 (2000).

57 Lin, A. & Karin, M. NF-kappaB in cancer: a marked target. *Seminars in cancer biology* **13**, 107-114 (2003).

58 Hacker, H. & Karin, M. Regulation and function of IKK and IKK-related kinases. *Science's STKE : signal transduction knowledge environment* **2006**, re13, doi:10.1126/stke.3572006re13 (2006).

59 Yang, J. *et al.* The essential role of MEKK3 in TNF-induced NF-kappaB activation. *Nature immunology* **2**, 620-624, doi:10.1038/89769 (2001).

60 Karin, M. Nuclear factor-kappaB in cancer development and progression. *Nature* **441**, 431-436, doi:10.1038/nature04870 (2006).

61 Karin, M. & Lin, A. NF-kappaB at the crossroads of life and death. *Nature immunology* **3**, 221-227, doi:10.1038/ni0302-221 (2002).

62 Gilmore, T. D. The Re1/NF-kappa B/I kappa B signal transduction pathway and cancer. *Cancer treatment and research* **115**, 241-265 (2003).

63 Pahl, H. L. Activators and target genes of Rel/NF-kappaB transcription factors. *Oncogene* **18**, 6853-6866, doi:10.1038/sj.onc.1203239 (1999).

64 Reis-Filho, J. S. & Pusztai, L. Gene expression profiling in breast cancer: classification, prognostication, and prediction. *Lancet* **378**, 1812-1823, doi:10.1016/S0140-6736(11)61539-0 (2011).

65 Harris, T. J. & McCormick, F. The molecular pathology of cancer. *Nature reviews. Clinical oncology* **7**, 251-265, doi:10.1038/nrclinonc.2010.41 (2010).

66 Cancer Genome Atlas Research, N. Integrated genomic analyses of ovarian carcinoma. *Nature* **474**, 609-615, doi:10.1038/nature10166 (2011).

67 Curtis, C. *et al.* The genomic and transcriptomic architecture of 2,000 breast tumours reveals novel subgroups. *Nature* **486**, 346-352, doi:10.1038/nature10983 (2012).

68 Tothill, R. W. *et al.* Novel molecular subtypes of serous and endometrioid ovarian cancer linked to clinical outcome. *Clinical cancer research : an official journal of the American Association for Cancer Research* **14**, 5198-5208, doi:10.1158/1078-0432.CCR-08-0196 (2008).

69 Bonome, T. *et al.* A gene signature predicting for survival in suboptimally debulked patients with ovarian cancer. *Cancer research* **68**, 5478-5486, doi:10.1158/0008-5472.CAN-07-6595 (2008).

70 Prat, A., Ellis, M. J. & Perou, C. M. Practical implications of gene-expression-based assays for breast oncologists. *Nature reviews. Clinical oncology* **9**, 48-57, doi:10.1038/nrclinonc.2011.178 (2012).

71 Bristow, R. E., Tomacruz, R. S., Armstrong, D. K., Trimble, E. L. & Montz, F. J. Survival effect of maximal cytoreductive surgery for advanced ovarian carcinoma during the platinum era: a meta-analysis. *J Clin Oncol* **20**, 1248-1259 (2002).

72 Burges, A. & Schmalfeldt, B. Ovarian cancer: diagnosis and treatment. *Deutsches Arzteblatt international* **108**, 635-641, doi:10.3238/arztebl.2011.0635 (2011).

73 Young, R. C. *et al.* Staging laparotomy in early ovarian cancer. *JAMA : the journal of the American Medical Association* **250**, 3072-3076 (1983).

74 Omura, G. A. *et al.* Long-term follow-up and prognostic factor analysis in advanced ovarian carcinoma: the Gynecologic Oncology Group experience. *J Clin Oncol* **9**, 1138-1150 (1991).

75 Lavin, P. T. *et al.* CA 125 for the monitoring of ovarian carcinoma during primary therapy. *Obstetrics and gynecology* **69**, 223-227 (1987).

76 Markman, M. *et al.* Epithelial ovarian cancer in the elderly. The Memorial Sloan-Kettering Cancer Center experience. *Cancer* **71**, 634-637 (1993).

77 Crawford, T. C. *et al.* Prognostic usefulness of left ventricular thrombus by echocardiography in dilated cardiomyopathy in predicting stroke, transient ischemic attack, and death. *The American journal of cardiology* **93**, 500-503, doi:10.1016/j.amjcard.2003.10.056 (2004).

78 Trimbos, J. B. *et al.* Impact of adjuvant chemotherapy and surgical staging in early-stage ovarian carcinoma: European Organisation for Research and Treatment of Cancer-Adjuvant ChemoTherapy in Ovarian Neoplasm trial. *Journal of the National Cancer Institute* **95**, 113-125 (2003).

79 Bell, J. *et al.* Randomized phase III trial of three versus six cycles of adjuvant carboplatin and paclitaxel in early stage epithelial ovarian carcinoma: a Gynecologic Oncology Group study. *Gynecologic oncology* **102**, 432-439, doi:10.1016/j.ygyno.2006.06.013 (2006).

80 Markman, M. Informing patients with cancer of "new findings" that may influence their willingness to participate in research studies. *Cancer* **98**, 885-887, doi:10.1002/cncr.11607 (2003).

81 Cannistra, S. A. Cancer of the ovary. *The New England journal of medicine* **351**, 2519-2529, doi:10.1056/NEJMra041842 (2004).

82 Eisenhauer, E. L. *et al.* The addition of extensive upper abdominal surgery to achieve optimal cytoreduction improves survival in patients with stages IIIC-IV epithelial ovarian cancer. *Gynecologic oncology* **103**, 1083-1090, doi:10.1016/j.ygyno.2006.06.028 (2006).

83 Aletti, G. D., Dowdy, S. C., Podratz, K. C. & Cliby, W. A. Surgical treatment of diaphragm disease correlates with improved survival in optimally debulked advanced stage ovarian cancer. *Gynecologic oncology* **100**, 283-287, doi:10.1016/j.ygyno.2005.08.027 (2006).

84 Bristow, R. E., Montz, F. J., Lagasse, L. D., Leuchter, R. S. & Karlan, B. Y. Survival impact of surgical cytoreduction in stage IV epithelial ovarian cancer. *Gynecologic oncology* **72**, 278-287, doi:10.1006/gyno.1998.5145 (1999).

85 Dowdy, S. C., Loewen, R. T., Aletti, G., Feitoza, S. S. & Cliby, W. Assessment of outcomes and morbidity following diaphragmatic peritonectomy for women with ovarian carcinoma. *Gynecologic oncology* **109**, 303-307, doi:10.1016/j.ygyno.2008.02.012 (2008).

86 Panici, P. B. *et al.* Systematic aortic and pelvic lymphadenectomy versus resection of bulky nodes only in optimally debulked advanced ovarian cancer: a randomized clinical trial. *Journal of the National Cancer Institute* **97**, 560-566, doi:10.1093/jnci/dji102 (2005).

87 Rowinsky, E. K. & Donehower, R. C. Paclitaxel (taxol). *The New England journal of medicine* **332**, 1004-1014, doi:10.1056/NEJM199504133321507 (1995).

88 Covens, A. *et al.* Systematic review of first-line chemotherapy for newly diagnosed postoperative patients with stage II, III, or IV epithelial ovarian cancer. *Gynecologic oncology* **85**, 71-80, doi:10.1006/gyno.2001.6552 (2002).

89 McGuire, W. P. *et al.* Cyclophosphamide and cisplatin compared with paclitaxel and cisplatin in patients with stage III and stage IV ovarian cancer. *The New England journal of medicine* **334**, 1-6, doi:10.1056/NEJM199601043340101 (1996).

90 Piccart, M. J. *et al.* Randomized intergroup trial of cisplatin-paclitaxel versus cisplatin-cyclophosphamide in women with advanced epithelial ovarian cancer: three-year results. *Journal of the National Cancer Institute* **92**, 699-708 (2000).

91 Ozols, R. F. *et al.* Phase III trial of carboplatin and paclitaxel compared with cisplatin and paclitaxel in patients with optimally resected stage III ovarian cancer: a Gynecologic Oncology Group study. *J Clin Oncol* **21**, 3194-3200, doi:10.1200/JCO.2003.02.153 (2003).

92 du Bois, A. *et al.* A randomized clinical trial of cisplatin/paclitaxel versus carboplatin/paclitaxel as first-line treatment of ovarian cancer. *Journal of the National Cancer Institute* **95**, 1320-1329 (2003).

93 Markman, M. *et al.* Tamoxifen in platinum-refractory ovarian cancer: a Gynecologic Oncology Group Ancillary Report. *Gynecologic oncology* **62**, 4-6, doi:10.1006/gyno.1996.0181 (1996).

94 Bowman, A. *et al.* CA125 response is associated with estrogen receptor expression in a phase II trial of letrozole in ovarian cancer: identification of an endocrine-sensitive subgroup. *Clinical cancer research : an official journal of the American Association for Cancer Research* **8**, 2233-2239 (2002).

95 Cannistra, S. A. Is there a "best" choice of second-line agent in the treatment of recurrent, potentially platinum-sensitive ovarian cancer? *J Clin Oncol* **20**, 1158-1160 (2002).

96 Markman, M. *et al.* Second-line platinum therapy in patients with ovarian cancer previously treated with cisplatin. *J Clin Oncol* **9**, 389-393 (1991).

97 Parmar, M. K. *et al.* Paclitaxel plus platinum-based chemotherapy versus conventional platinum-based chemotherapy in women with relapsed ovarian cancer: the ICON4/AGO-OVAR-2.2 trial. *Lancet* **361**, 2099-2106 (2003).

98 Markman, M. "Recurrence within 6 months of platinum therapy": an adequate definition of "platinum-refractory" ovarian cancer? *Gynecologic oncology* **69**, 91-92, doi:10.1006/gyno.1998.4997 (1998).

99 Ozols, R. F. The current role of gemcitabine in ovarian cancer. *Seminars in oncology* **28**, 18-24 (2001).

100 Markman, M. *et al.* Phase II trial of weekly single-agent paclitaxel in platinum/paclitaxel-refractory ovarian cancer. *J Clin Oncol* **20**, 2365-2369 (2002).

101 Homesley, H. D. *et al.* A dose-escalating study of weekly bolus topotecan in previously treated ovarian cancer patients. *Gynecologic oncology* **83**, 394-399, doi:10.1006/gyno.2001.6435 (2001).

102 Bookman, M. A. *et al.* Topotecan for the treatment of advanced epithelial ovarian cancer: an open-label phase II study in patients treated after prior chemotherapy that contained cisplatin or carboplatin and paclitaxel. *J Clin Oncol* **16**, 3345-3352 (1998).

103 Ozols, R. F. Systemic therapy for ovarian cancer: current status and new treatments. *Seminars in oncology* **33**, S3-11, doi:10.1053/j.seminoncol.2006.03.011 (2006).

104 Baselga, J. Why the epidermal growth factor receptor? The rationale for cancer therapy. *The oncologist* **7 Suppl 4**, 2-8 (2002).

105 Konner, J. *et al.* A phase II study of cetuximab/paclitaxel/carboplatin for the initial treatment of advanced-stage ovarian, primary peritoneal, or fallopian tube cancer. *Gynecologic oncology* **110**, 140-145, doi:10.1016/j.ygyno.2008.04.018 (2008).

106 Vasey, P. A. *et al.* A phase Ib trial of docetaxel, carboplatin and erlotinib in ovarian, fallopian tube and primary peritoneal cancers. *British journal of cancer* **98**, 1774-1780, doi:10.1038/sj.bjc.6604371 (2008).

107 Hirte, H. *et al.* A phase II study of erlotinib (OSI-774) given in combination with carboplatin in patients with recurrent epithelial ovarian cancer (NCIC CTG IND.149). *Gynecologic oncology* **118**, 308-312, doi:10.1016/j.ygyno.2010.05.005 (2010).

108 Blank, S. V. *et al.* Erlotinib added to carboplatin and paclitaxel as first-line treatment of ovarian cancer: a phase II study based on surgical reassessment. *Gynecologic oncology* **119**, 451-456, doi:10.1016/j.ygyno.2010.08.008 (2010).

109 Bookman, M. A., Darcy, K. M., Clarke-Pearson, D., Boothby, R. A. & Horowitz, I. R. Evaluation of monoclonal humanized anti-HER2 antibody, trastuzumab, in patients with recurrent or refractory ovarian or primary peritoneal carcinoma with overexpression of HER2: a phase II trial of the Gynecologic Oncology Group. *J Clin Oncol* **21**, 283-290 (2003).

110 Gordon, M. S. *et al.* Clinical activity of pertuzumab (rhuMAb 2C4), a HER dimerization inhibitor, in advanced ovarian cancer: potential predictive relationship with tumor HER2 activation status. *J Clin Oncol* **24**, 4324-4332, doi:10.1200/JCO.2005.05.4221 (2006).

111 Brown, M. R., Blanchette, J. O. & Kohn, E. C. Angiogenesis in ovarian cancer. *Bailliere's best practice & research. Clinical obstetrics & gynaecology* **14**, 901-918, doi:10.1053/beog.2000.0134 (2000).

112 Hefler, L. A. *et al.* Vascular endothelial growth factor gene polymorphisms are associated with prognosis in ovarian cancer. *Clinical cancer research : an official journal of the American Association for Cancer Research* **13**, 898-901, doi:10.1158/1078-0432.CCR-06-1008 (2007).

113 Burger, R. A., Sill, M. W., Monk, B. J., Greer, B. E. & Sorosky, J. I. Phase II trial of bevacizumab in persistent or recurrent epithelial ovarian cancer or primary peritoneal cancer: a Gynecologic Oncology Group Study. *J Clin Oncol* **25**, 5165-5171, doi:10.1200/JCO.2007.11.5345 (2007).

114 Cannistra, S. A. *et al.* Phase II study of bevacizumab in patients with platinum-resistant ovarian cancer or peritoneal serous cancer. *J Clin Oncol* **25**, 5180-5186, doi:10.1200/JCO.2007.12.0782 (2007).

115 Perren, T. J. *et al.* A phase 3 trial of bevacizumab in ovarian cancer. *The New England journal of medicine* **365**, 2484-2496, doi:10.1056/NEJMoa1103799 (2011).

116 Tagawa, T., Morgan, R., Yen, Y. & Mortimer, J. Ovarian cancer: opportunity for targeted therapy. *Journal of oncology* **2012**, 682480, doi:10.1155/2012/682480 (2012).

117 Agarwal, R. & Kaye, S. B. Ovarian cancer: strategies for overcoming resistance to chemotherapy. *Nature reviews. Cancer* **3**, 502-516, doi:10.1038/nrc1123 (2003).

118 Iyer, L. & Ratain, M. J. Pharmacogenetics and cancer chemotherapy. *European journal of cancer* **34**, 1493-1499 (1998).

119 Tomida, A. & Tsuruo, T. Drug resistance mediated by cellular stress response to the microenvironment of solid tumors. *Anti-cancer drug design* **14**, 169-177 (1999).

120 Teicher, B. A. Hypoxia and drug resistance. *Cancer metastasis reviews* **13**, 139-168 (1994).

121 Green, S. K., Frankel, A. & Kerbel, R. S. Adhesion-dependent multicellular drug resistance. *Anti-cancer drug design* **14**, 153-168 (1999).

122 Gillet, J. P. & Gottesman, M. M. Mechanisms of multidrug resistance in cancer. *Methods in molecular biology* **596**, 47-76, doi:10.1007/978-1-60761-416-6_4 (2010).

123 Trumpp, A., Essers, M. & Wilson, A. Awakening dormant haematopoietic stem cells. *Nature reviews. Immunology* **10**, 201-209, doi:10.1038/nri2726 (2010).

124 Magee, J. A., Piskounova, E. & Morrison, S. J. Cancer stem cells: impact, heterogeneity, and uncertainty. *Cancer cell* **21**, 283-296, doi:10.1016/j.ccr.2012.03.003 (2012).

125 Polyak, K., Haviv, I. & Campbell, I. G. Co-evolution of tumor cells and their microenvironment. *Trends in genetics : TIG* **25**, 30-38, doi:10.1016/j.tig.2008.10.012 (2009).

126 Bissell, M. J. & Hines, W. C. Why don't we get more cancer? A proposed role of the microenvironment in restraining cancer progression. *Nature medicine* **17**, 320-329, doi:10.1038/nm.2328 (2011).

127 Dick, J. E. Stem cell concepts renew cancer research. *Blood* **112**, 4793-4807, doi:10.1182/blood-2008-08-077941 (2008).

128 Shackleton, M., Quintana, E., Fearon, E. R. & Morrison, S. J. Heterogeneity in cancer: cancer stem cells versus clonal evolution. *Cell* **138**, 822-829, doi:10.1016/j.cell.2009.08.017 (2009).

129 Shimada, H. *et al.* Histopathologic prognostic factors in neuroblastic tumors: definition of subtypes of ganglioneuroblastoma and an age-linked classification of neuroblastomas. *Journal of the National Cancer Institute* **73**, 405-416 (1984).

130 Case records of the Massachusetts General Hospital. Weekly clinicopathological exercises. Case 26-1986. A 62-year-old man with progressive polyneuropathy. *The New England journal of medicine* **315**, 45-55, doi:10.1056/NEJM198607033150108 (1986).

131 Stenning, S. P. *et al.* Postchemotherapy residual masses in germ cell tumor patients: content, clinical features, and prognosis. Medical Research Council Testicular Tumour Working Party. *Cancer* **83**, 1409-1419 (1998).

132 Shimada, H. *et al.* Terminology and morphologic criteria of neuroblastic tumors: recommendations by the International Neuroblastoma Pathology Committee. *Cancer* **86**, 349-363 (1999).

133 Matthay, K. K. *et al.* Long-term results for children with high-risk neuroblastoma treated on a randomized trial of myeloablative therapy followed by 13-cis-retinoic acid: a children's oncology group study. *J Clin Oncol* **27**, 1007-1013, doi:10.1200/JCO.2007.13.8925 (2009).

134 Bonnet, D. & Dick, J. E. Human acute myeloid leukemia is organized as a hierarchy that originates from a primitive hematopoietic cell. *Nature medicine* **3**, 730-737 (1997).

135 Al-Hajj, M., Wicha, M. S., Benito-Hernandez, A., Morrison, S. J. & Clarke, M. F. Prospective identification of tumorigenic breast cancer cells. *Proceedings of the National Academy of Sciences of the United States of America* **100**, 3983-3988, doi:10.1073/pnas.0530291100 (2003).

136 O'Brien, C. A., Pollett, A., Gallinger, S. & Dick, J. E. A human colon cancer cell capable of initiating tumour growth in immunodeficient mice. *Nature* **445**, 106-110, doi:10.1038/nature05372 (2007).

137 Ricci-Vitiani, L. *et al.* Identification and expansion of human colon-cancer-initiating cells. *Nature* **445**, 111-115, doi:10.1038/nature05384 (2007).

138 Li, C. *et al.* Identification of pancreatic cancer stem cells. *Cancer research* **67**, 1030-1037, doi:10.1158/0008-5472.CAN-06-2030 (2007).

139 Bao, S. *et al.* Glioma stem cells promote radioresistance by preferential activation of the DNA damage response. *Nature* **444**, 756-760, doi:10.1038/nature05236 (2006).

140 Alvero, A. B. *et al.* Molecular phenotyping of human ovarian cancer stem cells unravels the mechanisms for repair and chemoresistance. *Cell cycle* **8**, 158-166 (2009).

141 Curley, M. D. *et al.* CD133 expression defines a tumor initiating cell population in primary human ovarian cancer. *Stem cells* **27**, 2875-2883, doi:10.1002/stem.236 (2009).

142 Stewart, J. M. *et al.* Phenotypic heterogeneity and instability of human ovarian tumor-initiating cells. *Proceedings of the National Academy of Sciences of the United States of America* **108**, 6468-6473, doi:10.1073/pnas.1005529108 (2011).

143 Zhang, S. *et al.* Identification and characterization of ovarian cancer-initiating cells from primary human tumors. *Cancer research* **68**, 4311-4320, doi:10.1158/0008-5472.CAN-08-0364 (2008).

144 Gao, M. Q., Choi, Y. P., Kang, S., Youn, J. H. & Cho, N. H. CD24+ cells from hierarchically organized ovarian cancer are enriched in cancer stem cells. *Oncogene* **29**, 2672-2680, doi:10.1038/onc.2010.35 (2010).

145 Selvakumaran, M. *et al.* Ovarian epithelial cell lineage-specific gene expression using the promoter of a retrovirus-like element. *Cancer research* **61**, 1291-1295 (2001).

146 Connolly, D. C. *et al.* Female mice chimeric for expression of the simian virus 40 TAg under control of the MISIIR promoter develop epithelial ovarian cancer. *Cancer research* **63**, 1389-1397 (2003).

147 Garson, K. *et al.* Generation of tumors in transgenic mice expressing the SV40 T antigen under the control of ovarian-specific promoter 1. *Journal of the Society for Gynecologic Investigation* **10**, 244-250 (2003).

148 Aunoble, B., Sanches, R., Didier, E. & Bignon, Y. J. Major oncogenes and tumor suppressor genes involved in epithelial ovarian cancer (review). *International journal of oncology* **16**, 567-576 (2000).

149 Tammela, J. & Odunsi, K. Gene expression and prognostic significance in ovarian cancer. *Minerva ginecologica* **56**, 495-502 (2004).

150 Landen, C. N., Jr., Birrer, M. J. & Sood, A. K. Early events in the pathogenesis of epithelial ovarian cancer. *J Clin Oncol* **26**, 995-1005, doi:10.1200/JCO.2006.07.9970 (2008).

151 Marino, S., Vooijs, M., van Der Gulden, H., Jonkers, J. & Berns, A. Induction of medulloblastomas in p53-null mutant mice by somatic inactivation of Rb in the external granular layer cells of the cerebellum. *Genes & development* **14**, 994-1004 (2000).

152 Jonkers, J. *et al.* Synergistic tumor suppressor activity of BRCA2 and p53 in a conditional mouse model for breast cancer. *Nature genetics* **29**, 418-425, doi:10.1038/ng747 (2001).

153 Corpet, D. E. & Pierre, F. How good are rodent models of carcinogenesis in predicting efficacy in humans? A systematic review and meta-analysis of colon chemoprevention in rats, mice and men. *European journal of cancer* **41**, 1911-1922, doi:10.1016/j.ejca.2005.06.006 (2005).

154 Dinulescu, D. M. *et al.* Role of K-ras and Pten in the development of mouse models of endometriosis and endometrioid ovarian cancer. *Nature medicine* **11**, 63-70, doi:10.1038/nm1173 (2005).

155 Tuveson, D. A. *et al.* Endogenous oncogenic K-ras(G12D) stimulates proliferation and widespread neoplastic and developmental defects. *Cancer cell* **5**, 375-387 (2004).

156 Heyer, J., Kwong, L. N., Lowe, S. W. & Chin, L. Non-germline genetically engineered mouse models for translational cancer research. *Nature reviews. Cancer* **10**, 470-480, doi:10.1038/nrc2877 (2010).

157 Flanagan, S. P. 'Nude', a new hairless gene with pleiotropic effects in the mouse. *Genetical research* **8**, 295-309 (1966).

158 Nonoyama, S., Smith, F. O., Bernstein, I. D. & Ochs, H. D. Strain-dependent leakiness of mice with severe combined immune deficiency. *Journal of immunology* **150**, 3817-3824 (1993).

159 Nomura, T. *et al.* SCID (severe combined immunodeficiency) mice as a new system to investigate metastasis of human tumors. *Journal of radiation research* **31**, 288-292 (1990).

160 Boermans, H. J., Percy, D. H., Stirtzinger, T. & Croy, B. A. Engraftment of severe combined immune deficient/beige mice with bovine foetal lymphoid tissues. *Veterinary immunology and immunopathology* **34**, 273-289 (1992).

161 Christianson, S. W. *et al.* Role of natural killer cells on engraftment of human lymphoid cells and on metastasis of human T-lymphoblastoid leukemia cells in C57BL/6J-scid mice and in C57BL/6J-scid bg mice. *Cellular immunology* **171**, 186-199, doi:10.1006/cimm.1996.0193 (1996).

162 Greiner, D. L. *et al.* Improved engraftment of human spleen cells in NOD/LtSz-scid/scid mice as compared with C.B-17-scid/scid mice. *The American journal of pathology* **146**, 888-902 (1995).

163 Shultz, L. D. *et al.* Multiple defects in innate and adaptive immunologic function in NOD/LtSz-scid mice. *Journal of immunology* **154**, 180-191 (1995).

164 Ito, M. *et al.* NOD/SCID/gamma(c)(null) mouse: an excellent recipient mouse model for engraftment of human cells. *Blood* **100**, 3175-3182, doi:10.1182/blood-2001-12-0207 (2002).

165 Koyanagi, Y. *et al.* High levels of viremia in hu-PBL-NOD-scid mice with HIV-1 infection. *Leukemia* **11 Suppl 3**, 109-112 (1997).

166 Yoshino, H. *et al.* Natural killer cell depletion by anti-asialo GM1 antiserum treatment enhances human hematopoietic stem cell engraftment in NOD/Shi-scid mice. *Bone marrow transplantation* **26**, 1211-1216, doi:10.1038/sj.bmt.1702702 (2000).

167 Lee, J. *et al.* Tumor stem cells derived from glioblastomas cultured in bFGF and EGF more closely mirror the phenotype and genotype of primary tumors than do serum-cultured cell lines. *Cancer cell* **9**, 391-403, doi:10.1016/j.ccr.2006.03.030 (2006).

168 Pardal, R., Clarke, M. F. & Morrison, S. J. Applying the principles of stem-cell biology to cancer. *Nature reviews. Cancer* **3**, 895-902, doi:10.1038/nrc1232 (2003).

169 Voskoglou-Nomikos, T., Pater, J. L. & Seymour, L. Clinical predictive value of the in vitro cell line, human xenograft, and mouse allograft preclinical cancer models. *Clinical cancer research : an official journal of the American Association for Cancer Research* **9**, 4227-4239 (2003).

170 Gage, F. H., Ray, J. & Fisher, L. J. Isolation, characterization, and use of stem cells from the CNS. *Annual review of neuroscience* **18**, 159-192, doi:10.1146/annurev.ne.18.030195.001111 (1995).

171 Rietze, R. L. & Reynolds, B. A. Neural stem cell isolation and characterization. *Methods in enzymology* **419**, 3-23, doi:10.1016/S0076-6879(06)19001-1 (2006).

172 Uchida, N. *et al.* Direct isolation of human central nervous system stem cells. *Proceedings of the National Academy of Sciences of the United States of America* **97**, 14720-14725, doi:10.1073/pnas.97.26.14720 (2000).

173 Geschwind, D. H. *et al.* A genetic analysis of neural progenitor differentiation. *Neuron* **29**, 325-339 (2001).

174 Dontu, G. *et al.* In vitro propagation and transcriptional profiling of human mammary stem/progenitor cells. *Genes & development* **17**, 1253-1270, doi:10.1101/gad.1061803 (2003).

175 Singh, S. K. *et al.* Identification of human brain tumour initiating cells. *Nature* **432**, 396-401, doi:10.1038/nature03128 (2004).

176 Pollard, S. M. *et al.* Glioma stem cell lines expanded in adherent culture have tumor-specific phenotypes and are suitable for chemical and genetic screens. *Cell stem cell* **4**, 568-580, doi:10.1016/j.stem.2009.03.014 (2009).

177 Pollard, S. M., Conti, L., Sun, Y., Goffredo, D. & Smith, A. Adherent neural stem (NS) cells from fetal and adult forebrain. *Cerebral cortex* **16 Suppl 1**, i112-120, doi:10.1093/cercor/bhj167 (2006).

178 Kuch, V., Schreiber, C., Thiele, W., Umansky, V. & Sleeman, J. P. Tumor-initiating properties of breast cancer and melanoma cells in vivo are not invariably reflected by spheroid formation in vitro, but can be increased by long-term culturing as adherent monolayers. *International journal of cancer. Journal international du cancer* **132**, E94-105, doi:10.1002/ijc.27785 (2013).

179 Subramanian, A. *et al.* Gene set enrichment analysis: a knowledge-based approach for interpreting genome-wide expression profiles. *Proceedings of the National Academy of Sciences of the United States of America* **102**, 15545-15550, doi:10.1073/pnas.0506580102 (2005).

180 Vermeulen, L. *et al.* Single-cell cloning of colon cancer stem cells reveals a multi-lineage differentiation capacity. *Proceedings of the National Academy of Sciences of the United States of America* **105**, 13427-13432, doi:10.1073/pnas.0805706105 (2008).

181 Richmond, A. & Su, Y. Mouse xenograft models vs GEM models for human cancer therapeutics. *Disease models & mechanisms* **1**, 78-82, doi:10.1242/dmm.000976 (2008).

182 Bankert, R. B. *et al.* Humanized mouse model of ovarian cancer recapitulates patient solid tumor progression, ascites formation, and metastasis. *PloS one* **6**, e24420, doi:10.1371/journal.pone.0024420 (2011).
183 Pan, Z. *et al.* Establishment of human ovarian serous carcinomas cell lines in serum free media. *Methods* **56**, 432-439, doi:10.1016/j.ymeth.2012.03.003 (2012).
184 Simon, W. E. & Holzel, F. Hormone sensitivity of gynecological tumor cells in tissue culture. *Journal of cancer research and clinical oncology* **94**, 307-323 (1979).
185 Balconi, G. *et al.* Human ovarian tumors in primary culture: growth, characterization and initial evaluation of the response to cis platinum treatment in vitro. *International journal of cancer. Journal international du cancer* **41**, 809-818 (1988).
186 Murdoch, W. J. Endothelial cell death in preovulatory ovine follicles: possible implication in the biomechanics of rupture. *Journal of reproduction and fertility* **105**, 161-164 (1995).
187 Warde-Farley, D. *et al.* The GeneMANIA prediction server: biological network integration for gene prioritization and predicting gene function. *Nucleic acids research* **38**, W214-220, doi:10.1093/nar/gkq537 (2010).
188 Yang, D. *et al.* Integrated analyses identify a master microRNA regulatory network for the mesenchymal subtype in serous ovarian cancer. *Cancer cell* **23**, 186-199, doi:10.1016/j.ccr.2012.12.020 (2013).
189 Maecker, H. T., Todd, S. C. & Levy, S. The tetraspanin superfamily: molecular facilitators. *FASEB journal : official publication of the Federation of American Societies for Experimental Biology* **11**, 428-442 (1997).
190 Boucheix, C. & Rubinstein, E. Tetraspanins. *Cellular and molecular life sciences : CMLS* **58**, 1189-1205 (2001).
191 Kazarov, A. R., Yang, X., Stipp, C. S., Sehgal, B. & Hemler, M. E. An extracellular site on tetraspanin CD151 determines alpha 3 and alpha 6 integrin-dependent cellular morphology. *The Journal of cell biology* **158**, 1299-1309 (2002).
192 Zijlstra, A., Lewis, J., Degryse, B., Stuhlmann, H. & Quigley, J. P. The inhibition of tumor cell intravasation and subsequent metastasis via regulation of in vivo tumor cell motility by the tetraspanin CD151. *Cancer cell* **13**, 221-234, doi:10.1016/j.ccr.2008.01.031 (2008).
193 Ang, J., Lijovic, M., Ashman, L. K., Kan, K. & Frauman, A. G. CD151 protein expression predicts the clinical outcome of low-grade primary prostate cancer better than histologic grading: a new prognostic indicator? *Cancer epidemiology, biomarkers & prevention : a publication of the American Association for Cancer Research, cosponsored by the American Society of Preventive Oncology* **13**, 1717-1721 (2004).
194 Tokuhara, T. *et al.* Clinical significance of CD151 gene expression in non-small cell lung cancer. *Clinical cancer research : an official journal of the American Association for Cancer Research* **7**, 4109-4114 (2001).
195 Chien, C. W. *et al.* Regulation of CD151 by hypoxia controls cell adhesion and metastasis in colorectal cancer. *Clinical cancer research : an official journal of the American Association for Cancer Research* **14**, 8043-8051, doi:10.1158/1078-0432.CCR-08-1651 (2008).
196 Kwon, M. J. *et al.* Clinical significance of CD151 overexpression in subtypes of invasive breast cancer. *British journal of cancer* **106**, 923-930, doi:10.1038/bjc.2012.11 (2012).

197 Rajasekhar, V. K., Studer, L., Gerald, W., Socci, N. D. & Scher, H. I. Tumour-initiating stem-like cells in human prostate cancer exhibit increased NF-kappaB signalling. *Nature communications* **2**, 162, doi:10.1038/ncomms1159 (2011).
198 Guo, W. & Giancotti, F. G. Integrin signalling during tumour progression. *Nature reviews. Molecular cell biology* **5**, 816-826, doi:10.1038/nrm1490 (2004).
199 Haeuw, J. F., Goetsch, L., Bailly, C. & Corvaia, N. Tetraspanin CD151 as a target for antibody-based cancer immunotherapy. *Biochemical Society transactions* **39**, 553-558, doi:10.1042/BST0390553 (2011).
200 Yarden, Y. & Sliwkowski, M. X. Untangling the ErbB signalling network. *Nature reviews. Molecular cell biology* **2**, 127-137, doi:10.1038/35052073 (2001).
201 Veeman, M. T., Axelrod, J. D. & Moon, R. T. A second canon. Functions and mechanisms of beta-catenin-independent Wnt signaling. *Developmental cell* **5**, 367-377 (2003).
202 Ichijo, H. From receptors to stress-activated MAP kinases. *Oncogene* **18**, 6087-6093, doi:10.1038/sj.onc.1203129 (1999).
203 Davis, R. J. Signal transduction by the JNK group of MAP kinases. *Cell* **103**, 239-252 (2000).
204 Siegel, R., Naishadham, D. & Jemal, A. Cancer statistics, 2012. *CA: a cancer journal for clinicians* **62**, 10-29, doi:10.3322/caac.20138 (2012).
205 Jemal, A. *et al.* Cancer statistics, 2009. *CA: a cancer journal for clinicians* **59**, 225-249, doi:10.3322/caac.20006 (2009).
206 Armstrong, D. K. *et al.* Intraperitoneal cisplatin and paclitaxel in ovarian cancer. *The New England journal of medicine* **354**, 34-43, doi:10.1056/NEJMoa052985 (2006).
207 Tentler, J. J. *et al.* Patient-derived tumour xenografts as models for oncology drug development. *Nature reviews. Clinical oncology* **9**, 338-350, doi:10.1038/nrclinonc.2012.61 (2012).
208 Schatton, T. *et al.* Identification of cells initiating human melanomas. *Nature* **451**, 345-349, doi:10.1038/nature06489 (2008).
209 Dobrynin, Y. V. Establishment and Characteristics of Cell Strains from Some Epithelial Tumors of Human Origin. *Journal of the National Cancer Institute* **31**, 1173-1195 (1963).
210 McQueen, H. A., Wyllie, A. H., Piris, J., Foster, E. & Bird, C. C. Stability of critical genetic lesions in human colorectal carcinoma xenografts. *British journal of cancer* **63**, 94-96 (1991).
211 Garson, K., Shaw, T. J., Clark, K. V., Yao, D. S. & Vanderhyden, B. C. Models of ovarian cancer--are we there yet? *Molecular and cellular endocrinology* **239**, 15-26, doi:10.1016/j.mce.2005.03.019 (2005).
212 Burleson, K. M. *et al.* Ovarian carcinoma ascites spheroids adhere to extracellular matrix components and mesothelial cell monolayers. *Gynecologic oncology* **93**, 170-181, doi:10.1016/j.ygyno.2003.12.034 (2004).
213 Barsotti, A. M. & Prives, C. Pro-proliferative FoxM1 is a target of p53-mediated repression. *Oncogene* **28**, 4295-4305, doi:10.1038/onc.2009.282 (2009).
214 Cliby, W. A., Lewis, K. A., Lilly, K. K. & Kaufmann, S. H. S phase and G2 arrests induced by topoisomerase I poisons are dependent on ATR kinase function. *The Journal of biological chemistry* **277**, 1599-1606, doi:10.1074/jbc.M106287200 (2002).
215 Kohno, M., Hasegawa, H., Miyake, M., Yamamoto, T. & Fujita, S. CD151 enhances cell motility and metastasis of cancer cells in the presence of focal adhesion

kinase. *International journal of cancer. Journal international du cancer* **97**, 336-343 (2002).

216 Testa, J. E., Brooks, P. C., Lin, J. M. & Quigley, J. P. Eukaryotic expression cloning with an antimetastatic monoclonal antibody identifies a tetraspanin (PETA-3/CD151) as an effector of human tumor cell migration and metastasis. *Cancer research* **59**, 3812-3820 (1999).

217 Shibata, W. *et al.* c-Jun NH2-terminal kinase 1 is a critical regulator for the development of gastric cancer in mice. *Cancer research* **68**, 5031-5039, doi:10.1158/0008-5472.CAN-07-6332 (2008).

218 Hui, L., Zatloukal, K., Scheuch, H., Stepniak, E. & Wagner, E. F. Proliferation of human HCC cells and chemically induced mouse liver cancers requires JNK1-dependent p21 downregulation. *The Journal of clinical investigation* **118**, 3943-3953, doi:10.1172/JCI37156 (2008).

219 Chen, T., Pengetnze, Y. & Taylor, C. C. Src inhibition enhances paclitaxel cytotoxicity in ovarian cancer cells by caspase-9-independent activation of caspase-3. *Molecular cancer therapeutics* **4**, 217-224 (2005).

220 Nateri, A. S., Spencer-Dene, B. & Behrens, A. Interaction of phosphorylated c-Jun with TCF4 regulates intestinal cancer development. *Nature* **437**, 281-285, doi:10.1038/nature03914 (2005).

221 Sancho, R. *et al.* JNK signalling modulates intestinal homeostasis and tumourigenesis in mice. *The EMBO journal* **28**, 1843-1854, doi:10.1038/emboj.2009.153 (2009).

222 Zoller, M. Tetraspanins: push and pull in suppressing and promoting metastasis. *Nature reviews. Cancer* **9**, 40-55, doi:10.1038/nrc2543 (2009).

223 Myant, K. B. *et al.* ROS Production and NF-kappaB Activation Triggered by RAC1 Facilitate WNT-Driven Intestinal Stem Cell Proliferation and Colorectal Cancer Initiation. *Cell stem cell* **12**, 761-773, doi:10.1016/j.stem.2013.04.006 (2013).

8 Abbreviations

ACS	American Cancer Society
AIM2	absent in melanoma 2
AJCC	American Joint Cancer Committee
Akt	Proteinkinase B
ANOVA	Analysis of Variance
APC	Adenomatous polyposis coli
ATCC	American Type Culture Collection
BRAF	Raf murine sarcoma viral oncogene homolog B1
BRCA1	Breast Cancer 1 susceptibility protein
BRCA2	Breast Cancer 2 susceptibility protein
CA125	carbohydrate antigen 125
CD133	Prominin-1
CD151	Cluster of Differentiation 151
CD24	Cluster of Differentiation 24
CD44	Cluster of Differentiation 44
CDKN2A	Cyclin-dependent kinase inhibitor 2A
CML	Chronic Myloid Leukemia
Cre	Cre Recombinase
CTNNB1	*ß-Catenin*
DN	Double negative
DNA	Deoxyribonucleic acid
DT	Derived Tumor
EGFR	Epidermal growth factor receptor
eIF4	Eukaryotic initiation factor 4
EMT	Epithelial-to-menenchymal transition
ER	Estrogen receptor
eSC	Embryonic Stem Cells
FACS	Flourescent activated cell sorting
FCS	Fetal calf serum
FDA	Food and Drug Administration
FIGO	International Federation of Gynecology and Obstetrics
G1	Gap 1 phase
G2/M	G2-M DNA damage checkpoint
GEM	Genetically engineered mouse model
GSEA	Gene set enrichement analysis
HER2	human epidermal growth factor receptor type 2
HER2	Human Epidermal Growth Factor Receptor 2
IC50	half-maximal inhibitory concentration
ICGC	International Cancer Genome Consortium
IL-6	Interleukin 6
iPS	Induced pluripotent stem cells
JNK	c-Jun N-terminal kinases

Ki67	Antigen KI-67
KRAS2	V-Ki-ras2 Kirsten rat sarcoma viral oncogene homolog
LOH	Loss of heterozygosity
MKK4	Dual specificity mitogen-activated protein kinase kinase 4
MSig	Molecular Signatures
mTOR	Mammalian target of Rapamycin
NLM	National Library of Medicine
NOD/SCID	Nonobese diabetic with severe combined immunodeficiency
NSC	Neural stem cells
NSG	NOD.Cg-*Prkdc*^{scid} *Il2rg*^{tm1Wjl}
OS	Overall survival
p70S6K	p70S6 kinase
PI3K	Phosphoinositide 3-kinase
PKB	Proteinkinase B
PR	Progesterone receptor
PR	Progesterone receptor
PRSS1	Trypsin-1
PT	Primary Tumor
PTEN	Phosphatase and tensin homolog
Rab25	Ras-related protein Rab-25
RAF-MAPK	Raf murine sarcoma viral oncogene - Mitogen-activated protein (MAP) kinases
RalGDS	Ral guanine nucleotide dissociation stimulator
Ser	Serine
SFK	Src family kinases
SOC	Serous Ovarian Cancer
Src	Tyrosinkinase Src
STAT3	Signal transducer and activator of transcription 3
TCGA	The Cancer Genome Atlas Network
TIC	Tumor initiating cell
TIC	Tumor initiating cell
TMN	Tumor Node Metastasis
TP53	tumor protein 53
TVS	Transvaginal ultrasound
Tyr	Tyrosine
VEGF	Vascular endothelial growth factor
VEGFR2	vascular endothelial growth factor receptor 2
WT1	Wilms Tumor 1
µg	microgram
µM	micromolar
µm	micrometer